REPORT NO. CG-D-09-80

LORAN-BASED BUOY POSITION AUDITING SYSTEMS--ANALYTICAL EVALUATION

U.S. DEPARTMENT OF TRANSPORTATION
RESEARCH AND SPECIAL PROGRAMS ADMINISTRATION
Transportation Systems Center
Cambridge MA 02142

FEBRUARY 1980

FINAL REPORT

Prepared for

U.S. DEPARTMENT OF TRANSPORTATION
UNITED STATES COAST GUARD
Office of Research and Development
Washington DC 20593

Technical Report Documentation Page

1. Report No.	2. Government Accession No.	3. Recipient's Catalog No.
CG-D-09-80		

4. Title and Subtitle	5. Report Date
LORAN-BASED BUOY POSITION AUDITING SYSTEMS--ANALYTICAL EVALUATION	February 1980
	6. Performing Organization Code
	8. Performing Organization Report No. DOT-TSC-USCG-80-2
7. Author(s) J.A. Wolfson,* P.D. Engels,* M.C. Poppe, Jr.,** J.M. Foltz,*** L.M. DePalma***	
9. Performing Organization Name and Address *U.S. Department of Transportation Research and Special Programs Administration Transportation Systems Center Cambridge MA 02142	10. Work Unit No. (TRAIS) CG019/R0004
	11. Contract or Grant No.
12. Sponsoring Agency Name and Address U.S. Department of Transportation United States Coast Guard Office of Research and Development Washington DC 20593	13. Type of Report and Period Covered Final Report Feb. to Dec. 1979
	14. Sponsoring Agency Code

15. Supplementary Notes

**Cambridge Engineering
Cambridge VT 05444

***The Analytic Science Corporation
Reading MA 01867

16. Abstract

An analytic evaluation and comparison of the following candidate Buoy Position Auditing System (BPAS) configurations is presented in this report: transmission of digital Time Difference (TD) data from a Loran-C receiver on the buoy, retransmission of Loran-C pulses from the buoy, and combination of helicopter Loran-C data and helicopter-to-buoy microwave ranging data in a variable geometry solution. The candidate BPAS configurations utilize Loran-C in the differential mode. A model is developed to characterize differential Loran-C errors, accounting for the expected effect of the land/sea water conductivity interface. The error model is utilized alone, or with a microwave ranging system error model, to estimate buoy position-fix accuracy afforded by each BPAS configuration. Accuracy estimates and data on cost, complexity, and technical risk are employed to recommend a BPAS configuration for testing. It is concluded that Loran-C pulse retransmission is not a viable BPAS configuration. The variable geometry BPAS configuration is highly accurate, due to calibration of Loran-C errors by processing of redundant data, but is not presently cost-effective. The digital TD transmission BPAS configuration is recommended for testing, due to its simplicity and low cost. An experiment is outlined whereby the accuracy of the TD transmission configuration can be assessed to determine its utility in the U.S. Coast Guard buoy audit mission.

17. Key Words	18. Distribution Statement
Buoy Position Finding Aids to Navigation Differential Loran-C Loran-C Pulse Retransmission	DOCUMENT IS AVAILABLE TO THE PUBLIC THROUGH THE NATIONAL TECHNICAL INFORMATION SERVICE, SPRINGFIELD, VIRGINIA 22161

19. Security Classif. (of this report)	20. Security Classif. (of this page)	21. No. of Pages	22. Price
Unclassified	Unclassified	258	

Form DOT F 1700.7 (8-72) Reproduction of completed page authorized

PREFACE

The purpose of this Transportation Systems Center (TSC) report is to:

1. provide an evaluation and comparison of methods for auditing the positions of U.S. Coast Guard buoys (aids to navigation) using retransmission of radio location signals,

2. recommend a buoy position audit system (BPAS) configuration,

3. provide a test method to determine the operational acceptability of the technique.

The project was sponsored by Captain Donald A. Feldman of the United States Coast Guard (G-DST-1). Peter D. Engels and Joseph A. Wolfson of the Transportation Systems Center were responsible for the preparation of the report as well as overseeing and contributing to all subject areas. The error analyses were performed by Leon M. DePalma and James M. Foltz of The Analytical Sciences Corporation (TASC) in Reading, Massachusetts. The BPAS system hardware configurations, availability, operations and associated costs studies were performed by Martin C. Poppe, Jr. of Cambridge Engineering in Cambridge, Vermont. These three gentlemen also contributed to all phases of this report.

The authors would also like to acknowledge Kathleen Kvicala whose typing skills were critical to the timely completion of this report. Acknowledgement is also due to William Nucefora for a splendid job of editing and compilation.

TABLE OF CONTENTS

TABLE OF CONTENTS (continued)

LIST OF ILLUSTRATIONS (Continued)

LIST OF TABLES

1. INTRODUCTION AND SUMMARY

1.1 BACKGROUND AND OBJECTIVES

The U.S. Coast Guard (USCG) maintains a network of moored buoys (aids to navigation) to control maritime traffic in the shipping channels of rivers, harbors and harbor entrances. These buoys can be moved off station or destroyed as a result of severe storms, ice flow or collision with vessels. Since an off-station buoy is presently identified by periodic inspections with a buoy tender or by an "aid discrepancy report" from a mariner, a significant time delay may occur before a warning is issued and the buoy is returned to its correct location. An effective Buoy Position Auditing System (BPAS) will both reduce this delay and enable the Coast Guard to maintain the navigational capability provided by the buoy network, thus minimizing the likelihood of property damage and shipping delays which can result from displaced buoys.

In October 1977, the USCG Research and Development Center published Report No. CG-D-61-77, "A Study of Aerial Semi-Precise Survey Systems for Position Auditing of Coast Guard Aids to Navigation". This report specified the following requirements for a buoy position auditing system:

1. Economical operation
2. Buoy position error less than ±30 meters
3. Response time of a few hours and completion within 48 hours
4. Minimal development time and modest equipment and manpower procurement requirements.

This report also concluded that no system is presently available which can meet all these requirements.

The Naval Research Laboratory (NRL) also studied the problem and arrived at a slightly different set of requirements:

1. Buoy position accuracy of 15 meters
2. Auditing up to four times a day.

position relative to a moving platform can be accomplished by two-way ranging. The platform emits a ranging signal which is transponded back by the buoy. As the platform moves, the changing geometry relative to the buoy will generate multiple lines of position, enabling buoy location by triangulation. Alternatively the ranging measurements could be made from a network of shore stations.

The configurations are referred to as "TD Transmission", "Pulse Retransmission", and "Variable Geometry", respectively, in this report.

All three candidate configurations employ differential Loran-C, which exhibits cost, accuracy and/or operational advantages over other methods of locating and tracking buoys (Appendix E contains a list of other methods). Implementation of a Buoy Position Auditing System based on differential Loran-C could lead to coordination of the buoy audit mission with harbor and harbor entrance navigation, for which differential Loran-C is also under consideration by the USCG.

The major objectives of this study are to:

- o Identify viable Loran-C system configurations meeting the requirements of a buoy-based system
- o Construct a tradeoff between cost/complexity and performance for the selected configurations
- o Define the associated base station equipment required to receive and process signals received from the buoys
- o Construct a typical operating scenario for each system to determine audit rates and buoy power requirements
- o Define a candidate system for experimental verification of the selected approach
- o Perform error analyses of the candidate BPAS configurations to estimate system accuracy and identify critical hardware parameters and operational restrictions

charged by solar cells thereby permitting a greater battery drain during a buoy audit than is presently feasible. Further, systems requiring sophisticated adjustments are also undesirable, as these would increase the level of training required for buoy tender personnel.

The following constraints pertain to the shore station used in the TD Transmission and Pulse Retransmission configurations:

- o Shore station-to-buoy communications link: line-of-sight
- o Antenna for communications link: mounted on existing tower
- o Maximum frequency of audits: daily
- o Equipment cost: $20,000 to $50,000 per control station.

Since communications from the shore station to the buoy must be line-of-sight from an antenna mounted on an existing tower, some buoys (particularly, ocean buoys) may have to be audited from a helicopter. Both a shore station and a helicopter may be needed to audit the buoys in each harbor, in the TD Transmission and Pulse Retransmission BPAS configurations.

The following constraints are applicable to the helicopter involved in all three configurations:

- o Typical altitude: 300 m (1,000 ft)
- o Maximum velocity: 150-220 km/hr (80-120 kt), depending on helicopter model
- o Maximum round-trip flight time: 3 hrs
- o Weather conditions at time of audit: good visibility
- o Helicopter-to-buoy communications link: line-of-sight

on accuracy guidelines for aerial "semi-precise" imaging systems, which are considered for the buoy position auditing problem in Ref. 8. The selected hardware should have a negligible effect on the potential accuracy of Loran-C. Further, the use of differential Loran-C (i.e. the measurement of Loran-C signals at a fixed location to calibrate the Loran-C signals received in the area of operation) is considered fundamental to meeting the stated less than 30 meter accuracy requirement. As part of establishing a buoy audit system, it is necessary to obtain authorization from the Federal Communication Commission (FCC) to use the necessary communication channels. Systems which permit the use of existing communication channels and further, which transmit data in a format permitted by the presently allocated use of those channels, are desirable. With the present crowded conditions in all frequency bands, the request for a wideband (e.g. 1MHz) communication channel would most likely be granted only in L-band or higher frequency ranges.

1.3 SYSTEM DESCRIPTIONS

The TD Transmission, Pulse Retransmission, and Variable Geometry BPAS configurations are described generically in this section. The candidate BPAS configurations all employ differential Loran-C operated in the hyperbolic mode. As in the case of conventional (non-differential) Loran-C, a position fix is computed as the intersection of two hyperbolas, each associated with a time difference measured at the Loran-C user location. However, the user TDs are first corrected based on the TDs measured at a pattern monitor (a Loran-C receiver which is established at a known location and operated continuously during the buoy audit). If the pattern monitor is located near the Loran-C user, differential Loran-C can significantly reduce the effect of temporal TD variations and thereby exhibit much smaller position-fix errors than conventional Loran-C. The differential Loran-C algorithm for the TD Transmission BPAS configuration is detailed in Appendix A (Section A.4.1). It is assumed that buoy TDs are recorded by personnel on the buoy tender when the BPAS equipment is first installed (time t_o). (The TDs are recorded with the buoy directly above the desired buoy anchor position.) Pattern monitor TDs are likewise assumed to be measured at time t_o, and are subtracted from the buoy TDs to form differential TDs. New differential TDs are computed based on buoy and pattern monitor TDs measured during the buoy audit. The change in differential TDs between time t_o and the audit time is used to estimate the new buoy position relative to the desired anchor position.

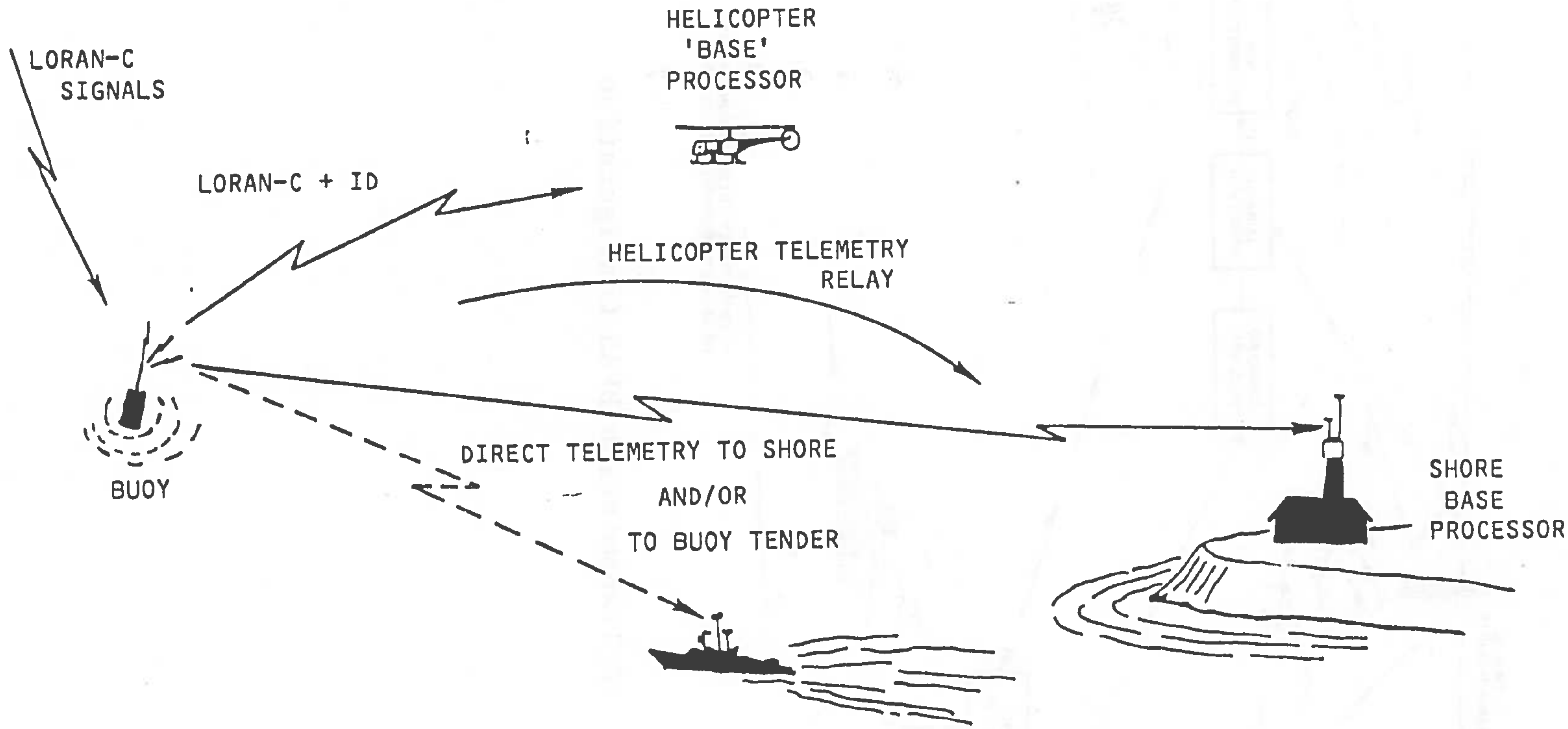

Figure 1.3-1 A Loran-C Based Buoy Audit System, System Configuration

1.3.2 Pulse Retransmission

The Pulse Retransmission BPAS configuration (Figure 1-3.3) differs from the TD Transmission configuration in that a Loran-C pulse retransmitter, instead of a Loran-C receiver, is installed on each buoy. The Loran-C signals are received at the buoy, and are processed by an analog pulse processor. The output of this processor is an analog signal which is a transformation of the original pulse. The processed pulse, pulse processing parameters necessary to complete the processing of the pulse, and identification data are transmitted back to the base station on a wideband telemetry link. At the base station, the processing of the Loran-C pulses is completed to obtain Loran-C time differences. This is accomplished using a special purpose Loran-C processor. As shown, the base station processor makes use of local Loran-C signals. Primary use of these signals is to aid in the processing of the retransmitted signals by providing timing and preliminary pulse information. The digital output from the special purpose Loran-C processor is recorded and directed to a data position processor/center where buoy position is determined using differential techniques. The primary reason for considering the pulse retransmission technique is the potential for cost reduction in the buoy electronics. Essentially, the electronics on the buoy may be thought of as the 'front end' of a Loran-C receiver, where the special purpose base station Loran-C procesor performs the remaining functions required to process the Loran-C signal to time difference data. By moving this electronics processing to the base station, the Loran-C processing in the buoy is simplified, resulting in a potential cost saving.

1.3.3 Variable Geometry

In the Variable Geometry BPAS configuration (Figure 1.3-4), the buoy audit is conducted from a helicopter which carries a Loran-C receiver, a precision ranging system, and an altimeter. The ranging system is used to determine the ranges from the helicopter to the buoys, where each buoy is equipped with a transponder. Simultaneous Loran-C TDs, range data, and altitude data are stored on magnetic tape and delivered to a USCG shore station for processing. The helicopter Loran-C TDs are combined with pattern monitor TDs in a differential Loran-C algorithm to compute helicopter position fixes. Buoy position fixes are then estimated from helicopter position-fixes, range data, and altitude data in a least-squares algorithm. The Loran-C and ranging equipment required for the Variable Geometry

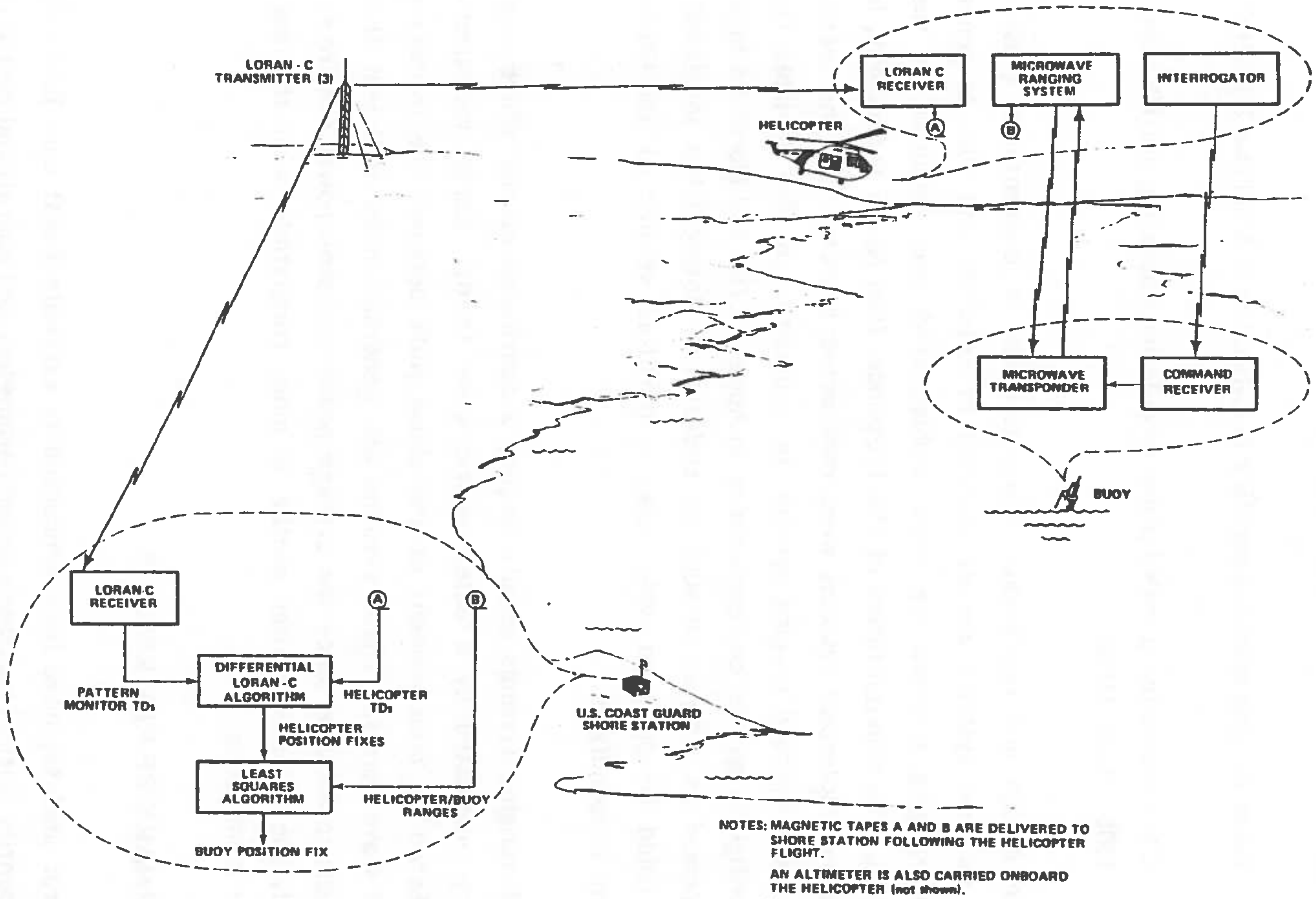

Figure 1.3-4 Variable Geometry BPAS Configuration

Loran-C error model (with GDOP = 1) which accounts for the expected effect of the land/sea water conductivity interface. This error model is used alone, or in combination with ranging system and altimeter error models (for the Variable Geometry configuration) to estimate buoy position-fix accuracy. A summary comparison of the three candidate BPAS configurations is contained in Table 1.4-1. The accuracy estimates presented in Table 1.4-1 are based on a selected subset of buoys in Boston Harbor, a differential Loran-C pattern monitor at Boston Light (a fixed aid), and certain assumptions regarding helicopter flight pattern and fix-taking strategy (Chapter 3).

Accuracy of the TD Transmission configuration is highly sensitive to buoy-to-pattern monitor separation. Estimated buoy position-fix errors are 10 to 30 m rms for a buoy-to-pattern monitor separation less than 11 km (the Loran-C error model results predict a maximum position error increase of 2.6 m per km of separation).* An improvement in TD Transmission accuracy can be achieved by deploying multiple pattern monitors so as to reduce the maximum buoy-to-monitor separation. However, a buoy-to-monitor separation less than 3 km is required to reduce the position error to less than 10 m rms. An alternative approach to reduce TD Transmission buoy position errors is to use data from multiple pattern monitors in a scheme to calibrate the Loran-C errors at the time of each audit. This scheme would permit accuracy improvement with a reasonable number of pattern monitors. Although detailed analyses of the calibration approach were beyond the scope of the present study, it is expected that significant improvement could be achieved with as few as three pattern monitors.

The TD Transmission BPAS configuration is very sensitive to Loran-C geometry. Buoy position fix errors are scaled by the Geometric Dilution of Precision (GDOP)--e.g., the position errors for San Francisco Harbor are approximately 4 times the position errors for Boston Harbor. However, in those locations where GDOP is poor the addition of more pattern monitors can reduce the buoy position errors to within acceptable limits. The Variable Geometry

---

*The reader is cautioned that this is a theoretical result based on "worst case" assumptions and should be interpreted accordingly.

position error accuracy is significantly less sensitive to Loran-C geometry Furthermore, the sensitivity can be reduced by taking additional fixes and/or constraining the helicopter trajectory.

Position errors for the Pulse Retransmission configuration are expected to be greater than for TD Transmission due to the adverse effect of Loran-C pulse modulation/demodulation on phase-tracking accuracy. However, detailed analyses of the modulation/demodulation process were not performed during this study because of the clear disadvantages of the Pulse Retransmission configuration with respect to cost and technical risk. As a result, a decision was made by the U.S. Coast Guard at an interim project briefing on 31 July 1979 to discontinue study of the Pulse Retransmission configuration.

Buoy position-fix errors for the Variable Geometry BPAS configuration can be reduced to less than 10 m without unduly constraining the helicopter flight pattern and Loran/ranging fix-taking strategies. Accuracy of the Variable Geometry configuration is less sensitive to buoy-to-pattern monitor separation than is the TD Transmission configuration (the maximum rate of increase is 0.8 m error per km of separation). Sensitivity can be further reduced by placing minor restrictions on the helicopter flight pattern or increasing the number of Loran/ranging fixes. It is important to recognize that the Variable Geometry BPAS configuration accuracy is not influenced by helicopter accelerations in the same manner as is a Loran-C airborne navigation system (e.g., see Ref. 28). This results because the phase-tracking loops in the Loran-C receiver for the Variable Geometry application are assumed to be designed to minimize acceleration-induced errors at the expense of increased measurement noise. Increased measurement noise can be tolerated in the BPAS application, in contrast to the airborne navigation application, because of the redundant information provided by ranging.

1.5 CONCLUSIONS AND RECOMMENDATIONS

Results of analyses of accuracy, cost, complexity, and technical risk presented in this report have demonstrated the feasibility of an electronic Buoy Position Auditing System based on differential Loran-C. The TD Transmission and Variable Geometry BPAS configurations are both feasible. The TD Transmission BPAS configuration exhibits less than half the estimated cost per buoy unit than

2. SYSTEM COMPONENT DESIGN AND COST ANALYSIS

2.1 INTRODUCTION

This section presents the system component design and cost analysis for all buoy position location schemes under consideration. In evaluating both systems, the following conditions were assumed:

- A maximum telemetry range of 40 km
- The availability of a wideband telemetry channel assignment at 1500 MHz
- The availability of a narrow band telemetry link assignment at 150 MHz
- The availability of a narrow band command and control telemetry link at 150 MHz
- The Loran-C signal environment listed in Table 2.1-1.

The specification and availability of the major system components along with component costs were developed following discussions with various manufacturers. The costs assumed for the telemetry equipment was extrapolated from costs currently being paid by various government agencies for similar equipment procured under competitive bid. In cases where exemplary equipment was identified, data sheets were obtained and included in Appendix G to give the reader an idea of off-the-shelf equipment that could be applied to an experiment.

The costing procedure used for the Loran-C equipment requires special comments. A large number of automatic Loran-C receivers designed for commercial marine applications are presently available. These vary in price from approximately $1700 to $3000. Because of the commercial retailing and distribution activity of the manufacturers, they are reluctant to talk about proposed competitive bid pricing for modifications of their standard equipment in reasonably large volume. For this reason, the dollars listed here were determined after:

- o Examining the dealer retail price for the equipment and taking into account normal dealer markups and manufacturer warranty provisions

- o Examining the physical equipment itself and estimating the dollars required to assemble that level of equipment complexity.

An exception to this is the Pulse Retransmission buoy direct/derived pulse processor. In this case, a company presently not manufacturing equipment for the Loran-C market had recently completed a design and pricing exercise for the analog portion of a Loran-C receiver, which they were willing to disclose.

A final comment is necessary regarding the system parameters used in the component design for cost analysis and tradeoff purposes. Transmission powers, telemetry bandwidths, frequencies and digital message formats are all preliminary and do not represent final system design values, but are felt to be typical and suitable for the purposes intended.

2.2 TD TRANSMISSION SYSTEM

2.2.1 TD Transmission Buoy

A block diagram of TD Transmission buoy electronics is shown in Figure 2.2-1. A common antenna is assumed for the reception of the LF Loran-C signals, the VHF command signals and the transmission of the digital Loran-C data. The use of a single antenna for all these functions was assumed for two reasons:

- o first, the space available for mounting antennas on the buoy is limited, therefore the use of a single antenna will simplify the mechanical installation

- o second, placed in such close proximity, problems of interference between the various elements (e.g. jamming of the command receiver by the VHF transmitter or pattern alteration) must be considered even if multiple antennas are used. By employing a single antenna and a properly designed triplexer, these problems can be solved during the equipment design phase, reducing the potential for electronic problems at the time of installation.

The received Loran-C signals are directed to a Loran-C monitor receiver. This receiver is similar in design concept to an automatic Loran-C receiver, but differs in that:

- The front end of the receiver and the resolution in the timing logic have been increased to provide additional accuracy and resolution of measurement

- There is no need for front panel display and control electronics.

The Loran-C monitor receiver produces information regarding the time differences between the various received Loran-C stations, the envelope-to-cycle differences for each station, the signal quality for each station and the Master station/receiver oscillator offset. It is assumed that the receiver design selected will be capable of tracking all received Loran-C signals in a given operating area. Therefore, provisions will be made in the digital message for the retransmission of data from up to five stations (Master plus 4 Secondaries). It is further assumed that the Loran-C receiver will be based on microprocessor technology and therefore will be capable of integrating buoy identification data with the Loran-C data. The output of the Loran-C monitor receiver is a formatted message ready for modulation on a narrowband FM VHF transmitter.

The operation of the TD Transmission buoy electronics is controlled by a VHF command receiver. Upon receipt of a suitable coded command from the base station, the command receiver initiates a power control sequence. This sequence allows time for the automatic lockup and settling of the Loran-C monitor receiver, followed by the transmission of the digitized Loran-C and buoy identification data.

A typical TD Transmission buoy message is shown in Table 2.2-1. A total transmission time of approximately 700 msec/buoy is projected, of which 300 msec is 'dead' time provided for link capture and data demodulator synchronization. The message provides for the retransmission of 16 bits of identification data and complete time difference and signal quality data from the stations. In addition, a bit sequence equal in length to the message is provided for error correction/detection bits.

The TD Transmission data can be transmitted back to the base station using a narrow band VHF communication channel at a data transmission rate of 1200 bits/second. A typical telemetry budget for such a channel is shown in Table 2.2-2. Assuming a transmitter power output of 1 Watt, and a buoy antenna gain of 2dB, a total received signal strength of -93dBm is calculated. The major received noise sources are thermal noise and man-made noise. The available signal and noise combine to yield an IF signal-to-noise ratio of 31dB and a post-demodulation signal-to-noise ratio of 43dB assuring proper data demodulation even under conditions of severe multipath fading.

In order to establish the buoy power requirements, it is necessary to assume an operating cycle for the system. In the standby state, only the buoy command receiver is powered. At the start of an audit, the Loran-C receiver is turned on. The time required for lockup varies with receiver design and signal quality, however times ranging from 4-6 minutes are typical. Following lockup, it is further necessary for the receiver to smooth or integrate the time difference data to provide a single output value representing a statistical average over a period of several minutes. These two steps require a total time of 8 minutes from system turn on to the availability of data. Once smoothed time difference data is computed, the receiver is put in a standby mode in which only the time difference and signal quality data are kept in active storage pending readout of the data by the base station. During the receiver acquisition and settling time, there is no need for a buoy to transmit to the base station, and hence no competition for the telemetry link. Therefore, all buoys within radio range can be commanded to obtain Loran-C data simultaneously.

A typical TD Transmission operating cycle is shown in Figure 2.2-2. The command transmitter issues an ALL call which is received and processed by all buoys in radio range. This causes each buoy to power up the onboard Loran-C receiver.

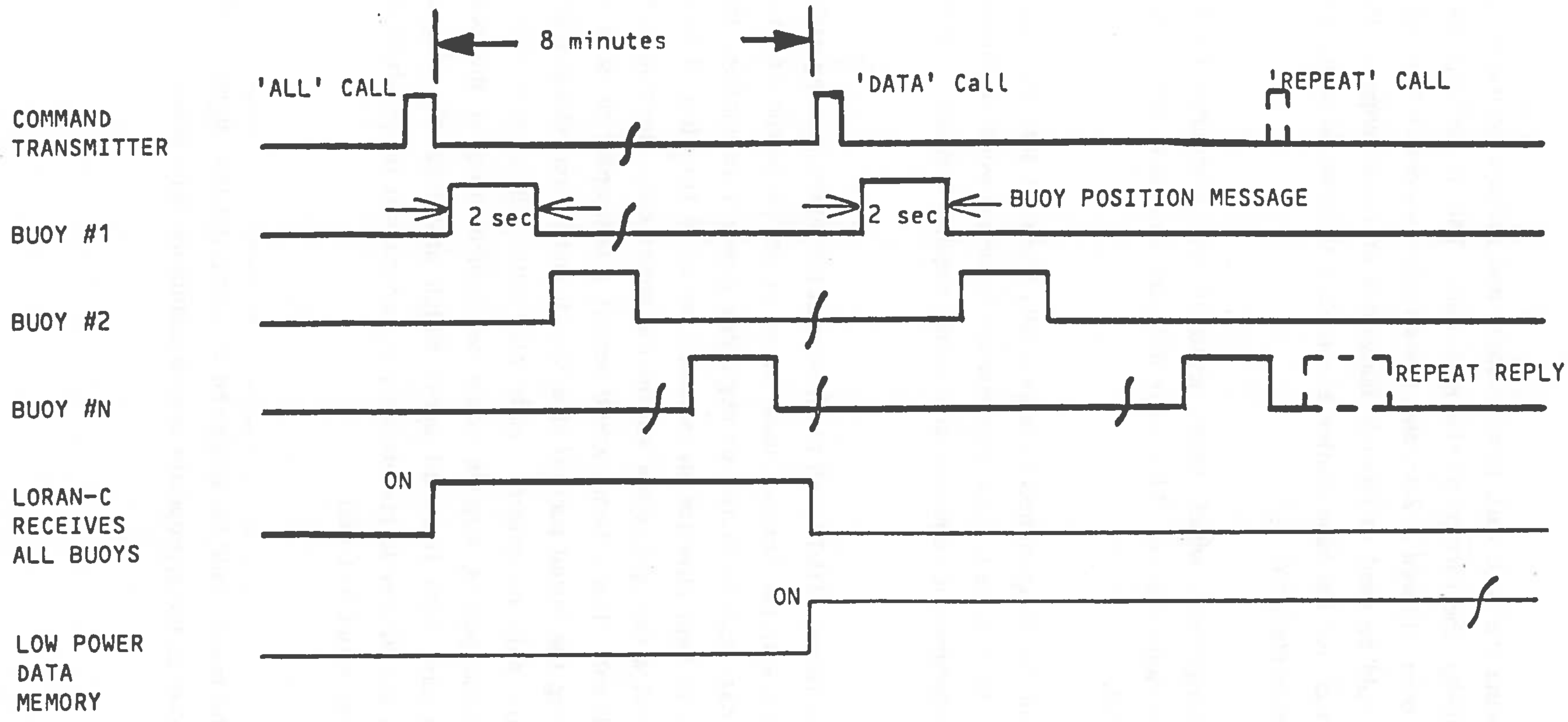

Figure 2.2-2 A Typical TD Transmission Operating Cycle

A buoy power budget for a TD Transmission scheme employing the operating cycle depicted in Figure 2.2-2 is shown in Table 2.2-3. The power consumptions listed for the command receiver, the Loran-C receiver and the transmitter are taken from devices presently available or under development. The major power consumer on the buoy is the command receiver. Although its current consumption is quite low, 15 mA, it is operated continuously. One obvious technique of reducing power consumption from the command receiver is to employ a daylight photo switch. This will reduce the power by approximately 50% averaged over the year. Other schemes could employ micropower clocking schemes which would only enable the command receiver during specific periods of the day. The Loran-C receiver requires the largest amount of operational power, 10 Watts, however its relatively short duty cycle of 8 minutes keeps its total contribution to the power budget low. The power requirements for the control logic and the transmitter are negligible. The control logic power is minimized through the use of CMOS logic, while the transmitter power requirement reflects its very low transmission duty cycle. Average ampere-hours/day numbers are presented for both a 1 read-cycle/day and a 1 read-cycle/week situation. In addition, these numbers are computed assuming both the use of a plot switch and a continuous operating receiver. The worst case power consumption is .5 ampere-hours/day for daily readings; and the minimum, with photo switch and 1 read-cycle/week is .225 ampere hours/day average.

2.2.2 TD Transmission Base Station

The functions required of the TD Transmission base station are:

- o The generation and transmission of audit control signals
- o The reception and demodulation of buoy data
- o The recording of data for reduction to position.

A block diagram of the TD Transmission base station electronics is shown in Figure 2.2-3. The audit control electronics generate audit signals. The process starts with the issue of a CALL to an individual buoy or an ALL call to the field of buoys. This digital message is transmitted to the buoys by the transmitter. Data from the buoys are received by a narrow band VHF FM receiver.

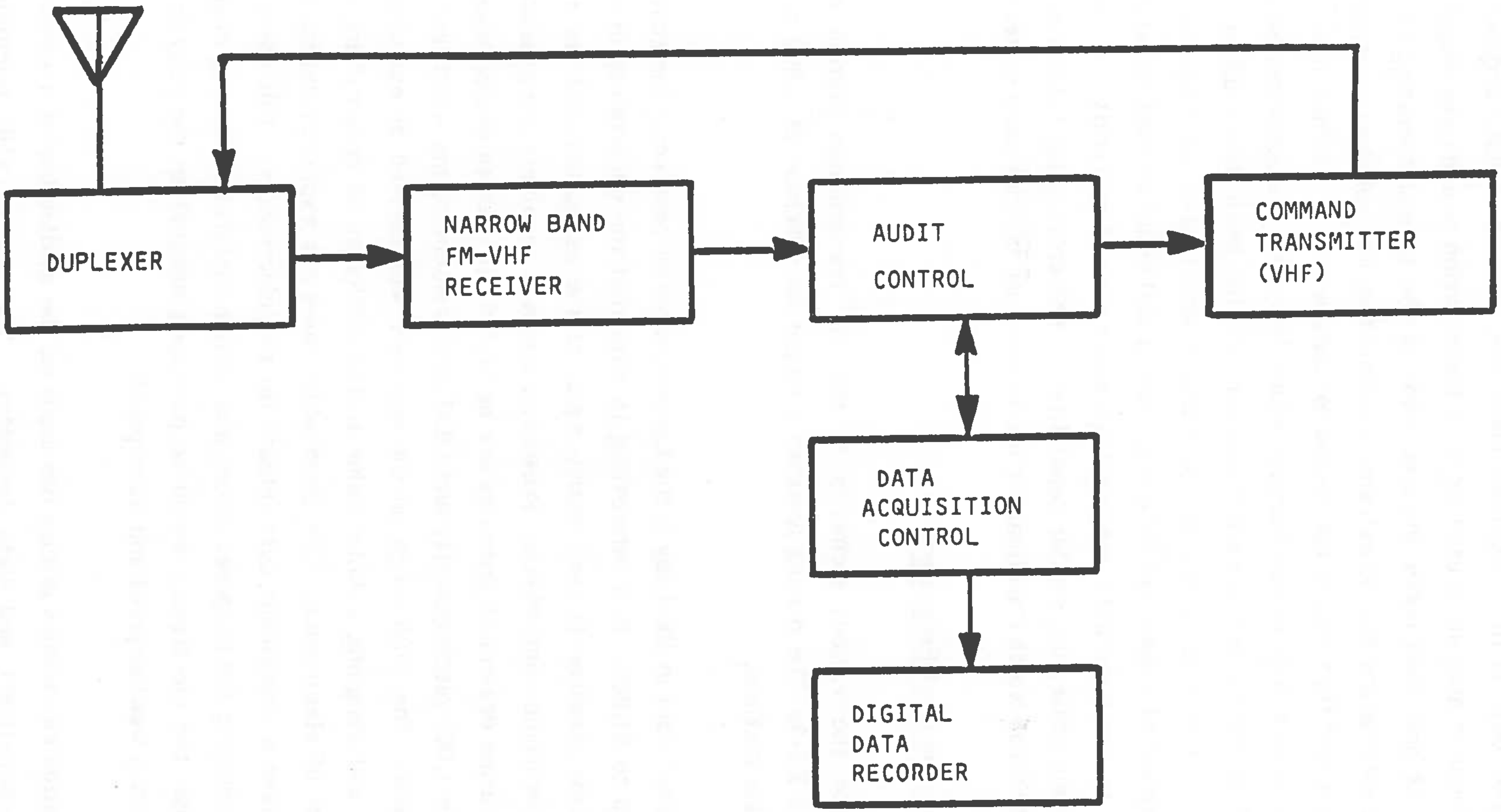

Figure 2.2-3 TD Transmission - Base Station Electronics

BUOY ELECTRONICS (1000-pc Lot)	
ANTENNA, COUPLER, DUPLEXER	$ 40
LORAN-C MONITOR RECEIVER	$ 700 - $1,000
COMMAND RECEIVER	$ 70
POWER CONTROLLER	$ 10
TRANSMITTER	$ 90
SYSTEM INTEGRATION & TESTING	$ 150
TOTAL ESTIMATED COSTING......	$1,060 - $1,360

BASE STATION (10-pc Lot)	
VHF RECEIVER/DEMODULATOR	$2,000
DATA RECORDER	$1,000
COMMAND TRANSMITTER	$1,000
AUDIT & DATA ACQUISITION CONTROL UNIT	$2,000
SYSTEM INTEGRATION & TESTING	$1,000
TOTAL ESTIMATED COSTING......	$7,000

*Assumes Specification and Initial Development during Experimental Phases.

Does not include non-recurring post-experiment costs.

Does not include system documentation beyond that provided with standard commercial equipment.

Table 2.2-4 TD Transmission Estimated Costing*

- Preservation of the pulse envelope fidelity to assure accurate cycle selection at the base station

- Preservation of Loran-C pulse fidelity at the tracking point to assure position accuracy

- The need to provide a telemetry signal-to-noise ratio which does not degrade the overall quality of the Loran-C signal

- The requirement to preprocess the Loran-C signal to assure that the dynamic range of the signal does not exceed the capability of the telemetry link.

A block diagram of the Pulse Retransmission buoy electronics is shown in Figure 2.3-1. As in the case of the TD Transmission electronics, a common antenna is used for both telemetry transmission and reception as well as Loran-C signal reception.

The Loran-C signals are processed by a Loran-C analog pulse amplifier/processor. Several variations of this amplifier/processor have been considered and are discussed in Section 2.3.2. For the present, it is only necessary to assume that the processor prepares the signals for transmission back to the base station in such a manner that they may be processed at the base station to obtain the required time difference information. The output of the amplifier/processor and data encoder are directed by a wideband telemetry transmitter. Due to the fidelity with which the pulse information is to be retransmitted, a 1 MHz bandwidth has been assumed for the modulated signal.* A transmitter power of 5 Watts has been selected for the purposes of this analysis.

---

*While slightly narrower bandwidths may be possible, they are not felt to alter substantially the proposed system design presented.

The operation of the buoy electronics is controlled by a VHF command receiver. A system command simply turns the buoy on and for selected pulse processing techniques, selects a processing mode. Note that because the Pulse Retransmission approach does not reduce the data to storable time difference, sequencing of the power, first to the Loran-C amplifier/processor and then to the transmitter, is not possible.

Table 2.3-1 shows the telemetry budget for the Pulse Retransmission system. A telemetry frequency of 1500 MHz has been assumed consistent with the desire to obtain authorization for a 1 MHz bandwidth. Despite the increase in transmitter power from 1 Watt to 5 Watts, the IF signal-to-noise ratio is only 12 dB compared to 31 dB for the TD Transmission system. This reduction is attributable to the increased path loss at 1500 MHz and the increased noise due to the 1 MHz IF bandwidth. The 12 dB IF signal to noise ratio yields an anticipated dynamic range of 32 dB from the point at which a pulse will be contaminated by -10 dB of telemetry noise to a signal level which provides the maximum telemetry carrier frequency deviation. The anticipated 32 dB dynamic range is 32 dB less than the 64 dB range required to transmit the anticipated Loran-C signals. This implies that it is not possible to simply amplify the received Loran-C pulses and use them to modulate the transmitter directly and therefore further pulse processing is required.

At this point the reader can assess the reasonableness of the 5 Watt power level selected. First, 5 Watts is a convenient power level to produce with combinations of power transistor devices available in this frequency range. Secondly, to increase the projected dynamic range by 10 dB would require a 10 dB increase in transmitter power, or a transmitter output of 50 Watts. Assuming that the transmitter efficiency stays relatively constant as the power is increased, this 10-fold increase in power would require increases in the prime power well beyond the 1 ampere-hour/day specified, and the cost of such a transmitter would be an order of magnitude more than a 5 Watt unit.

POST-DEMODULATION SNR		
INPUT SNR (1 MHz BW)	12 dB	
FM IMPROVEMENT	24 dB	$-3\left[\frac{BW}{2\ BW_0}\right]^3$
OUTPUT SNR AT FULL DEVIATION	36 dB	
SNR IMPROVEMENT FOR 85-115 kHz FILTER	6 dB	$10\ Log_{10}\left[1-\left(\frac{fi}{fn}\right)^3\right]$
DESIRED TELEMETRY NOISE TO LORAN-C SIGNAL RATIO	-10 dB	
DYNAMIC RANGE........................	32 dB	

Table 2.3-1 Pulse Retransmission - Assumed Telemetry Budget at 1500 MHz (continued)

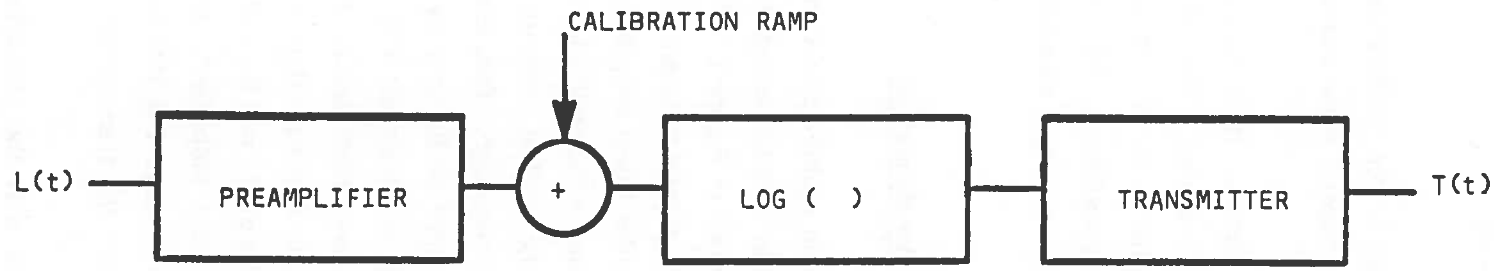

Figure 2.3-2   Pulse Retransmission - Pulse Compression

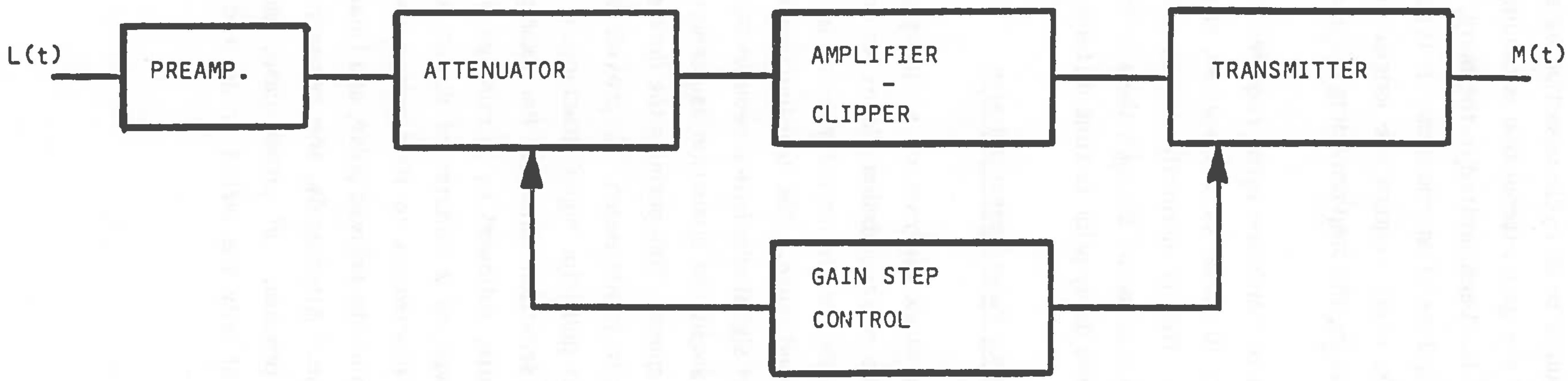

Figure 2.3-3 Pulse Retransmission - Stepped Gain Amplification

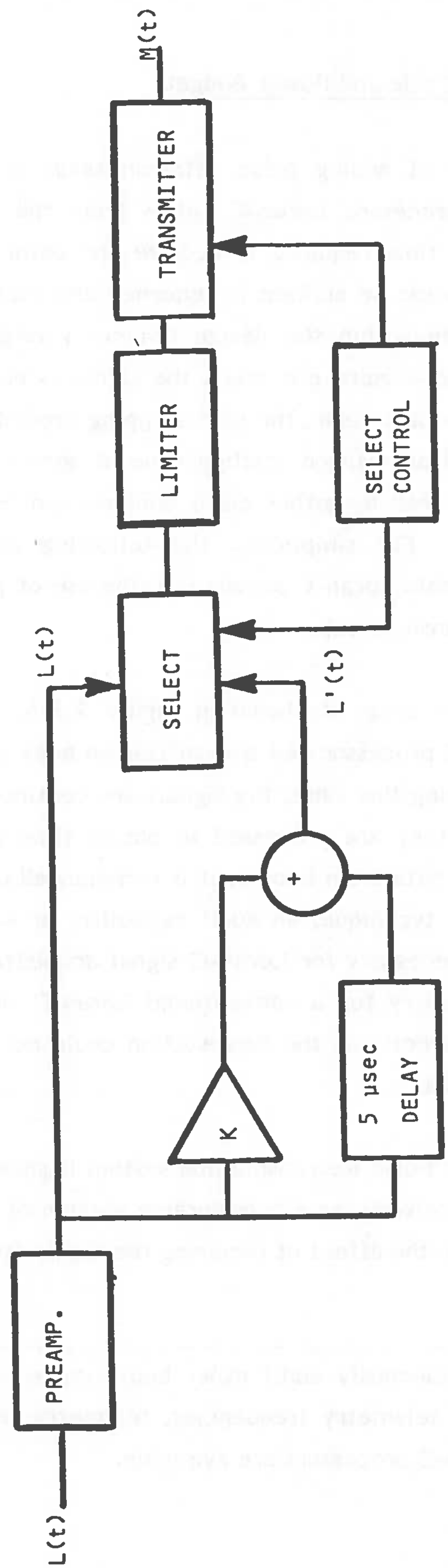

Figure 2.3-4 Pulse Retransmission - Direct and Derived

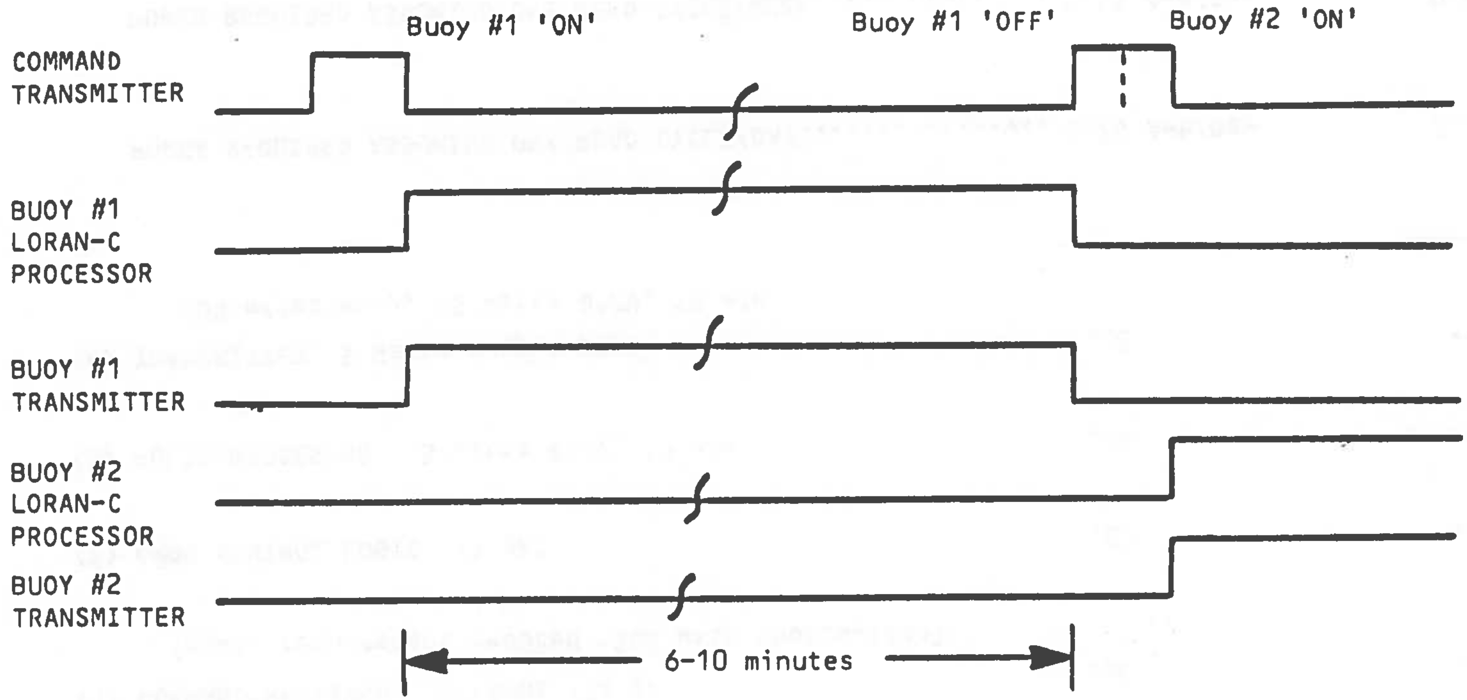

Figure 2.3-5 Pulse Retransmission - Typical Operating Cycle

processor to remain on for the duration of the audit period. The transmitter also draws additional power due to the decreased efficiency of transmitters operating at 1500 MHz. In all cases, both 1 read-cycle/day and 1 read-cycle/week, either with or without a command receiver photo-switch, the power is below the required maximum of 1 ampere-hour/day, with the numbers generally running higher than the equivalent cases for the TD Transmission electronics.

2.3.4 Pulse Retransmission Base Station

The Pulse Retransmission base station is much more complicated than the TD Transmission base station. This is due to the requirement for a special purpose Loran-C processor and the desirability of aiding that processor with local Loran-C signals. Both base stations provide the necessary functions of generating and transmitting audit control signals as well as recording the Loran-C time difference data for reduction to buoy position. In addition to these functions, the Pulse Retransmission base station must acquire, perform cycle selection and track the analog pulses transmitted from the buoy. It is also necessary that the special purpose Loran-C processor be capable of monitoring and editing out telemetry fades to prevent false acquistion and/or poor data due to the presence of temporarily noisy conditions. Further, the processor must compensate for helicopter flight dynamics.* A block diagram of the base station is shown in Figure 2.3-6. Here again a common antenna is proposed for the command transmitter, buoy telemetry receiver and base station Loran-C reception. The practicality of using a single antenna for this application on a helicopter will have to be explored further; however, the desirability of only a single antenna is recognized. The buoy telemetry signal is received by an L-band receiver and the output directed to both the audit control electronics for determination of buoy identification and the special purpose Loran-C processor. The output of this special purpose processor is

---

*The velocity of the helicopter is impressed on both the locally received Loran-C signals (due to helicopter-to-Loran-C station Doppler) and on the buoy signals (due to Doppler imposed on the helicopter-to-buoy telemetry path).

Loran-C time difference data, which is recorded on a digital data recorder for reduction to position. The audit control electronics keep track of the time for which a given buoy has been audited and controls the command transmitter which can selectively turn on and off the various buoys being audited.

2.3.5 Estimated Cost of Pulse Retransmission System

Two buoy electronic configurations have been estimated, a pulse-only scheme, assuming a pulse compressor, and a unit which retransmits both the direct and derived pulse. The major expense for both systems is the transmitter. This high cost is due to the necessity of providing the 5 Watt crystal-controlled transmitter at 1500 MHz. The reduction in transmitter price for the direct/derived pulse retransmitter is attibuted to a decrease in the required telemetry link dynamic range. All other items are assumed to be equal, except for the command receiver, where a small additional expense has been allowed to permit the base station to command switching between the direct and derived pulse (Table 2.3-3). These costs are based on a 1000-piece single lot purchase of the buoy electronics and the procurement of 10 base stations.

The base station estimates reflect the increased cost anticipated for a wideband L-band receiver, however this is overshadowed by the cost estimate for the special purpose Loran-C processor. Involved in this cost estimate are:

- o The special nature of the unit (i.e. the design would most likely not find application in other types of systems)
- o The device must be capable of airborne operation and be capable of processing both local and buoy Loran-C signals.

2.4 VARIABLE GEOMETRY TECHNIQUES

Buoy location can also be determined by ranging techniques. The measurement of range or distance from a buoy to a known location establishes the buoy on a fixed line of position which is a circle centered on the known location.

Several such measurements from different locations can then fix the buoy position. In principle, a field of buoys about a harbor could be monitored in this way from a network of shore stations. However, in practice multiple sites over a large area will be required to optimize the geometry; such a network will be large, complex and require substantial amounts of real estate.

An alternative technique is to make the range measurements from a moving platform such as a helicopter. The motion of the helicopter generates multiple position lines from a series of range measurements; this is known as a "variable geometry" system. In order to locate the helicopter precisely, differential Loran-C measurements are obtained by making Loran-C TD measurements aboard the helicopter and comparing them, post facto, with those made by a network of pattern monitors. In addition the accuracy of the knowledge of the helicopter's position as derived from the differential Loran-C, can be improved by use of the over-determined solution of buoy position which results from multiple range measurements to multiple buoys. This technique is incorporated into the variable geometry measurements described in this report.

2.4.1 Range Measurement Techniques

Two basically different range measurement techniques are under consideration. They are:

1. Pulse Ranging - In this technique the helicopter emits a stream of pulses of RF energy. These are received by the buoy, and retransmitted to the helicopter. The helicopter receives the return pulse and measures the elapsed time between pulse transmission and pulse reception. An onboard computer multiplies this measurement by the speed of light to calculate the round-trip range.

2. CW Ranging - This technique uses a continuous RF carrier rather than a stream of pulses. The carrier is modulated by a suitable waveform; the helicopter measures the round trip phase shift of this wave form and thus determines the round trip time delay. Since this system allows for both low average and low peak power requirements on the buoy, it can also be used in a one-way range-measurement where the ranging signal

amp-hr per audit for the command receiver* yields a total drain of 24 amp-hr. The battery drain can be reduced by transponder innovations and/or a different interrogation schedule. For example, data could be collected for only a few segments of the flight pattern and the transponders deactivated between segments.

2.4.3 CW Ranging

The primary difference between CW Ranging and Pulse Ranging lies in the ratio of peak to average RF power. In a CW Ranging system, the peak RF power is equal to the average power; a Pulse Ranging system typically has peak/average ratios of 1000 or greater. A Pulse Ranging system operates by detection of the time of arrival of the leading edge of the pulse. CW Ranging on the other hand, impresses a distinctive wave form on the carrier by phase or frequency modulation. Two wave forms have been investigated in this report. They are pseudo-random codes (PRN Codes), and an ensemble of CW tones known as Stiffler codes (Refs. 35 and 36).

2.4.3.1 PRN Codes

Pseudo-Random Noise (PRN) codes belong to a family of two-level or binary codes. These codes, while completely deterministic, possess certain unique properties which cause them to be extremely recognizable when perturbed or masked by noise. The most important of these is the autocorrelation function. The autocorrelation function of a signal represents its "signature" in time, i.e. the mark, or determining factor, which when comparing two signals tells whether the two are identical or different. Ideally, an autocorrelation function--that is, the correlation function between a received signal, and a synthesized replica of the transmitted signal would have a uniform low value when the two differ, and a single sharp peak when the two are identical. In particular, binary correlation is defined as follows:

---

*Assuming a command receiver drain of .36 amp-hr/day for seven days.

synchronism. Obviously to acquire a sequence it is necessary to observe and compare all possible states, or bit positions, for positive identification. A sequence of length P, may require P trials, or correlations, before acquisition is complete. After acquisition, range is determined by measurement of the time shift between transmitted and received codes.

The performance of a typical design is analyzed in Appendix I.

2.4.3.2 Stiffler Codes

A promising waveform for the BPAS application is presented and analyzed in Ref. 36. This waveform can be viewed as a form of tone ranging, which determines range by measurement of the phase shift of a composite set of tones (sine-waves) modulated on an RF carrier (Refs. 35, 38 & 39). The tones are coherent in phase and commensurate in frequency; this is usually achieved by digital division from a common master oscillator. The specific implementation under consideration uses square waves which are submultiples of two from a highest frequency tone of 100 KHz. The implementation details and performance calculations are contained in Appendix I.

It is apparent from the calculations in Appendices H and I that CW ranging systems are strong contenders, in that the measurement standard deviation due to random noise is substantially less than 10 meters rms. The attainment of such a high level of precision is, in practise, extremely difficult due to instrumental biases in the measurement process. However, these are areas under the control of the designer. Careful design will ensure correct system performance.

2.4.4 One-Way Ranging

All Variable Geometry systems considered so far have been two-way techniques; that is, the ranging signal emanates from the same station that makes the final measurement - the buoy merely transponds the ranging signal. In so doing, however, a substantial uncertainty is inserted into the measurement process - not only does the buoy transponder become a major source of noise error, but bias errors due to phase delay changes in the transponder (due to temperature and component drift) also increase the total error. These errors are primarily in the

Now form time differences $T_1' - T_2'$ and $T_1' - T_3'$

$$(2.4\text{-}2) - (2.4\text{-}3) = T_1' - T_2' = (T_1 + \alpha) - (T_2 + \beta) \qquad (2.4\text{-}5)$$

$$\text{and } T_1' - T_3' = (T_1 + \alpha) - (T_3 + \gamma) \qquad (2.4\text{-}6)$$

Here the assumption is that the timing error Δt is (to a first approximation) common to all three measurements, i.e., the oscillator does not change frequency (drift) during the time period which contains all three measurements. These measurements then locate the buoy on a line of position defined by a hyperbola whose foci are at positions 1 and 2. Position 3 then defines a second hyperbola whose intersection with the first one determines the buoy's position.

a. Oscillator Stability Requirements

The ranging signal is set in time by a clock, whose time stability is determined by a highly stable oscillator. See Figure 2.4-2 below, for a typical design.

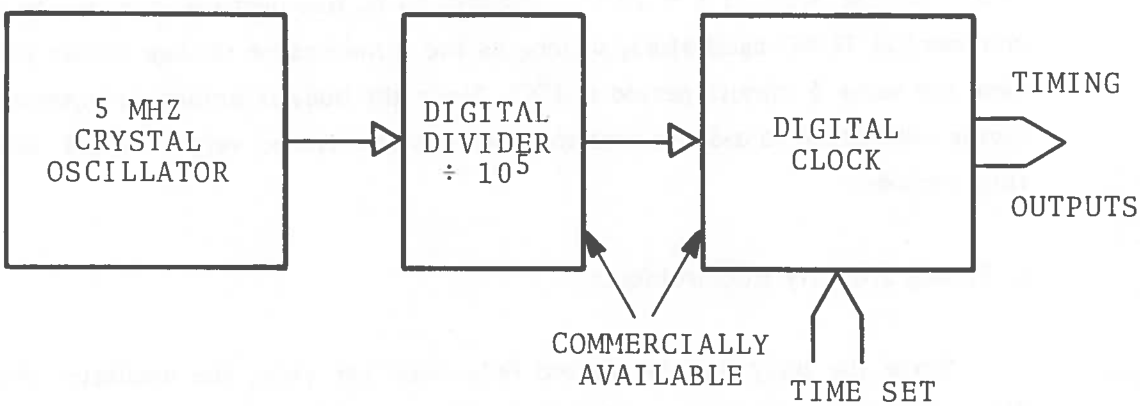

Figure 2.4-2 Typical Digital Clock

If the oscillator drift results in a timing error change of 5 nanoseconds over the course of one buoy position measurement, this will add 5 feet of error to the buoy position (not including GDOP). This timing error analysis applies during the time interval required to do a buoy position fix. Typically, the helicopter will fly at 80 - 120 knots, which is 1.3 - 2.0 miles per minute of flight time. If the buoy is 10 - 20 miles to one side of the flight path, 5 minutes will result in 7 - 10 miles of

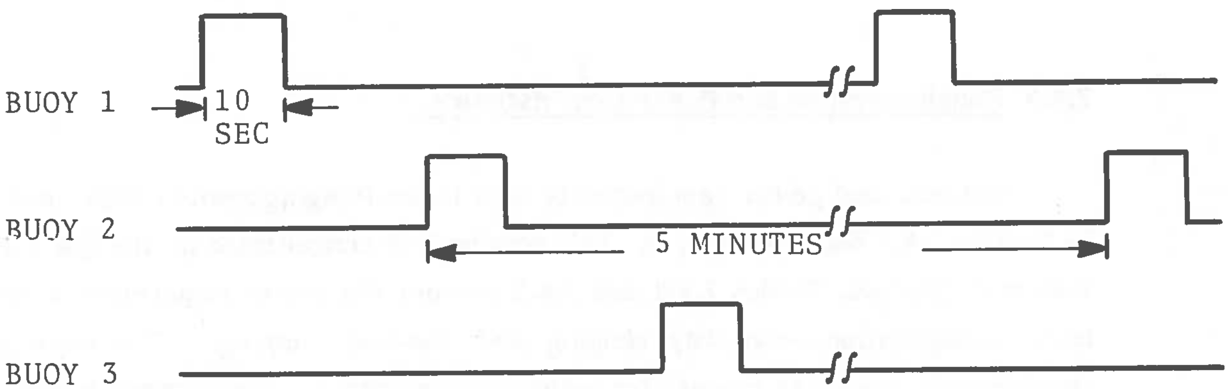

Approximately 5 Minutes

Figure 2.4-4 Typical Buoy Transmission Sequence

In this simplified description, each buoy would transmit a total of 3 times, at 5 minute intervals. Each transmission would provide a burst of 10 seconds of the selected ranging signal, encoded with data for buoy I.D. The helicopter would make three range measurements, and process them to form two sets of range differences. The buoy would then be located at the intersection of the two hyperbolas defined by the two sets of range difference measurements.

In practice, operational and geometrical considerations, as discussed in Section 3.0, would result in multiple measurements for each buoy. This section does not present a complete operational scenario; rather it demonstrates by simple calculation, the feasibility of the one-way ranging approach. Such an approach is very attractive for the following reasons:

(1) The buoy electronics package is greatly simplified, thus resulting in a lower cost operational package. Neither the command receiver, its associated control logic, nor the ranging receiver are required by this system.

(2) A significant (and presently unquantified) system error source, namely bias errors in the buoy transponder receiver, has been removed from the system.

TABLE 2.4-1

CW RANGING - BUOY POWER BUDGET (TWO-WAY)

	Ampere-Hours
COMMAND RECEIVER	
(0.015 Amp @ 12V) - ON 12 HOURS/DAY AVERAGE	0.180
SYSTEM CONTROL (CMOS LOGIC - 1 MA)	0.024
TRANSPONDER (5 WATT TRANSMITTER, 20% EFFICIENCY)	
RECEIVER POWER DRAIN - 50MA. TRANSMITTER POWER DRAIN - 2.08 AMPERES TOTAL TRANSPONDER DRAIN - 2.13 AMPERES 15 SECONDS PER MEASUREMENT, 6 MEASUREMENTS/AUDIT	0.053
FOR ONE AUDIT/DAY -	0.26 A/H per day
FOR ONE AUDIT/WEEK -	0.21 A/H per day

The cost estimates, particularly Tables 2.4-3 and 2.4-4, showing cost estimates for the buoy electronics in production quantities, illustrate clearly one basic fact. That is that a two-way ranging system which is tailored to solving the BPAS problem, will be about 5 times as expensive (per buoy) as the TD Transmission system. The primary expense is the transponder which is a special design for this program and has no obvious other function. The cost is primarily due to the receiver requirements--namely, that over the dynamic range of signal level and frequency change and over an unattended operational period of one year, the phase shift (group time delay) must remain constant to within a few nanoseconds. The only easy way to accomplish this is to design the receive portion of the transponder to have a bandwidth of about 40 MHz--however, this will result in a receiver noise power level greater than the signal power. In this event, the transponder will saturate on noise power, suppress the signal energy and the performance will be severely degraded (potentially) by any interference and/or intermodulation problems. Therefore, the design bandwidth can be only slightly wider than the signal RF bandwidth of about 4 MHz, the design effort (and maintenance effort) then becomes a serious problem. From these points of view, two-way CW ranging systems, requiring the development of a dedicated transponder, seem to represent a poor choice, both from system cost and technical risk viewpoints.

However, one-way ranging seems to offer significantly more potential. The design of the electronics package is substantially simpler, as it consists of an oscillator, clock, ranging signal generator and transmitter. The antenna needs to deal with only one signal, thus eliminating the requirement for a diplexer and/or signal combiner. The result of this simplification is a substantially lower cost for the buoy electronics. (Costs for the one-way ranging base station electronics is presented in Table 2.4-5). The overall comparison, however, must note that the helicopter electronics is an order of magnitude more complex for any ranging approach than for TD Transmission. Thus, on balance, TD Transmission appears to be the lowest risk <u>and</u> lowest <u>overall</u> cost approach.

TABLE 2.4-4

BUOY ELECTRONICS - UNIT COSTS

ONE-WAY RANGING - PURCHASE 1000 UNITS

OSCILLATOR	$100.00
TIMING SUBSYSTEM & CONTROL LOGIC	25.00
TONE GENERATOR	50.00
TRANSMITTER	1000.00
ANTENNA	25.00
PACKAGE & TEST	150.00
TOTAL	$1350.00

3. BUOY POSITION AUDITING SYSTEM ERROR ANALYSIS RESULTS

3.1 INTRODUCTION

Error analysis results for the candidate Buoy Position Auditing System (BPAS) configurations, ie., TD Transmission, Pulse Retransmission, and Variable Geometry -- are presented in this chapter. Boston Harbor has been chosen as the specific scenario for the error analyses, since initial experimental verification of the recommended BPAS configuration is proposed to take place there. Seventeen buoys and three fixed aids (lights) which have been selected for consideration are listed in Table 3.1-1 and indicated on a chart of Boston Harbor in Figure 3.1-1*. Loran-C coverage for Boston Harbor is provided by the master/secondary W/secondary X transmitter triad of the Northeast U.S. Loran-C chain (transmitter locations are indicated in Table 3.1-2 and Figure 3.1-2). A detailed analysis of BPAS errors for other U.S. harbors is beyond the scope of the present study. However, BPAS accuracy for a U.S. harbor which exhibits a different Loran-C geometry or expected pattern monitor-to-buoy spacing than Boston Harbor can be estimated using sensitivity analysis results presented herein. The simulation capability developed for this study is general enough to permit more detailed error analyses for other harbors, if required in the future by the U.S. Coast Guard.

The estimates of buoy position error presented in this chapter are based on error models for the candidate BPAS configurations. The error models for the TD Transmission and Variable Geometry configurations are derived in Appendices A and C, respectively, and are summarized in Section 3.2. Error analysis results for the TD Transmission and Variable Geometry configurations, including the sensitivity of errors to operational and error model parameters, are presented in Sections 3.3 and 3.4, respectively. The error analysis results are used to identify the critical hardware design parameters and operational restrictions for each configuration. After initial investigations, the Pulse Retransmission BPAS configuration was eliminated from further consideration because of high cost and technical risk (Chapter 2). Although a detailed analysis of Pulse Retransmission errors has not been conducted during this study, coarse simulations have been performed to analyze the effect of Pulse Retranmission on Loran-C third-cycle identification. The simulations are detailed in Appendix F, and the initial results are presented in Section 3.5. The candidate BPAS configurations are compared on the basis of buoy position-fix accuracy in Section 3.6.

---

*The charts of Boston Harbor presented in this report are computer-produced.

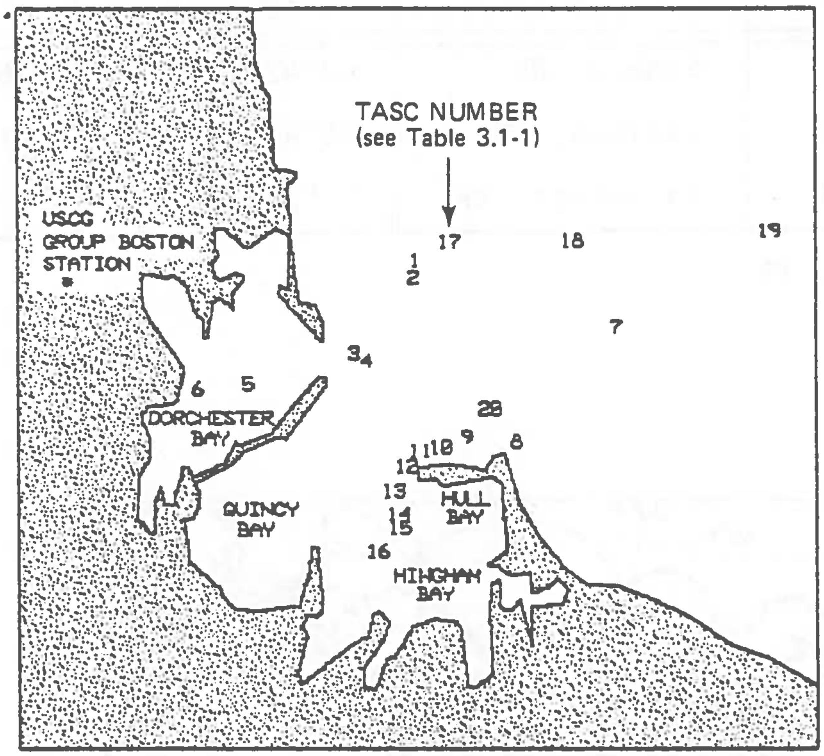

Figure 3.1-1 Locations of Selected Buoys And Fixed Aids in Boston Harbor

3.2 ERROR MODELING SUMMARY

3.2.1 TD Transmission

The candidate BPAS configurations employ differential Loran-C, either alone (for TD Transmission and Pulse Retransmission) or in combination with a microwave ranging system and altimeter (for Variable Geometry). The differential Loran-C error model is discussed below, with specific reference to the TD Transmission configuration. Aspects of the model which differ for the Variable Geometry configuration are discussed in Section 3.2.2.

An adequate data base is not presently available to permit development of an empirical differential Loran-C error model. Differential Loran-C experiments have been performed, such as the eight-week "Time Stability Study" conducted by the U.S. Coast Guard along the shores of Delaware Bay (Ref. 22). However, development of an empirical differential Loran-C error model for the BPAS application would require a minimum of one year of data, collected in various harbors, at an array of sites within each harbor. The alternative to an empirical model is a theoretical model, whereby Loran-C propagation theory is employed to establish upper bounds on differential Loran-C errors. The following attributes of a theoretical error model make it attractive for an initial feasibility study:

- o Applicable assumptions and restrictions can be readily identified and clearly stated
- o Model utility is not necessarily limited to a specific geographic region or time interval.

The differential Loran-C error model developed for this study is a theoretical model.

Loran-C position errors result from atmospheric noise (which corrupts the Loran-C TD measurements) and from propagation approximations (which are made in converting TDs to geodetic position coordinates i.e. latitude and longitude.*

*The TD-to-position transformation is referred to as the "TD grid."

The assumed propagation medium is simpler than may be encountered in reality but it is expected to describe the important features of the actual medium. Classical Loran-C groundwave propagation theory (Ref. 14) and Millington's method (Ref. 15) are applied to relate the transmitter-to-receiver signal propagation delay (travel time) to the parameters which characterize the propagation medium (i.e. refractive index, vertical lapse rate, and conductivity). The strong correlation between surface refractive index and vertical lapse rate (reported in Ref. 16) permits the atmospheric component of the propagation delay to be expressed by a function of surface refractive index, alone. This delay component is approximated by a linear dependence on transmitter-to-receiver range. However, the propagation delay component associated with conductivity (secondary phase delay (SF), including effects of land and sea water) is nonlinear in range, especially near the land/sea water interface. (See also extensive analysis and calculations concerning this effect in Ref. 24). The nonlinear dependence of SF on the range from the coastline to the receiver (along the transmitter-to-receiver path) is illustrated in Figure 3.2-1, where SF has been referenced to SF at the coastline. It is important to realize that the shape of the nonlinearity depends on the conductivity of the land path segment, even though the path between the coastline and the receiver is all sea water. However, the shape does not depend on the length of the land segment, for lengths greater than 2000 km.* For simplicity, it is assumed that SF is linear for those ranges relevant to a particular transmitter and harbor. It is further assumed that the paths for a particular transmitter and harbor are of one of the following types, where R is the coastline-to-receiver range:

Type I : $R < 15$ km

Type II : $15 \text{ km} < R < 200$ km

Type III : $R > 200$ km

The three path types are illustrated in Figure 3.2-2 for a hypothetical harbor. Classification of the path types for an actual harbor may be complicated by an irregular coastline. The slopes of the nonlinear SF curves for the three types of propagation paths are summarized in Table 3.2-1. The slope is termed the "Loran-C scale factor" in this report. Note that the range of scale factor values, corresponding to a particular range of conductivity values, is largest in magnitude for Type I paths and smallest for Type III paths.

---

*The value of SF does depend on land segment length.

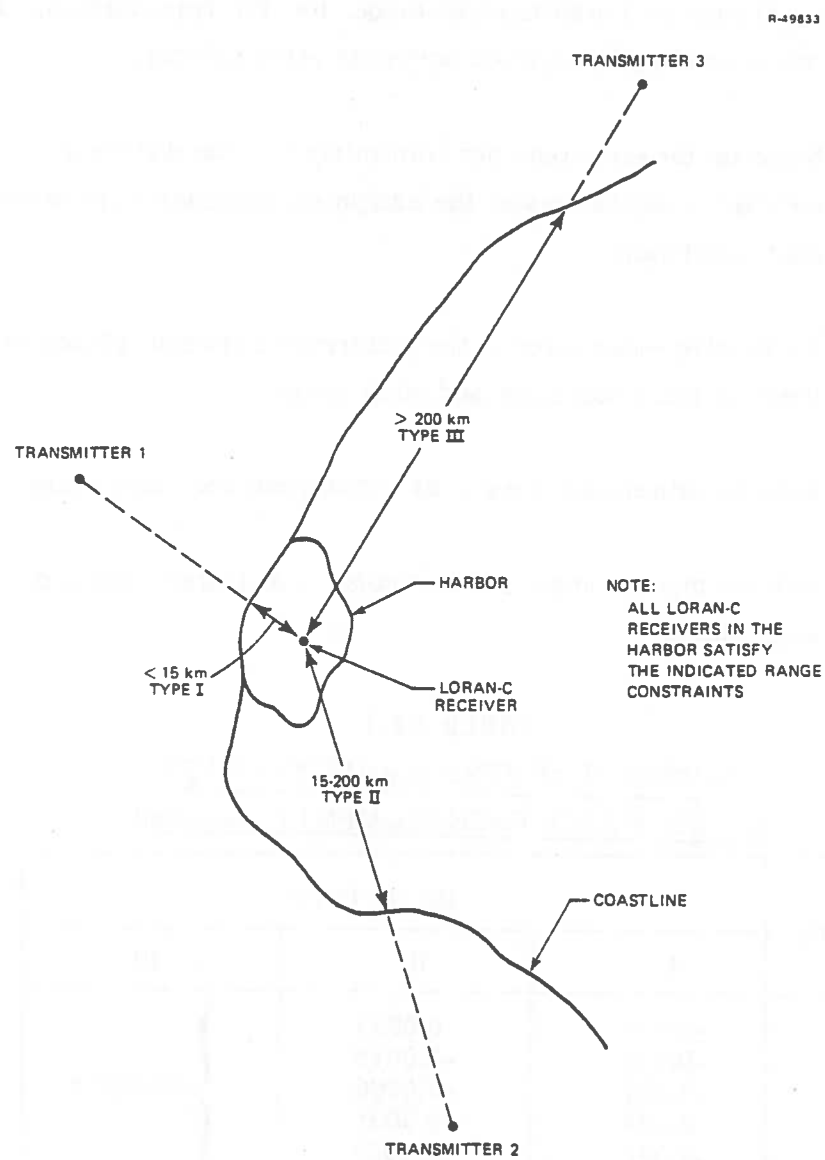

Figure 3.2-2 Definition of Propagation Path Types For A Hypothetical Harbor

The nominal standard deviations assumed for the error sources are derived in Appendix A and are listed in Table 3.2-2. Scale factor error standard deviation is based on the following assumptions:

- o Land conductivity can double between winter and summer (theoretical result from Ref. 11; based on 1-2 m of snow or frozen ground in winter and average ground in summer)
- o Seasonal conductivty variations are characterized by a uniform probability distribution between the extreme values
- o Buoy Loran-C equipment is installed at the time of a conductivity extreme
- o Propagation paths are Type I for all three transmitters.

TABLE 3.2-2

NOMINAL ERROR LEVELS FOR TD TRANSMISSION

ERROR SCALE	VARIABILITY DURING AUDIT	NOMINAL STANDARD DEVIATION
Scale Factor Error	Constant	12×10^{-6} μsec/m
Refractive Index Error	Constant	50×10^{-6}
Buoy Measurement Noise	Random	0.02 μsec
Pattern Monitor Measurement Noise	Random	0.02 μsec

These assumptions are expected to represent a worst case. In particular, note that conductivity would not be expected to double between winter and summer in the Southeast U.S. and West Coast Loran-C chain coverage areas, because winters in these regions are characterized by minimal snow cover. Furthermore, many harbors will have at least one transmitter path which is not monitor to the helicopter, using the TD grid prediction model and the differential Loran-C algorithm presented in Apendix A (Section A.4.2.).

In the absence of TD benchmarks, the differential Loran-C error sources for the Variable Geometry configuration are:

- o Scale Factor error (one per transmitter) -- the difference between the scale factor in the hypothesized model and the actual scale factor at the buoy audit time
- o Refractive index error -- the difference between refractive index in the model at the audit time
- o Helicopter measurement noise -- at the audit time
- o Pattern monitor measurement noise -- at the audit time.

The scale factor and refractive index errors depend on the accuracy of the TD grid prediction model. Note that helicopter and pattern monitor measurement noise only contribute to Loran-C error at the audit time, since no TD measurements are made at an initial (equipment installation) time.

The nominal standard deviations assumed for the Loran-C error sources are listed in Table 3.2-3. The scale factor error standard deviation is based on the following worst-case assumptions:

- o Land conductivity is only known to lie between extreme values of 0.0005 mho/m and 0.01 mho/m
- o Uncertainty in conductivity is characterized by a uniform distribution between the extremes
- o The hypothesized scale factor is based on an extreme conductivity value
- o Propagation paths are Type I for all three transmitters.

seasonal variations (Ref. 12). Pattern monitor measurement noise standard deviation is the same as in the TD Transmission configuration (0.02 μsec). However, a helicopter Loran-C measurement noise standard deviation of 0.02 μsec is not expected to be achievable, due to the increased bandwidth of the Loran-C phase-locked loops required to compensate for helicopter motion. In the absence of specific data on the required bandwidth, a noise standard deviation of 0.02 μsec has been selected as a nominal value, and sensitivity analyses have been performed to study the effect of increased Loran-C noise standard deviation on Variable Geometry accuracy.

In the Variable Geometry configuration error analyses, the differential Loran-C error model is used in conjunction with microwave ranging system and altimeter error models. The microwave ranging system error model includes the following error sources:

- Propagation velocity error -- the difference between actual and assumed microwave signal propagation velocities

- Common timing error (same for all buoys) -- uncompensated bias in round-trip signal travel time; could arise from helicopter receiver bias or common temperature -- dependent transponder delay

- Independent timing errors (one per buoy) -- uncompensated bias in round-trip travel time; could arise from differences in transponder delays from buoy to buoy, caused by manufacturing tolerances

- Measurement noise -- includes all random timing errors.

Note that the microwave propagation velocity error and the common and independent timing errors are assumed to be constant during the audit. All random errors are included in the microwave measurement noise.

Nominal standard deviations for the microwave error sources are listed in Table 3.2-3. Propagation velocity error standard deviation is based on seasonal variations in refractive index at Washington, D.C. Standard deviations for the

3.3 TD TRANSMISSION ERROR ANALYSIS RESULTS

3.3.1 Sensitivity to Pattern Monitor Location

The error ellipses for the 17 buoys in Boston Harbor (fixed aids are excluded) are shown in Figure 3.3-1 for a pattern monitor located at Boston Light (fixed aid 20 in Table 3.1-1). Note that the major axis of each error ellipse is oriented in the direction of the pattern monitor. Table 3.3-1 lists the rms error for each buoy. Buoy position error increases with increasing distance from the pattern monitor, from approximately 10 m rms for the closest buoys (8 and 9) to over 30 m rms for the farthest buoy (19).

Buoy position error is a function of the geometry of the Loran-C stations as well as the location of the pattern monitor with respect to the buoy. However, in the case that the Loran-C lines-of-position cross nearly at right angles, as in Boston Harbor, rms buoy position error is a function only of the range to the pattern monitor, in the manner shown in Figure 3.3-2. The 10 m rms position error for a buoy coincident with the pattern monitor is contributed by measurement noise. It should be noted that averaging the TDs for longer than 5-10 min. is not justified, because of the existence of other error sources (unmodeled) such as buoy motion (during the audit) and TD receiver biases.

The above results show the importance of locating the pattern monitor as near as possible to all buoys. For large harbors, multiple pattern monitors could be used. If a U.S. Coast Guard facility near the center of the buoy network is not available, buoy position error will degrade accordingly. For example, if the pattern monitor is located at the U.S. Coast Guard Group Boston Station (Figure 3.1-1), the maximum rms buoy position error (buoy 19) increases from 31.5 m to 60 m.

3.3.2 Nominal Error Budget

Buoy position error is caused by the following Loran-C error sources:

- Scale factor error
- Refractive index error

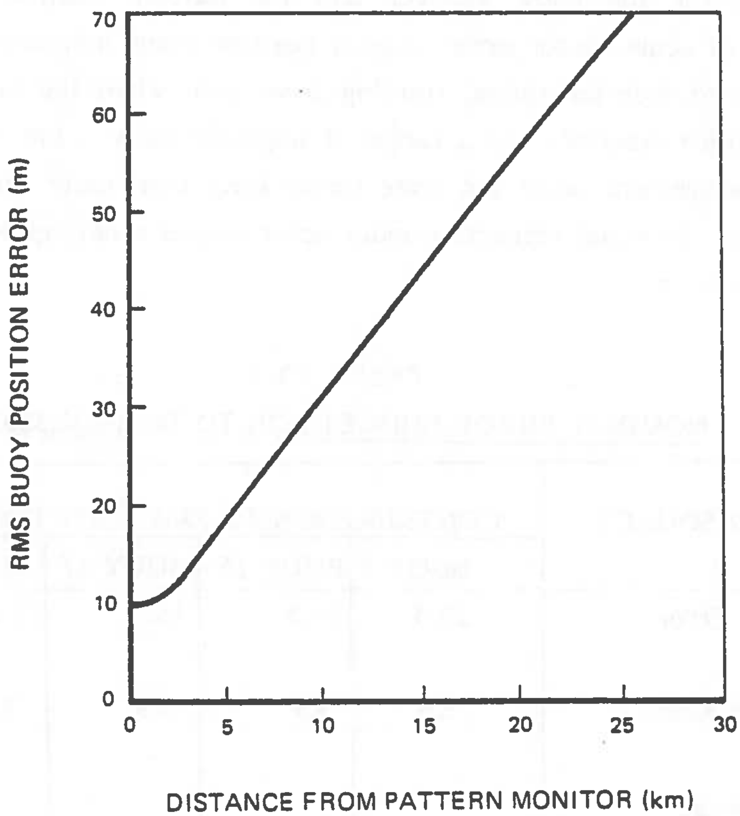

Figure 3.3-2 Dependence of Buoy Position Error on Distance from Pattern Monitor (TD Transmission)

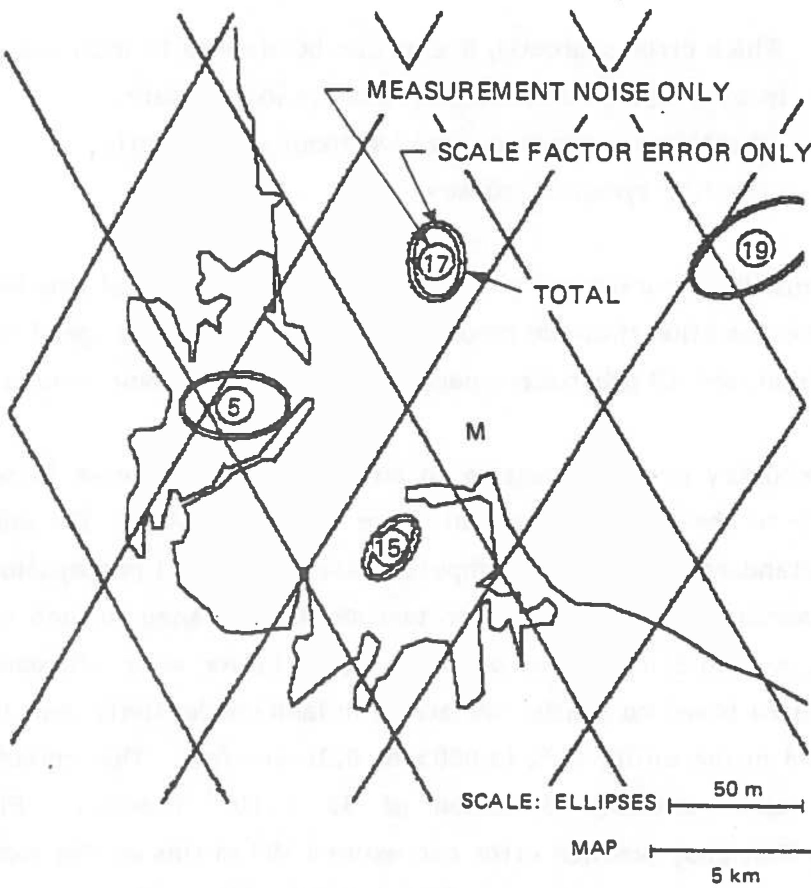

Figure 3.3-3 Measurement Noise and Scale Factor Error Contributions to Buoy Position Error (TD Transmission)

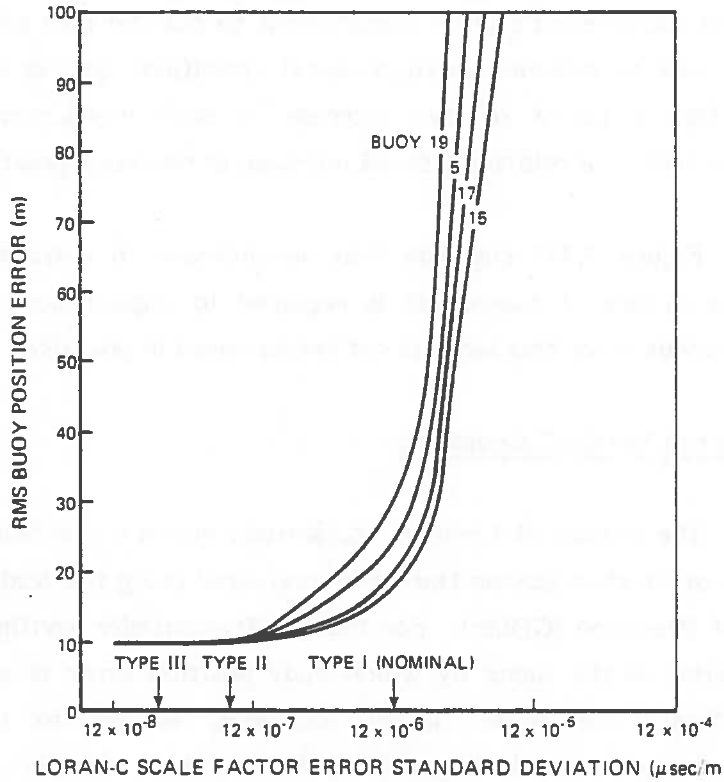

Figure 3.3-4 Buoy Position Error Sensitivity to Loran-C Scale Factor Error (TD Transmission)

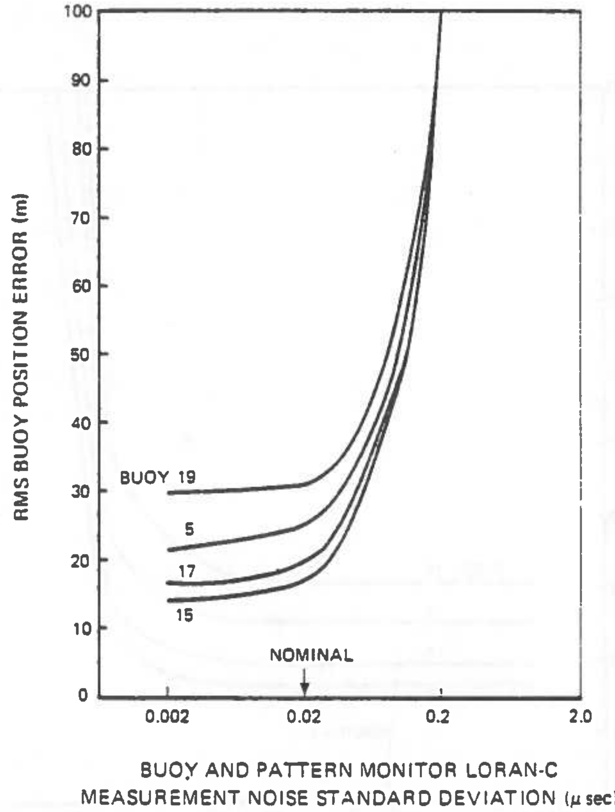

Figure 3.3-5 Buoy Position Error Sensitivity to Buoy <u>and</u> Pattern Monitor Loran-C Measurement Noise (TD Transmission)

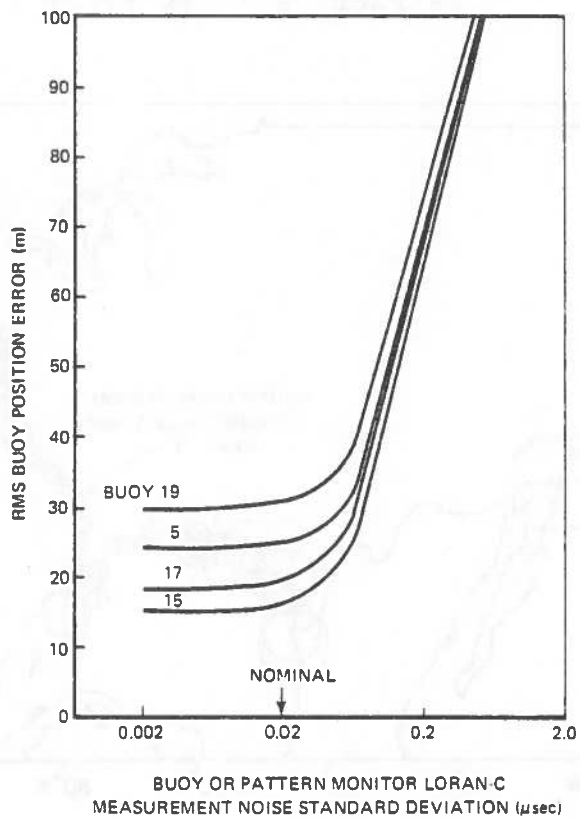

Figure 3.3-6 Buoy Position Error Sensitivity to Buoy <u>or</u> Pattern Monitor Loran-C Measurement Noise (TD Transmission)

- o Loran-C scale factor error
- o Measurement noise.

Nominal measurement noise contributes 10 m rms to buoy position error for all buoys. The contribution of scale factor error to buoy position error increases with increasing buoy-to-pattern monitor range, starting from zero when the buoy is coincident with the pattern monitor. At ranges beyond approximately 3 km, scale factor dominates measurement noise. The position errors for the TD Transmission errors are particularly sensitive to the Loran-C geometry.

3.4 VARIABLE GEOMETRY ERROR ANALYSIS RESULTS

3.4.1 Introduction

Processing of redundant measurements by the least-squares algorithm in the Variable Geometry configuration produces an estimate of constant error source parameters as well as buoy position error (Appendix C). The standard deviation of each error is reduced in accordance with the relative "observability" of the error source. Observability depends on the helicopter-to-buoy geometry and the a priori standard deviation of each error source. While the standard devation of noise error sources cannot be reduced by the algorithm, the impact of noise is reduced by averaging as more measurements are processed. It is the combination of calibration of observable constant error sources and noise averaging that produces a reduction in buoy position error in the least-squares algorithm.

Accuracy of the Variable Geometry configuration is a function of:

- o Loran-C transmitter geometry and pattern monitor location
- o Helicopter trajectory
- o Loran-C error levels
- o Microwave ranging system and altimeter error levels.

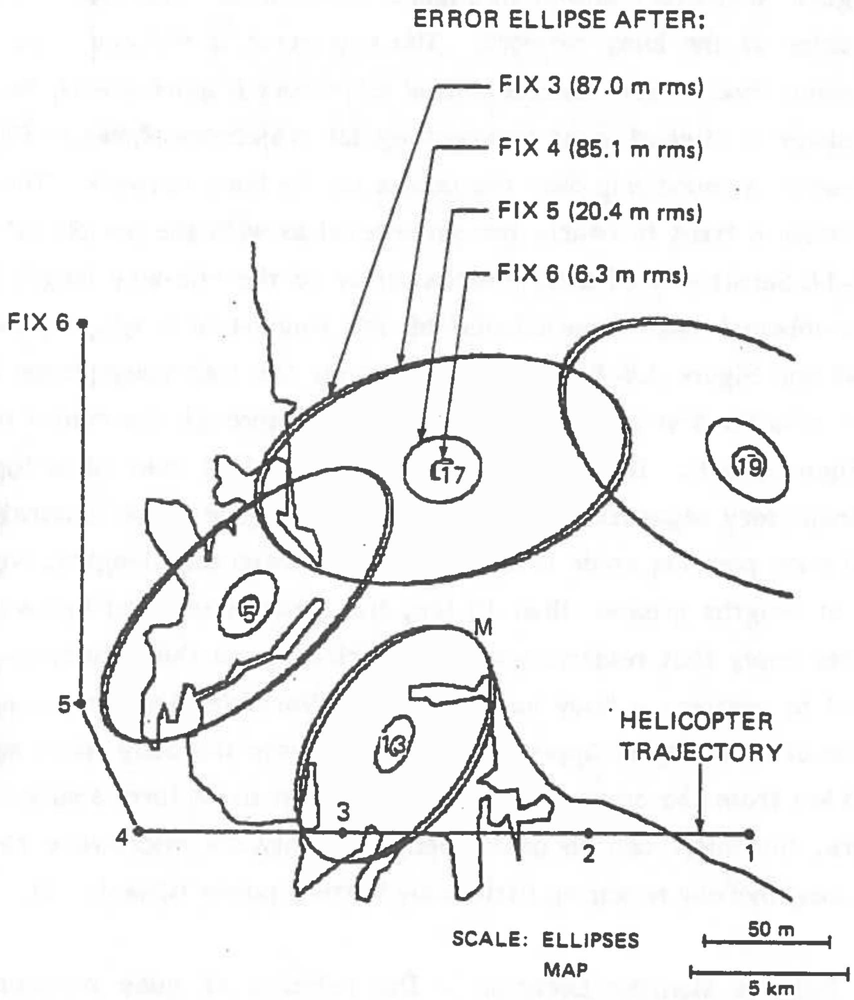

Figure 3.4-1 Buoy Position Error Ellipses For a Peripheral Trajectory (Variable Geometry)

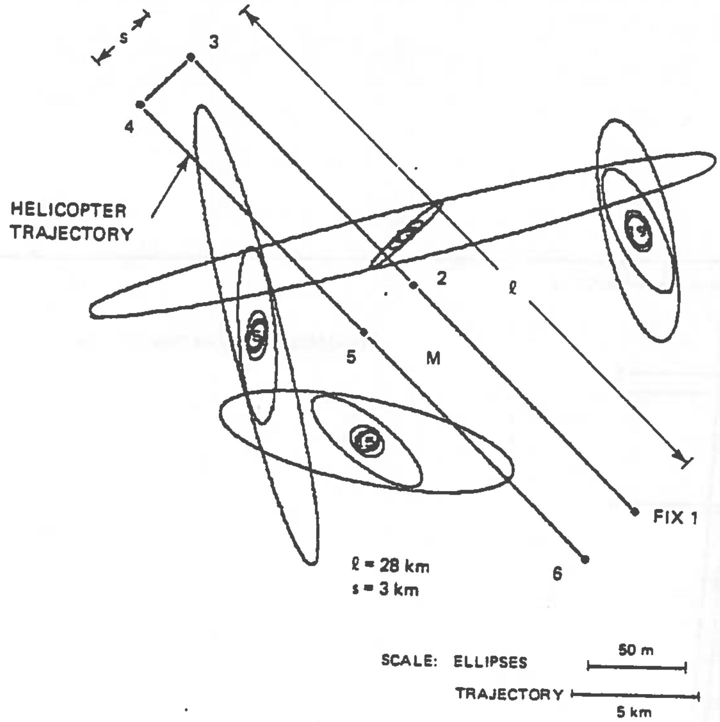

Figure 3.4-2 Buoy Position Error Ellipses for a Round-Trip Trajectory (Variable Geometry)

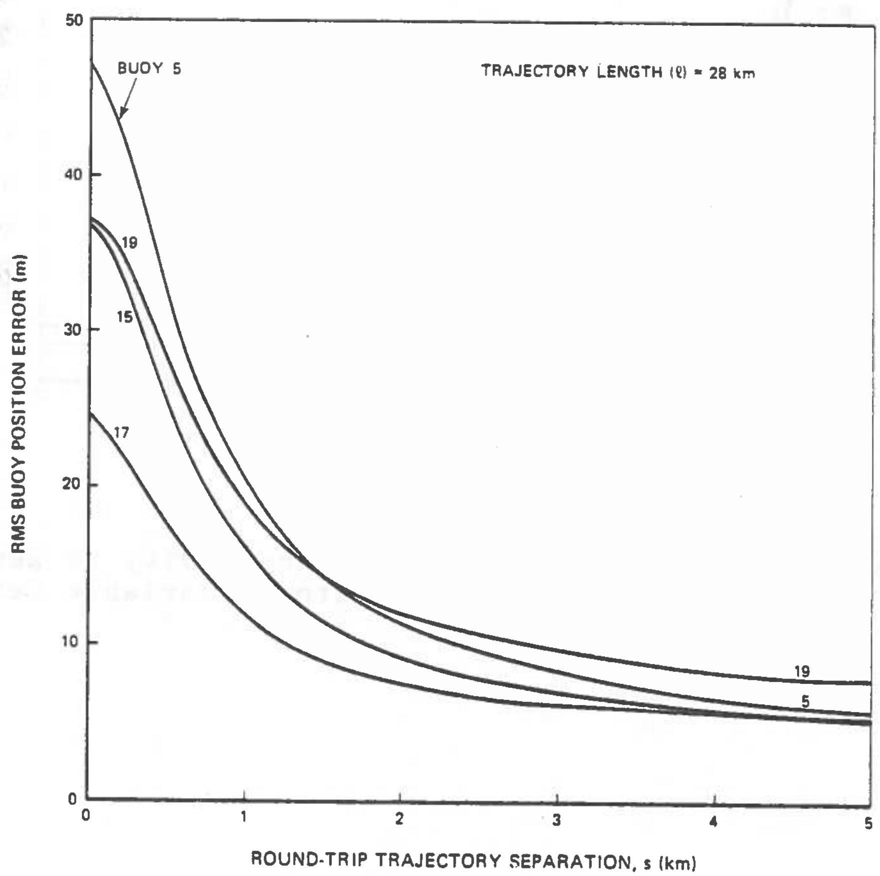

Figure 3.4-3 Buoy Position Error Sensitivity to Separation of Round-Trip Trajectory (Variable Geometry)

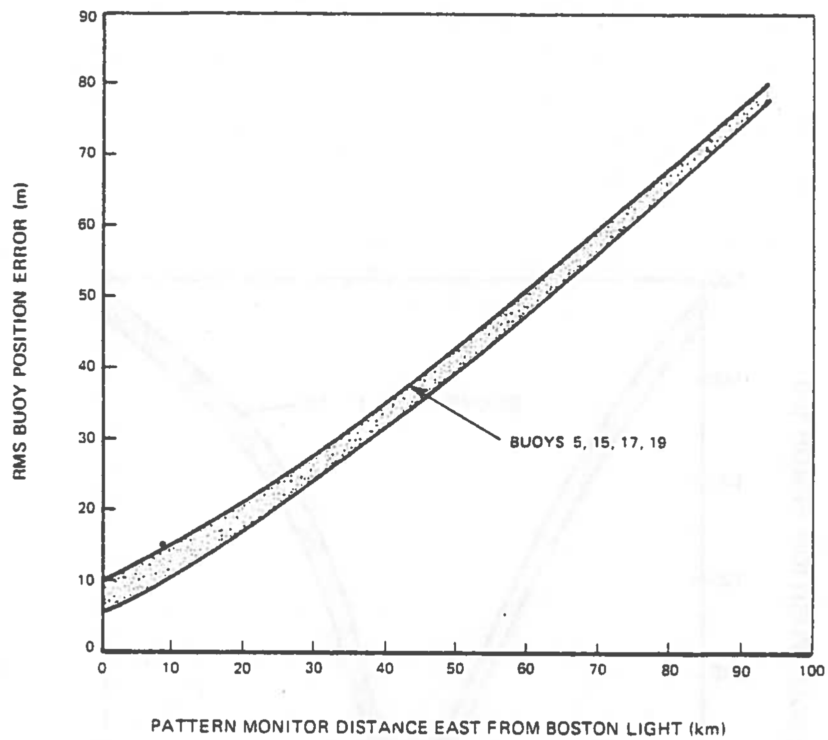

Figure 3.4-5 Buoy Position Error Sensitivity to Pattern Monitor Location (Variable Geometry)

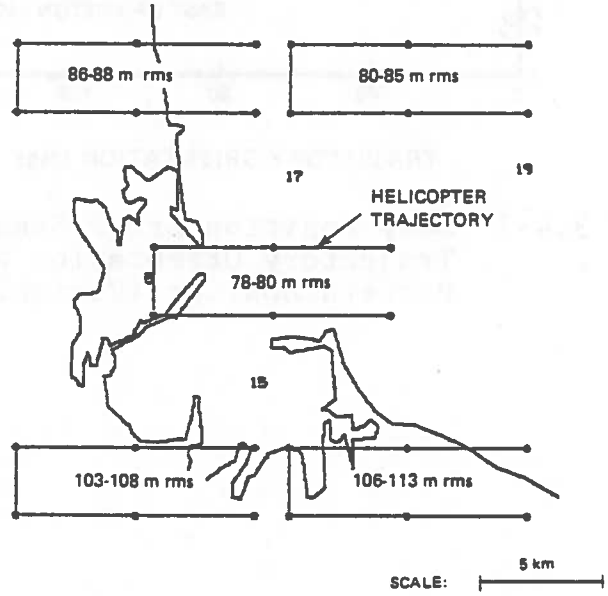

Figure 3.4-6 Buoy Position Error Sensitivity to Trajectory Location With Remote Pattern Monitor (Variable Geometry)

much less than in the TD Transmission configuration (Figure 3.3-2) because of error calibration by the least-squares algorithm. Note that when the pattern monitor is far from the buoys, the Loran-C transmitter-to-receiver paths for the pattern monitor and buoys may not all be of the same type, in violation of the modeling assumptions made in Section 3.2 and Appendix A. Modeling the entire harbor as Type I in this case provides a worst-case scale factor error.

Helicopter Trajectory with Remote Pattern Monitor - As the pattern monitor is moved from its nominal central location, accuracy not only degrades, as shown in Figure 3.4-5, but accuracy becomes more sensitive to helicopter trajectory. Figure 3.4-6 and Figure 3.4-7 illustrate the sensitivity of buoy position error to helicopter trajectory when the pattern monitor is at a remote location (94 km east of Boston Light). Maximum rms buoy position error over the four buoys increases from 80 m for the central trajectory shown in Figure 3.4-6, to a maximum of 113 m for the southeastern trajectory. When the pattern monitor is at its nominal location, the corresponding range of rms buoy position errors is 10 to 25 m. Figure 3.4-7 indicates that buoy position error is somewhat more sensitive to the orientation of the trajectory when the pattern monitor is remotely located. (Orientation angle is measured to the long axis of the trajectory, clockwise from north; the orientation of the trajectories in Figure 3.4-6 is 90 deg.) When the orientation of the central trajectory is rotated by 90 deg. rms buoy position error increases from 80 m to 175 m. There is little sensitivity to trajectory orientation for the nominal pattern monitor location.

The sensitivity to the helicopter trajectory with a remote pattern monitor is caused by the ability or inability of the least-squares algorithm to calibrate the Loran-C scale factor error. As discussed in Section 3.3, scale factor error causes a position error which is larger along the direction from the Loran-C user to the pattern monitor. The scale factor error is more observable to the least-squares algorithm when the helicopter trajectory exhibits large changes in position along this direction, as is the case for trajectories oriented at 90 deg. (east/west). This explanation of the sensitivity can be seen clearly in Figure 3.4-8, which shows the error ellipses after 6 fixes for the best-case (90 deg) and worst-case (0 deg) trajectories. Buoy position errors for the two trajectories are significantly different along the direction from the helicopter to the pattern monitor (east/west) because of the difference in observability, but nearly equal in the orthogonal direction (north/south).

Number of Fixes - Note that the sensitivity studies detailed above were performed with six fixes. Under nominal conditions, buoy position error is not reduced significantly by taking more than six fixes. This is shown by the lower curve in Figure 3.4-9. When the pattern monitor is located remotely, however, six fixes are not sufficient to calibrate the Loran-C scale factor error to its steady-state value, because the helicopter-to-pattern monitor geometry does not vary sufficiently. If more fixes are taken, the restricted geometry effect can be partially offset by the effect of measurement noise averaging. The upper curve in Figure 3.4-9 shows rms buoy position error to be reduced from 80 m to 27 m with 80 fixes; more fixes further reduce the error. While buoy position error can be significantly reduced by taking a large number of fixes, practical limications on the number of fixes must be considered. Limitations are imposed by available buoy battery power, shore station computer capacity and line-of-sight ranging requirement.

Number of Buoys Audited - In the least-squares algorithm, range measurements to all buoys are processed together. The algorithm is thus able to obtain information about the position of a given buoy from measurements to other buoys, and the error is smaller than it would be if measurements to the buoy were processed alone. Figure 3.4-10 demonstates how rms position error for buoy 17 increases as fewer buoys are audited (using a 3 km by 10 km trajectory with 6 fixes); the rms error is more than doubled when buoy 17 is audited alone.

3.4.3 Sensitivity to Error Model Parameter Values

Non-Sensitive Error Parameters - Buoy position error sensitivity to error model parameters was performed with a 3 km by 10 km trajectory oriented as the trajectory shown in Figure 3.4-2. Buoy position error is not sensitive to the following parameters over a factor of 1,000 on either side of nominal:

- o Loran-C scale factor error
- o Loran-C refractive index error
- o Helicopter altitude error
- o Microwave common timing error.

The least-squares algorithm can effectively calibrate each of these error sources even from very large initial values.

Sensitive Error Parameters - Buoy position error is sensitive to the following error sources:

- Microwave propagation velocity error
- Microwave independent timing error
- Microwave measurement noise
- Loran-C measurement noise

An increase in microwave propagation velocity error by more than a factor of 10 is required to affect accuracy (Figure 3.4-11). It is not likely that a significant increase in propagation velocity error would be cuased by refractive index variations. Figure 3.4-11 may also be used, however, to assess the impact of propagation velocity errors caused by other phenomena, such as multipath interference, which were not addressed specifically in this study. Sensitivity to the independent component of the microwave timing error (Figure 3.4-12) is moderate for a factor of 10 increase in the error source. Larger microwave timing errors cause buoy errors to increase rapidly and then level off; the filter can calibrate the independent timing errors when they are large with respect to other error sources. Recall that sensitivity to the common microwave timing error is small; an error which is common to all buoys is more observable to the least-squares algorithm. Although the nominal values for the common and independent microwave timing errors were chosen conservatively, the likelihood of either parameter exceeding its nominal value cannot be readily estimated. Note, however, that the sensitivity to the microwave independent timing error can be reduced by taking more fixes. Figure 3.4-13 shows that when microwave independent timing error is a factor of 100 above nominal (an extremely) unlikely value chosen to better illustrate the point), rms buoy position error for each of the four buoys can be reduced by a factor of 3 by processing 100 fixes.

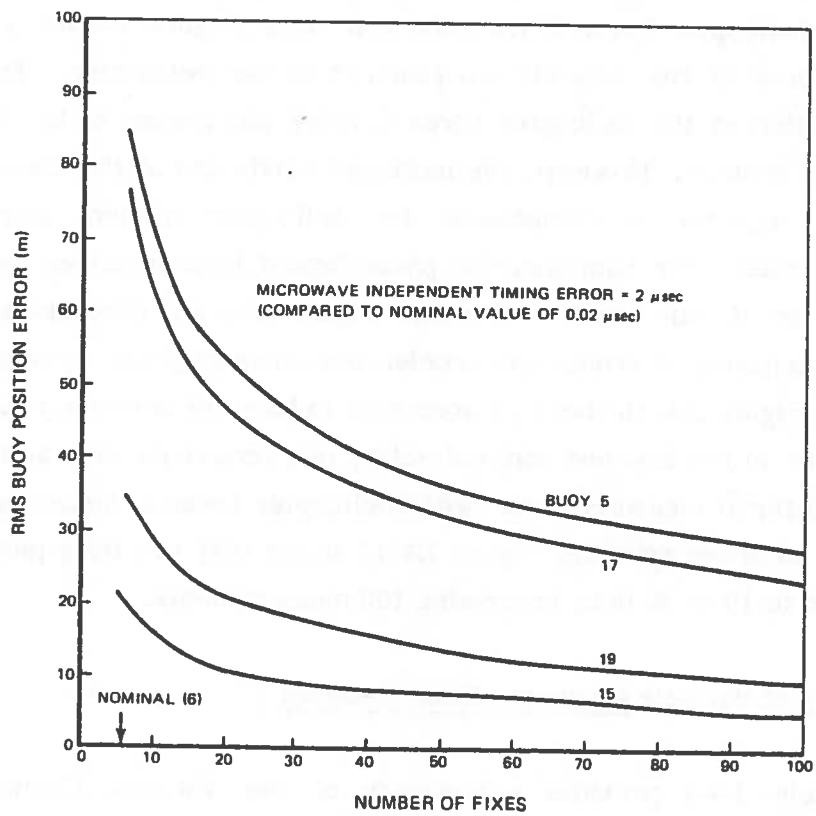

Figure 3.4-13 Buoy Position Error Sensitivity to Number of Fixes With Large Microwave Independent Timing Error (Variable Geometry)

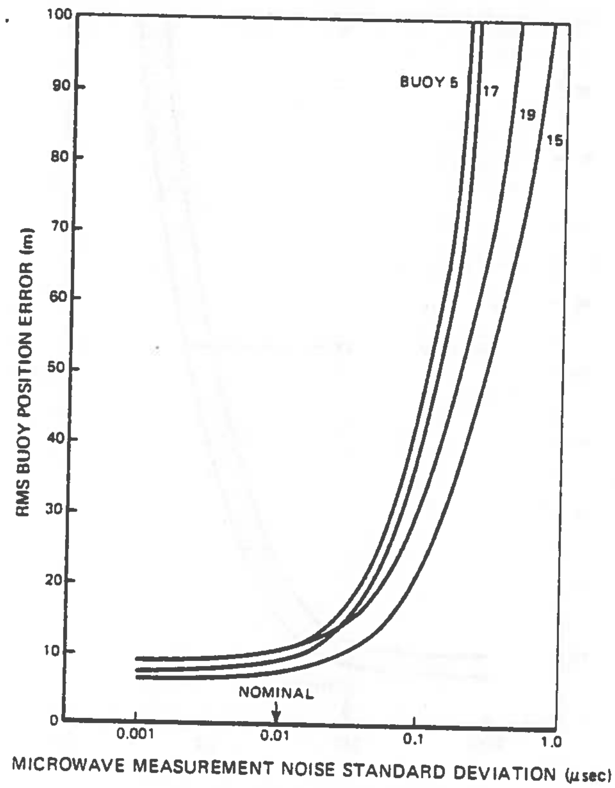

Figure 3.4-14 Buoy Position Error Sensitivity to Microwave Measurement Noise (Variable Geometry)

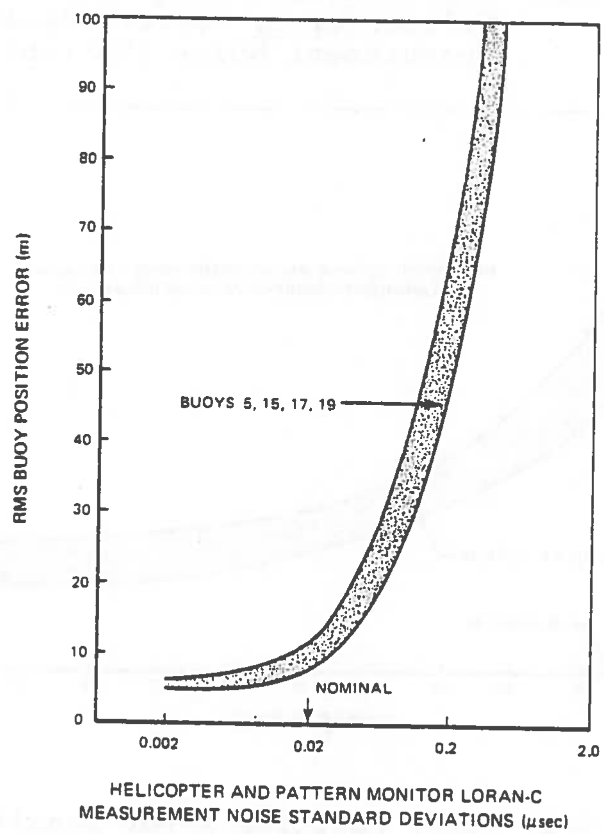

Figure 3.4-15 Buoy Position Error Sensitivity to Pattern Monitor and Helicopter Loran-C Measurement Noise (Variable Geometry)

TABLE 3.4-1
SUMMARY OF VARIABLE GEOMETRY ERROR ANALYSES

	PARAMETER	FIGURES	COMMENTS ON BPAS ERRORS
OPERATIONAL PARAMETERS	Helicopter Trajectory	3.4-1 to 3.4-4	Moderate Constraints On Trajectory To Achieve Small Errors
	Straight-Line	3.4-1, 3.4-3	Large Errors
	Peripheral	3.4-1	Small Errors
	Round-Trip	3.4-2, 3.4-3, 3.4-4	Relatively Insensitive To Increases In Round-Trip Separation > 3 km Or Length > 10 km
	Pattern Monitor Location	3.4-5	Increased Errors With Increased Distance From Buoy Network
	Remote Pattern Monitor	3.4-6 to 3.4-9	More Sensitive To Trajectory And Number Of Fixes With Remote Than With Local Pattern Monitor
	Trajectory Location	3.4-6	Smallest Errors With Trajectory In Center Of Buoy Network
	Trajectory Orientation	3.4-7, 3.4-8	Smallest Errors When Trajectory Aligned With Radial To Pattern Monitor
	Number Of Fixes	3.4-9	Reduced Errors With More Fixes
	Number Of Buoys Audited	3.4-10	Increased Errors If Only One Or Two Buoys Audited
ERROR MODEL PARAMETERS	Loran-C Scale Factor Error Refractive Index Error Helicopter Altitude Error Microwave Common Timing Error	Not Shown	Insensitive To These Parameters For A Factor Of 1,000 Range On Either Side Of Nominal
	Microwave Propagation Velocity Error	3.4-11	Relatively Insensitive To Changes In Propagation Velocity Error
	Microwave Independent Timing Error	3.4-12	Moderately Sensitive To Increased Independent Timing Error
		3.4-13	Reduced Errors With More Fixes
	Microwave Measurement Noise	3.4-14	Sensitive To Increased Measurement Noise
		3.4-17	Reduced Errors With More Fixes
	Loran-C Measurement Noise	3.4-15, 3.4-16	Sensitive To Increased Measurement Noise; Reduced Errors With More Fixes

It is concluded from the Pulse Retransmission simulations that Loran-C third-cycle identification is not significantly affected by the following parameters:

- o Manufacturing tolerances (from buoy to buoy) on the center frequency and bandwidth of Loran-C bandpass filters employed in the pulse retransmission equipment on the buoy

- o Static (memoryless) nonlinearities in the modulation/demodulation process.

These results are based on a simple model of a complex system and are intended to be used only as a foundation for more detailed analytical studies. In order to estimate TD measurement errors for the Pulse Retransmission BPAS configuration, a detailed nonlinear dynamic model would have to be developed for the modulation/demodulation process. If an estimate of TD measurement errors becomes available, the sensitivity analysis results presented for TD Transmission in Section 3.3 can be applied to estimate buoy position error for the Pulse Retransmission configuration.

4. COMPUTATIONAL AND MANPOWER REQUIREMENTS

4.1 INTRODUCTION

Implementation of a Buoy Position Auditing System (BPAS) by the U.S. Coast Guard would impose certain computational and manpower requirements. The expected requirements for the TD Transmission and Variable Geometry BPAS configurations are discussed in this chapter. For convenience, the buoy audit mission is divided into the following phases:

- Data Collection phase -- collect and store the necessary data, and determine data validity
- Position computation phase -- process the data to compute buoy position fixes
- Decision-making phase -- employ the position fixes to decide whether or not the buoys are "on station".

The three phases are discussed in Sections 4.2 to 4.4, respectively, and summarized in Section 4.5.

4.2 DATA COLLECTION PHASE

The data collection phase of the buoy audit mission requires minimal computation and manpower. Data collection equipment can be designed to operate semi-automatically, only involving manual interfaces for initialization and data validation.

4.2.1 TD Transmission

In the TD Transmission configuration, the buoy audit is conducted either from a U.S. Coast Guard shore station or from a moving platform such as a helicopter. When the audit is conducted from the shore station, the command sequence discussed in Section 2.2 is employed to "turn on" the buoy Loran-C receivers and request time-averaged TD's. In this command sequence, the TD's for all buoys are averaged during a common 5-10 min. time interval. It is desirable to average the pattern monitor TD's during the same

The use of staggered buoy interrogations requires that pattern monitor TD data also be staggered during the flight. Furthermore, if the pattern monitor does not lie in the line-of-sight of the helicopter, it may be necessary to interrogate the pattern monitor continuously from the shore station, during the flight. This approach necessarily requires time-tagging of buoy and pattern monitor TD's.

4.2.2 Variable Geometry

In the Variable Geometry configuration, the buoy audit is always conducted from a helicopter. Since the helicopter is not equipped to interrogate the pattern monitor, the helicopter data (Loran-C, microwave ranging, and altitude) are stored with time-tags. Pattern monitor TD data are received continuously at the shore station (over a telephone or VHF data link) and also stored with time tags for later processing.

The Variable Geometry error analysis results presented in Chapter 3 show that buoy position-fix errors are not reduced sufficiently when the Loran/microwave fixes are taken along a straight-line helicopter path. To obtain maximum variability in helicopter-to-buoy geometry, it is recommended that fixes be taken at points distributed along the entire round-trip flight path. This fix scenario could be accomplished by the following command sequence:

- o Determine when (e.g., at present times) or where (e.g. using Loran-C) the next fix is to be taken
- o "Turn on" the microwave transponders on all buoys
- o Range to the buoys in sequence, triggering each buoy transponder with a different identification code
- o All buoy transponders "turn off" after a preset time interval.

In this command sequence, the transponders are deactivated between fixes to conserve buoy battery power. Some buoys may not be within the line-of-sight of the helicopter when a fix is taken, or the ranges may be greater than the range for which the microwave system is designed. To accommodate this situation, the microwave interrogator ranges to the next buoy in sequence if a buoy response is not received within a certain period of time.

The computation and data storage requirements of the above procedure are minimal and can be accommodated with a desk-top calculator.

4.3.2 Variable Geometry

Computation of buoy position fixes in the Variable Geometry configuration involves the following steps:

- Assemble the relevant data -- helicopter and pattern monitor Loran-C TDs, microwave ranging and altitude data, pattern monitor position coordinates, and Loran-C chain transmitter coordinates

- Estimate helicopter Loran-C range differences at each point on the flight path, using the differential Loran-C algorithm described in Appendix A (Section A.4.2)

- Solve for helicopter position fixes at each point on the flight path

- Employ the helicopter position fixes, together with microwave ranging and altitude data, to compute coarse buoy position fixes (Appendix C)

- Refine the coarse fixes with the least-squares algorithm (Appendix C) to determine fine buoy position fixes.

The first four steps require minimal computation and data storage. Estimates of data-processing time and computer storage for the least-squares algorithm are presented in Table 4.3-1. The estimates are based on direct implementation of the equations detailed in Appendix C, and include only arithmetic operations and floating-point variables. A significant reduction in storage and a moderate reduction in data-processing time should be achievable by designing the computer software for maximum efficiency. It is apparent from Table 4.3-1 that computation requirements increase exponentially with an increase in the number of buoys audited. If a large number of buoys are audited in a harbor, Variable Geometry computation and storage can be reduced significantly by processing the

In the first method, the buoy station contour is established by identifying all locations for which the buoy serves its intended function as an aid to navigation. For example, a traffic separation buoy may serve its intended function anywhere in a rectangle whose long side is aligned with the direction of traffic flow, while a major obstruction buoy may have to be located to one side of the obstruction (Figure 4.4-1a). This method of establishing the buoy station contour emphasizes the location of the buoy, rather than the buoy anchor, and recognizes that a buoy may drag anchor without necessarily affecting its use as an aid to navigation.

In the second method, the buoy station contour is established by measuring the buoy position with the Buoy Position Auditing System under different tide and wind conditions, prior to implementation of the operational system. If the buoy anchor does not move during the measurement process, an estimate of the buoy watch circle* is obtained and the watch circle may be employed as the buoy station contour (see Figure 4.4-1b). Alternatively, the buoy position measurements can be employed to establish a number of buoy station contours corresponding to different categories of tide and wind conditions.) This method of establishing the buoy station contour emphasizes the location of the buoy anchor since the buoy position measurements are assumed to be obtained when the buoy anchor is in the single location mandated by the U.S. Coast Guard (surveyed by a buoy tender to a stated 1 to 2 m accuracy).

4.4.2 BPAS Decision Algorithms

It is recommended that the decision algorithm in an operational Buoy Position Auditing System provide the following outputs to U.S. Coast Guard personnel:

- o Buoy position fix
- o Decision that the buoy is on or off station
- o Confidence in the decision.

Two decision algorithms are outlined below.

---

*The path followed by the buoy may be elongated, rather than circular (Ref. 23).

The first decision algorithm is based on the buoy station contour defined in Section 4.4.1. The buoy position fix is compared to the buoy station contour, preferably on a graphical display. It is decided that the buoy is on station if the fix falls within the station contour, and off station if the fix is outside of the contour (See Figure 4.4-2).

In this approach, the confidence in the decision is based on expected buoy position fix errors. Position-fix error is characterized statistically by a bivariate normal probability density function. Contours of equal probability density are ellipses centered on the position fix (Figure 4.4-2). The probability density function is based on a theoretical error model (validated by experiment) from which an error covariance matrix is computed. The error model includes the various error sources (e.g., Loran-C propagation errors and measurement noise) and the relative geometry of the buoy and helicopter flight path (for Variable Geometry configuration, only), as described in Section 3.2. The probability that the true buoy position is within a particular region can be computed by integrating the probability density function over the region. If the position fix is inside the station contour, the Probability of a Correct Decision (PCD) is the integral of the probability density function inside the station contour; if the position fix is outside the station contour, the PCD is the integral of the probability density function outside the station contour.

If the decision is made that a buoy is off station, the U.S. Coast Guard may, depending on the value of the PCD, choose either to service the buoy immediately or to issue a marine alert pending further verification. The PCD may also be employed to rank off-station buoys to aid in scheduling buoy-tender operations. Similarly, if the decision is made that a buoy is on station, the PCD may aid in the scheduling of future position audits.

In the second decision algorithm, the buoy station contour concept is not used. Instead of defining a specific boundary which encompasses the acceptable buoy locations, a scatter pattern is accumulated for each buoy by measuring its position with the Buoy Position Auditing System over a range of tide and wind conditions, prior to implementing an operational system. (Alternatively, the buoy position measurements can be employed to establish a number of scatter diagrams, corresponding to specific tide and wind conditions.) For a given audit, the buoy position fix is compared to the appropriate scatter diagram. An on-station (or off station) decision is made if the position fix falls near to (or far from) the center of the scatter pattern.

The confidence in a correct decision is a function of the density of the scatter pattern and the distance of the buoy position fix from the center of the pattern. A quantitative algorithm for making the decision and for computing the associated confidence in the decision could be developed based on BPAS experimental data.

The candidate BPAS decision algorithms discussed herein (summarized in Figure 4.4-3) range from the "theoretical" involving a buoy station contour and theoretical probability density function, to the "empirical", relying on a BPAS-generated scatter pattern. The BPAS data required in the empirical decision algorithm (or in the theoretical algorithm with a BPAS-indicated station contour) must be collected prior to implementing the operational system. The data also must cover a range of tide and wind conditions, and, therefore, may require numerous audits to assemble. Acquisition of the necessary data would be more convenient if performed from a shore station rather than from a helicopter. However, this is not considered to be a major advantage of the TD Transmission configuration over the Variable Geometry configuration, since the data collection will require a several month period in either case.

4.5 SUMMARY OF COMPUTATIONAL AND MANPOWER REQUIREMENTS

Consideration of the computational and manpower requirements of the TD Transmission and Variable Geometry BPAS configuratjions leads to the following conclusions:

- o Neither configuration imposes excessive computational and manpower requirements during the data collection phase of the buoy audit mission
- o The position computation phase can be implemented on a desk-top calculator for TD Transmission, but requires a mini-computer or large-scale computer facility for Variable Geometry
- o Both configurations require that trained U.S. Coast Guard personnel be available to interpret the results of the buoy audit in the decision-making phase.

Further consideration should be given to computational and manpower issues during the BPAS experiment.

5. COMPARISON AND RECOMMENDATIONS

5.1 PERFORMANCE COMPARISON OF BPAS SYSTEM CONFIGURATIONS

A comparison between the TD Transmission, Pulse Retransmission and Variable Geometry approaches is shown in Table 5.1-1 . Position errors for the Pulse Retransmission configuration are expected to be greater than for TD Transmission due to the adverse effect of the Loran-C pulse processing. Since there is also a clear disadvantage of the Pulse Retransmission configuration with respect to cost and technical risk, a decision was made at an interim project briefing on 31 July 1979 to discontinue detailed analysis of the accuracy of the Pulse Retransmission configuration. Therefore, accuracy results for the Pulse Retransmission system are not included in this report. A comparison of the accuracy of the TD Transmission and Variable Geometry BPAS configurations is summarized in Table 5.1-2.

Under the nominal conditions assumed for this study, the Variable Geometry configuration is more accurate than the TD Transmission configuration. Nominal buoy position error is less than 10 m rms in the Variable Geometry configuration, while errors range from 10 m rms to 30 m rms* (with best case GDOP) in the TD Transmission configuration. The TD Transmission configuration has the advantage of minimal impact on U.S. Coast Guard operations, but the requirements of the Variable Geometry configuration are not severe. Only six microwave ranging fixes, taken along a 3 km by 10 km rectangular helicopter trajectory, are required to achieve a 10 m rms buoy position-fix accuracy in the Variable Geometry configuration. The Pulse Retransmission configuration is expected to be less accurate than the TD Transmission configuration because of degradation caused by increased Loran-C measurement noise. Figure 3.3-6 can be used to assess the impact of increased measurement noise on Pulse Retransmission buoy position error.

Loran-C scale factor error impacts the TD Transmission and Variable Geometry configurations differently. The TD Transmission configuration has the advantage of calibrating the Loran TD reading at the time the equipment is installed on the buoy. This calibration reduces the Loran-C scale factor error

*Dependent on range from buoy to pattern monitor and GDOP.

TABLE 5.1-2

TD TRANSMISSION AND VARIABLE GEOMETRY ACCURACY COMPARISON

	CONSIDERATION	TD TRANSMISSION	VARIABLE GEOMETRY
	Nominal rms Error	10-30 m	<10 m
	Operational Requirements	Minimal	3 km By 10 km Rectangular Trajectory With Six Fixes
LORAN-C ERRORS	Scale Factor Error	Initial Calibration When Equipment Is Installed; BPAS Errors Sensitive To Scale Factor Error	No Initial Calibration; BPAS Errors Not Sensitive To Scale Factor Error Because Of Calibration By Least-Squares Algorithm
LORAN-C ERRORS	Pattern Monitor Measurement Noise	BPAS Errors For Both Configurations Sensitive To An Increase In Pattern Monitor Measurement Noise; Nominal Should Be Achievable, However	
LORAN-C ERRORS	Buoy Or Helicopter Measurement Noise	Factor Of Five Increase In Measurement Noise Produces 50 m rms BPAS Error; Subject To Extremes In Buoy Environment	Factor Of Five Increase In Measurement Noise Produces 30 m rms BPAS Error; Dependent On Receiver Tracking-Loop Bandwidth
LORAN-C ERRORS	Refractive Index Error	Negligible Impact On BPAS Error For Both Configurations	
MICROWAVE ERRORS	Propagation Velocity Error	The TD Transmission Configuration Is Not Subject To Microwave Ranging And Altimeter Errors	Factor of 10 Increase In Propagation Velocity Error Produces Negligible Increase In BPAS Errors
MICROWAVE ERRORS	Common Timing Error		BPAS Errors Not Sensitive To An Increase In Common Timing Error
MICROWAVE ERRORS	Independent Timing Error		Factor Of 10 Increase In Independent Timing Error Produces 30 m rms Buoy Position Error
MICROWAVE ERRORS	Measurement Noise		Factor Of Five Increase In Measurement Noise Produces 30 m rms Buoy Position Error
	Altimeter Error		BPAS Errors Not Sensitive To Altimeter Error
	Pattern Monitor Location	BPAS Errors Sensitive To Distance Of Pattern Monitor From Buoys	Less Sensitive Than TD Transmission; Sensitivity Can Be Further Reduced By Additional Fixes And/Or Improved Helicopter Trajectory
	Potential For Improved Accuracy	Multiple Pattern Monitors	BPAS Error Estimates Significantly Less Than 10 m rms Are Unrealistic Because Of Potential Impact Of Unmodeled Error Sources
	Loran-C Geometry (GDOP)	Very Sensitive - Proportional to GDOP	Relatively Insensitive

because of calibration of the Loran-C scale factor error by the least-squares algorithm at the time of the audit. Redundant information also makes the Variable Geometry configuration more adaptable in the event of adverse system constraints, such as a remote pattern monitor location. Accuracy can normally be improved under adverse conditions by increasing the number of fixes or altering the helicopter trajectory.

Sensitivity of Variable Geometry accuracy to ranging errors is relatively small for most error sources. Propagation velocity and common timing errors are well-calibrated by the least-squares algorithm. Hardware performance requirements relative to these error sources could therefore be relaxed from the assumed nominal requirements, if warranted by cost savings. It is more important to control the source of an independent timing error, but a factor of ten increase in this error beyond the assumed nominal value only causes an increase in buoy position error to 30 m rms (Figure 3.4-12). Measurement noise is the most critical hardware parameter in the ranging system. The nominal value of 0.01 sec rms applies to a Pulse Ranging system operating in C-band or X-band; measurement noise for a CW Ranging system operating at L-band is expected to be higher. An increase in measurement noise to 0.05 sec rms causes an increase in buoy position error to 30 m rms (Figure 3.4-14). However, a decrease in measurement noise achieved with a higher quality system will not improve accuracy substantially.

The nominal accuracy of the Variable Geometry configuration estimated (less than 10 m rms buoy position error) meets the expected accuracy requirements for a Buoy Position Auditing System. A study of methods to further improve the accuracy of the Variable Geometry configuration is therefore not warrented. Note that the influence of unmodeled error sources becomes important for estimated buoy position errors less than 10 m rms. For example, errors introduced by buoy motion, or by a Loran-C receiver TD bias, are not modeled.

Improvement of TD Transmission accuracy to 10 m rms for all buoys requires reduction of Loran-C scale factor error, the primary error contributor. The most straight forward approach is to reduce the buoy-to-pattern monitor separation. It is shown in Section 3.3, however, that a separation of less than 3 km is required to achieve 10 m rms accuracy. In order to obtain a separation of less than 3 km, The base station costs again reflect the expense involved in the design and development of technically sophisticated equipment for limited use. The TD Transmission system can be constructed out of standard hardware components with the majority of the custom system design contained in the software programming for the audit control and data acquisition electronics. Pulse Retransmission, on the other hand, requires the special purpose Loran-C receiver which must be designed, produced and documented solely for this application.

The Loran-C pulse retransmission concept has been successfully applied to the tracking of weather balloons, using equipment manufactured by Beukers Laboratories, Inc. (Ref. 25). In addition, the U.S. Coast Guard has conducted analyses and testing of the concept in support of the Distress Alerting and Locating System (DALS) development effort (Refs. 9 and 21). Experience has shown that the modulation/demodulation process can distort the Loran-C pulse envelope, which contains information needed to identify the third cycle of the 100 kHz Loran-C carrier. Since the third-cycle, positive-going zero crossing must be tracked to meet the requirements of a precision buoy audit,* the pulse distortion issue is critical in the assessment of the Pulse Retransmission BPAS configuration. The following approaches for reducing the effect of pulse distortion are considered in this report:

- o Logarithmic (or similar) pulse compression
- o Stepped-gain pulse amplification
- o Time-multiplexed transmission of direct and derived pulses.

Each approach requires a specialized Loran-C receiver to process the coded pulses. There is considerable technical risk involved in pursuing these approaches since Loran-C equipment for their implementation has not been developed and tested.

The audit capability of the two systems differs markedly. Due to the parallel nature of the processing which is performed on the TD Transmission buoy electronics and the relatively short period of time required to transmit the

---

*Other Loran-C carrier cycles may be tracked for non-precision applications such as DALS.

Since the pulse ranging system assumed here is a relatively simple modification of an off-the-shelf unit, the power drain is a given from its manufacturer. The CW ranging system, on the other hand, is a new development, whose specifications are tailored to the BPAS application. It is probable that a pulse ranging system design could be developed for this program, with an acceptable power drain; however, the development costs would be similar to those for the CW ranging system and considerably in excess of the total cost of the pulse ranging system assumed in this report.

The decision over which type of ranging system to use will require a careful analysis, including the design requirements of all subsystems and a detailed compilation of all error sources for each system. This is beyond the scope of the present study.

The Variable Geometry BPAS configuration requires a greater data processing capability than the TD Transmission and Pulse Retransmission configurations. The differential Loran-C algorithm is somewhat different than the algorithm used in the other configurations, although its computational burden is still minimal. The algorithm employs helicopter and pattern monitor TDs measured at the audit time, but no TD data are assumed to be available for use as an initial reference (Appendix A, Section A.4.2). The difference between helicopter and pattern monitor TDs is used in a simple TD grid prediction model to estimate the position of the helicopter relative to the pattern monitor. The least-squares algorithm, which combines helicopter Loran-C position fixes with range and altitude data, may require a fairly large-scale computer facility for implementation. The buoy positions are all computed together in the least-squares algorithm, in contrast to separately, as in the TD Transmission and Pulse Retransmission BPAS configurations. The optimal integration of data from all buoys enables calibration of certain error sources and reduction of the effect of others (Section 3.4).

fixed sites, and on a U.S. Coast Guard vessel, and by installing VHF interrogation equipment at a shore station. Data are collected periodically from the shore station for one year, and additional data are collected using the vessel, at selected times during the year.

5.2.1 Equipment Evaluation

Although equipment performance will be evaluated during the entire experiment, certain special tests are recommended. Proper operation of the Loran-C receivers on the buoys and fixed aids should be verified for a range of environmental conditions. This can be accomplished by periodically positioning the ship next to each buoy or fixed aid, measuring the TDs with the ship's Loran-C receiver, and comparing the TDs with those transmitted from the buoy or fixed aid to the shore station. The incremental position-fixing resolution of the Loran-C receiver selected for the experiment should be determined by navigating the ship along short radials originating at a fixed aid (pattern monitor). The length of the radials should be at least 100 m and the ship's position relative to the fixed aid should be determined by transit theodolite and a measuring line. Data from this experiment permits an evaluation of the contribution of measurement noise to differential Loran-C errors, since propagation effects are negligible within 100 m of a pattern monitor.

5.2.2 Accuracy Assessment for Boston Harbor

Differential Loran-C accuracy in Boston Harbor is determined from TD data collected at five to ten fixed-sites, equipped with Loran-C receivers and VHF transmitters, and placed such that site-to-site distances vary from 1 km to 20 km (with priority given to distances between 3 km and 12 km). Fixed aids to navigation, as well as island facilities, are candidates for fixed sites. Each fixed site should be automatically interrogated periodically from the shore station (e.g., the TSC facility in Cambridge) and its TDs recorded on magnetic tape. It is important to realize that the fixed-site data must be collected for a year to properly assess differential Loran-C accuracy. The data are analyzed by interpreting one fixed site to be a pattern monitor and all other fixed sites to be ranging system, the scale factor can be computed for each radial. A relatively large clock drift can be tolerated because a 10 km radial is navigated in less than an hour; the clock phase offset is not important because the data are only used to measure the change in TOA along the radial. The test should be repeated four times during the year to ascertain the seasonal scale factor variation for each path type.

5.2.4 Testing Decision Algorithms

It is recommended that the TD Transmission equipment be installed on an operational buoy and on an experimental buoy, to provide data for testing BPAS decision algorithms (Section 4.4). Each buoy should be interrogated hourly for a month, and daily, thereafter to develop a history of buoy dynamics. The purpose of the operational buoy is to provide the opportunity to demonstrate the system to U.S. Coast Guard personnel presently charged with maintaining buoys on station. The experimental buoy is used to simulate off-station conditions. The anchor of the experimental buoy should be moved (without informing the data analysts) and the candidate decision algorithms employed in an attempt to detect the motion.

5.2.5 Recommended Experimental Hardware

This section defines the hardware necessary for an experimental program to determine the performance of the TD Transmission system. The experimental buoy system is based on the system block diagram shown in Figure 2.2-1. It is assumed that the experimental buoy system will be used both on floating navigational aids and as a differential Loran-C monitor when placed at a fixed site. The suggested experimental buoy equipment and costs are shown in Table 5.2-1. Also listed in this table are the model numbers of typical commercial equipment meeting the system requirements.

Table 5.2-2 shows the development costs associated with the buoy equipment. These costs include modification of the buoy's Loran-C processor firmware to incorporate buoy identification information and other modifications of the output

Buoy Loran-C Processor	$ 4,000
Power Sequence and Control Logic	$ 4,000
Antenna System	$ 3,000
Integration/Packaging/Testing	$15,000
BUOY DEVELOPMENT TOTAL........................	$26,000

Table 5.2-2

Experiment Electronic Equipment Cost,

Develop Buoy Electronics

Telemetry Receiver (Communitronics MR-11)	$ 1,100
Command Transmitter (Communitronics MT-11-10 Watts)	$ 1,500
Audit & Data Acquisition Control	$ 8,000
Antenna System	$ 200
QUICK-LOOK DATA CAPABILITY	$20,000
Integrate/Package/Test	$15,000
BASE ELECTRONICS TOTAL....................	$45,800

Table 5.2-3

Experiment Electronic Equipment Cost,

Develop Base Electronics

contained in Appendix G. The quoted costs do not include money for data reduction hardware or software; thus these costs are sufficient to pay for experimental hardware, but not the experiment itself. However, very recent data indicates that some of the quoted costs can be substantially reduced. Hardware being developed for the Suez Canal Vessel Traffic System, which uses differential Loran-C with time differences transmitted to a base station via a digital data link, may be applicable to the BPAS requirement. In this event, it appears that the total in Table 5.2-4 would reduce to about $90,000.

APPENDIX A
DIFFERENTIAL LORAN-C ERROR MODEL

A.1 INTRODUCTION

The candidate Buoy Position Auditing System (BPAS) configurations considered herein employ differential Loran-C, either alone (for TD Transmission and Pulse Retransmission) or in combination with a microwave ranging system (for Variable Geometry). In this appendix, a model is derived which characterizes differential Loran-C position errors in terms of signal propagation parameter variations and measurement noise.

The relationship between position error and range difference error is reviewed in Section A.2. Loran-C signal propagation is discussed in Section A.3, where an equation is derived to express measured time difference (TD) in terms of propagation parameters and measurement noise. The TD equation is employed in Section A.4 to derive the range difference error equations, the structures of which are identical for the three candidate BPAS configurations. In Section A.5, the error statistics applicable to the individual BPAS configurations are discussed.

A.2 RELATIONSHIP BETWEEN POSITION ERROR AND RANGE DIFFERENCE ERROR

The candidate BPAS configurations employ the hyperbolic mode of Loran-C, whereby a position fix for a buoy or helicopter is computed as the intersection of two hyperbolic lines-of-position, each defined by a range difference. The

Bearing angles from the user to transmitter i, measured clockwise from north, are denoted by β_i in Eq. A.2-2. The transformation matrix B is very nearly the same for all user locations in a harbor, unless the harbor is located near a Loran-C transmitter. However, range difference errors depend critically on the location of the user within the harbor, specifically his location with respect to the pattern monitor.

Geometric Dilution of Precision (GDOP) is a scalar index which can be used to characterize the transformation matrix B, for the purpose of comparing Loran-C geometries in various U.S. harbors. GDOP is the ratio of radial position error, $(\delta N^2 + \delta E^2)^{\frac{1}{2}}$, to range difference error, under the assumption that the two range difference errors have equal standard deviations and are correlated with correlation coefficient 0.5 (Ref. 10):

$$\text{GDOP} = \frac{a}{2\sin\theta}\left[\frac{1}{\sin^2\alpha} + \frac{1}{\sin^2\gamma} - \frac{\cos\theta}{\sin\alpha\,\sin\gamma}\right]^{\frac{1}{2}} \qquad \text{(A.2-3)}$$

where

$\alpha = (\beta_1 - \beta_m)/2$
$\gamma = (\beta_2 - \beta_m)/2$
$\theta = (\beta_1 - \beta_2)/2$
$a = \sqrt{2}$ (normalizes GDOP to unity for perfect geometry)

Some care must be exercised in employing GDOP as an indicator of Loran-C geometry when one range difference error is expected to be much larger than the other. In this case, the actual transformation matrix B must be considered in comparing Loran-C geometries.

Each propagation delay appearing in Eq. A.3-1 can be expressed in terms of three parameters which describe the signal propagation path for the 100 kHz Loran-C groundwave:

- Atmospheric refractive index at the surface (n)
- A parameter (α) related to the vertical lapse rate of atmospheric refractive index
- Effective ground conductivity (σ), including terrain effects.

It is assumed that refractive index and vertical lapse rate are homogeneous for all propagation paths relevant to a harbor. This is a reasonable assumption since seasonal variations in these parameters are significantly greater than the spatial parameter variations which exist in a Loran-C chain coverage area at any one time (see Ref. 12). Conductivity, on the other hand, typically varies more from path to path for widely spaced paths, than it does from season to season for any one path (see Ref. 13). Therefore, conductivity is assumed to be the same for paths from a particular transmitter to all users in a harbor, but different for different transmitters. Note that conductivity is not necessarily homogeneous along a path.

Under the above assumptions, the propagation delay from i to u is given by the equation:

$$\phi_i(u,t) = \frac{n(t)}{c} R_i(u) + SF(\sigma_i(u,t),\ R_i(u)) + \widetilde{SF}(\alpha(t),\ R_i(u)) \quad \text{(A.3-2)}$$

where

c = speed of light in free space = 0.299792 km/μsec

n(t) = refractive index

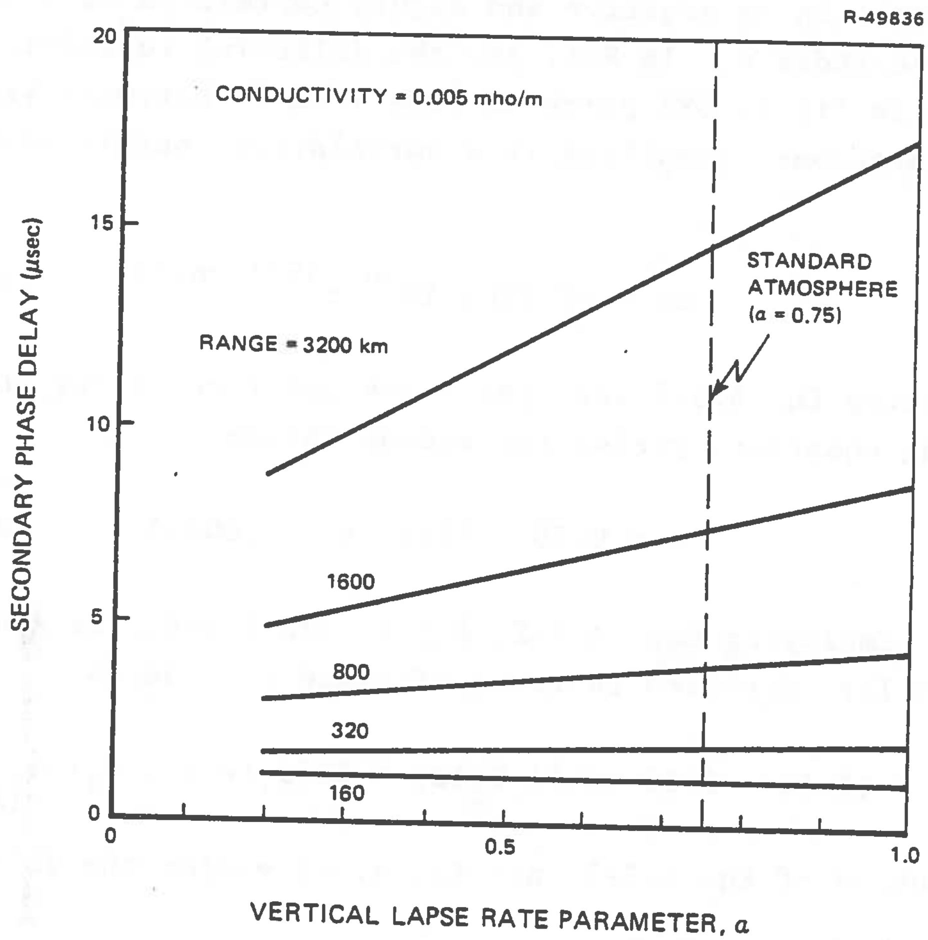

Figure A.3-1 Effect of Non-Standard Atmosphere on Secondary Phase Delay

$$\widetilde{SF} = 0.00373\ R_i(u)\ [\alpha(t) - 0.75] \qquad \text{(A.3-3)}$$

with $R_i(u)$ in km and SF in μsec. It is assumed that there is no coupling between σ and α, implying that Eq. A.3-3 is applicable for all conductivities.

To relate α and n, consider the definition of α in terms of the change in refractive index between the surface and 1.0 km altitude (Δn):

$$\alpha \doteq 1 + 6378\ \Delta n \qquad \text{(A.3-4)}$$

Range difference errors are caused by approximations in estimating range differences from TDs measured at the user and pattern monitor locations. In order to derive the range difference error equation, a mechanization for differential Loran-C must be assumed. The assumed mechanization has the following characteristics:

- One pattern monitor is employed in each harbor (utilization of multiple monitors is not considered in the present study)
- TDs are measured simultaneously at the user and pattern monitor locations (requires post-mission data processing in Variable Geometry configuration)
- If the user is a buoy, the user and pattern monitor TDs are measured when the Loran-C equipment is installed on the buoy (ideally, with the buoy located at its correct anchor position)
- If the user is a helicopter, a TD grid prediction model is hypothesized for the harbor.

The assumed mechanizations are different for cases of buoy and helicopter Loran-C users because initial TD measurements are available for buoys but not for helicopters. The range difference error equations are derived separately in Sections A.4.1 and A.4.2, and their common structure is summarized in Section A.4.3.

A.4.1 Buoy Loran-C User (TD Transmission and Pulse Retransmission)

If the user is a buoy, the objective is to determine any change in buoy range difference between the time of equipment installation (t_o) and the time of buoy position audit (t). Four measured TDs are available for this purpose -- $TD_i(u_o,t_o)$, be expanded in terms of propagation parameters and noise to yield the following equation*:

$$\frac{1}{c}\,\delta RD_i(u) = -3.06\,[n(t) - n(t_o)]\,[RD_i(u) - RD_i(p)]$$
$$+ [SF_i(u,t) - SF_i(p,t)] - [SF_i(u,t_o) - SF_i(p,t_o)]$$
$$- [SF_m(u,t) - SF_m(p,t)] + [SF_m(u,t_o) - SF_m(p,t_o)]$$
$$+ [v_i(u,t) - v_i(u,t_o)]$$
$$- [v_i(p,t) - v_i(p,t_o)] \qquad \text{(A.4-3)}$$

The error equation does not involve the emission delay, whose effect is nullified by the pattern monitor.

Four terms which appear in brackets in Eq. A.4-3 involve the difference between SF at the user and SF at the pattern monitor. It is assumed that the SF versus range curve for a particular time and transmitter is linear over those ranges relevant to the users and pattern monitor in a given harbor. The circumstances under which this assumption holds are discussed in Section A.5. The scale factor (slope of SF curve) for transmitter i at time t_i is denoted by $\zeta_i(t)$ and depends on the conductivity structure of the path between transmitter i and the harbor at time t. The resulting range difference error equation is

$$\frac{1}{c}\,\delta RD_i(u) = -3.06\,[n(t) - n(t_o)]\,[RD_i(u) - RD_i(p)]$$
$$+ [\zeta_i(t) - \zeta_i(t_o)]\,[R_i(u) - R_i(p)]$$
$$- [\zeta_m(t) - \zeta_m(t_o)]\,[R_m(u) - R_m(p)]$$
$$+ [v_i(u,t) - v_i(u,t_o)]$$
$$- [v_i(p,t) - v_i(p,t_o)] \qquad \text{(A.4-4)}$$

*The more compact notation $SF_i(u,t) = SF(\sigma_i(u,t), R_i(u))$ is used here.

to be biases over the time interval of the buoy audit, and measurement noises which are assumed to be random (both in time and space) during the audit. The biases for the buoy Loran-C user are the differences between propagation parameters at the audit time and at the equipment installation time; for the helicopter Loran-C user, the biases are the differences between propagation parameters at the audit time and for the hypothesized model. The Loran-C biases comprise the following state vectors:

$$\underline{x}_L = \overset{\text{Buoy}}{\begin{bmatrix} n(t) - n(t_o) \\ \zeta_1(t) - \zeta_1(t_o) \\ \zeta_2(t) - \zeta_2(t_o) \\ \zeta_m(t) - \zeta_m(t_o) \end{bmatrix}} \quad \text{or} \quad \overset{\text{Helicopter}}{\begin{bmatrix} n(t) - \bar{n} \\ \zeta_1(t) - \bar{\zeta} \\ \zeta_2(t) - \bar{\zeta} \\ \zeta_m(t) - \bar{\zeta} \end{bmatrix}} \qquad \text{(A.4-7)}$$

where scale factor errors for both secondary transmitters (i = 1 and 2) have been included. Measurement noise includes components for TDs measured at the user and pattern monitor. In the case of a buoy Loran-C user, noise is included at both the audit time and the equipment installation time, while noise is only included at the audit time for the helicopter Loran-C user. The Loran-C measurement noise vectors are

$$\underline{v}_L = \overset{\text{Buoy}}{\begin{bmatrix} v_1(u,t) - v_1(u,t_o) \\ v_2(u,t) - v_2(u,t_o) \\ v_1(p,t) - v_1(p,t_o) \\ v_2(p,t) - v_2(p,t_o) \end{bmatrix}} \quad \text{or} \quad \overset{\text{Helicopter}}{\begin{bmatrix} v_1(u,t) \\ v_2(u,t) \\ v_1(p,t) \\ v_2(p,t) \end{bmatrix}} \qquad \text{(A.4-8)}$$

where cov $\underline{x}_L$ and cov $\underline{v}_L$ are the covariance matrices for the state and noise vectors, respectively. The buoy position error covariance matrix for the Variable Geometry configuration is presented in Appendix C.

A.5 ERROR STATISTICS

A.5.1 State Vector

Each Loran-C bias (Eq. A.4-7) is the difference between the values of a propagation parameter at times t and t_o (for a buoy), or between the value at time t and the value assumed in a hypothesized model (for a helicopter). Standard deviations are assigned to the biases based on available information concerning maximum seasonal and spatial variations in the Loran-C propagation parameters.

Refractive index (n) is assumed to be spatially homogeneous since seasonal variations dominate spatial variations. Seasonal variations differ for different regions of the United States, but are largest for the northeastern region. Maximum, minimum, and mean seasonal cycles in refractive index are plotted from historical data (Ref. 12) in Fig. A.5-1 for Washington, D.C., illustrating a spread of approximately 110 x 10^{-6}. The following worst-case assumptions are made:

- $n(t_o)$ or $\bar{n}$ is at an extreme of the historical data
- n(t) obeys a uniform distribution between the extremes.

These assumptions result in a computed standard deviation of 50 x 10^{-6} for the refractive index error. This value is em-

The following characteristics apply to the transmitter-to-user propagation paths for analysis purposes (see Fig A.5-2):

- The transmitter is separated from the coastline by land of homogeneous conductivity σ_L and range R_L
- The harbor is separated from the coastline in the transmitter direction by sea water with conductivity σ_S and range R_S; R_S depends on specific user location
- The harbor itself, covering all Loran-C users*, is entirely sea water with conductivity σ_S.

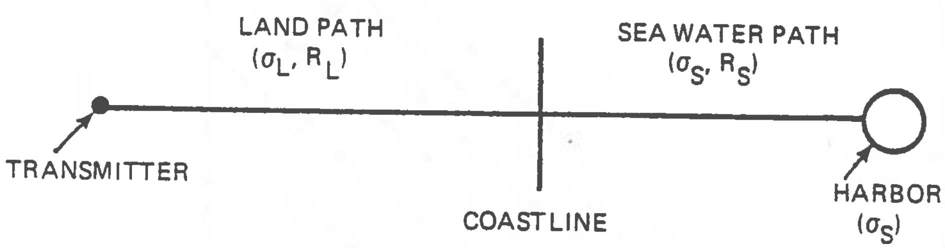

Figure A.5-2 Mixed Land and Sea Water Path

If the harbor is close to the coastline in the transmitter direction, the range R_L may depend on the bearing angle from the particular user to the transmitter. The shape of the coastline is important in this case. For tractability, it is assumed that R_L is the same for all users in the harbor.

Millington's method of expressing SF for the assumed mixed path includes six terms (Ref. 15):

---

*Although helicopter tracks or pattern monitor locations may be on land, they are assumed to be close to the water.

theory results into Eq. A.5-1 reveals that SF decreases on crossing the coastline from land to sea water. This phenomenom is illustrated in Fig. A.5-4 for various land conductivity values and land path lengths. Note that the slope of the SF curve on the sea water path segment depends on land conductivity (σ_L) and sea water path length (R_S), but not on land path length (R_L). For R_S less than 200 km, the slopes depend on σ_L in the manner shown in Fig. A.5-5, where the incremental SF (relative to SF at the coastline) is plotted versus R_S. Slope is independent of σ_L for R_S greater than approximately 200 km. It is assumed that all paths for a particular transmitter and harbor fall into one of the following categories:

Type I: $R_S < 15$ km
Type II: 15 km $< R_S <$ 200 km
Type III: $R_S > 200$ km

Slopes of the SF versus range curves for the three path types are summarized in Table A.5-1 for the spread of land conductivities found in the United States (see Ref. 13).

Interpretation of the slopes listed in Table A.5-1 depends on whether the Loran-C user is a buoy or helicopter. In the case of a helicopter Loran-C user, the scale factor error is $\zeta_i(t) - \bar{\zeta}$. Note that $\zeta_i(t) - \bar{\zeta}$ may be large, even if there are no temporal variations in land conductivity. This follows from the fact that spatial variations in land conductivity, which must be known to correctly hypothesize $\bar{\zeta}$, cannot be mapped reliably at present. Since $\bar{\zeta}$ would be based on a conductivity map which may have significant errors, the following worst-case assumptions are made:

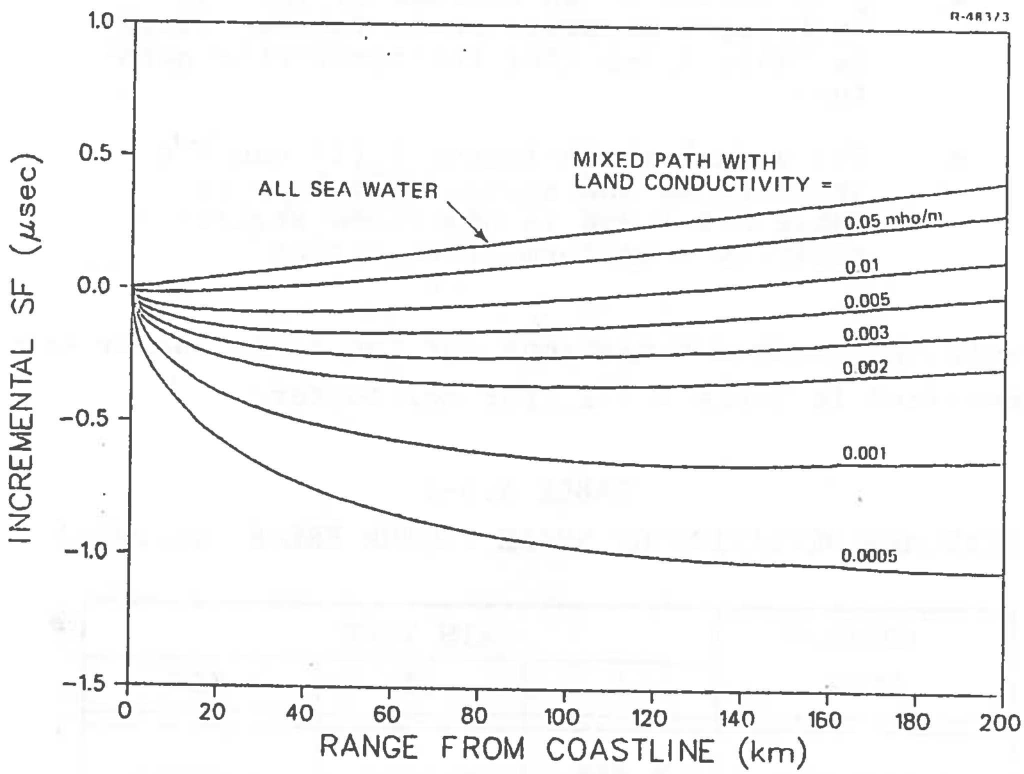

Figure A.5-5 Incremental SF on Sea Water Propagation Path Segment

TABLE A.5-1

SLOPES OF SF VERSUS RANGE CURVES ON SEA WATER PATH SEGMENT (μsec/km)

LAND CONDUCTIVITY (mho/m)	PATH TYPE I	PATH TYPE II	PATH TYPE III
0.0005	-0.076	-0.0035	+0.0021*
0.001	-0.056	-0.0019	
0.002	-0.041	-0.0006	
0.003	-0.034	-0.0001	
0.005	-0.027	+0.0005	
0.01	-0.020	+0.0010	

*Based on a sea water conductivity of 5 mho/m. Maximum spread assumed to be ±10 percent of value shown.

The standard deviations listed for Type I paths are employed as the nominal values in the covariance simulations herein, representing a worst case. The three scale factor errors (for i = 1,2, and m) are assumed to be independent.

A.5.2 Measurement Noise Vector

The measurement noise vector (Eq. A.4-8) includes two noises (corresponding to two measured TDs) for the Loran-C user and two noises for the pattern monitor. In the case of a buoy Loran-C user, each noise includes components at times t and t_o. In the case of a helicopter Loran-C user, each noise involves only a component at time t.

Noise in the Loran-C frequency band (90-110 kHz) is primarily atmospheric, rather than internal to the receiver. Since the distance from p to u and the time between t_o and t are generally large compared to the expected correlation distance and correlation time for atmospheric noise, it is assumed that the noises in all receiver channels are independent. However, the noises associated with two TDs measured at the same location at the same time both involve the master station channel, and are thus correlated with correlation coefficient 0.5. Denoting the standard deviations of user and pattern monitor TDs by σ_u and σ_p*, the measurement noise covariance matrix for a helicopter Loran-C user is

$$\text{cov } v_L = \left[\begin{array}{c|c} \sigma_u^2 \begin{bmatrix} 1 & 0.5 \\ 0.5 & 1 \end{bmatrix} & 0 \\ \hline 0 & \sigma_p^2 \begin{bmatrix} 1 & 0.5 \\ 0.5 & 1 \end{bmatrix} \end{array}\right] \quad \text{(A.5-2)}$$

*Not to be confused with conductivities.

pheric noise. The second-order tracking loop for the Micrologic ML-120 receiver is analyzed in Ref. 19. It is shown that the standard deviation of the tracking error (error in tracking third-cycle zero crossing) is proportional to $\sqrt{G}$, where G is the first-order loop gain (the second-order loop gain is adjusted to keep the damping ratio at a fixed value). On the other hand, the steady-state tracking error due to receiver acceleration is proportional to $1/G^2$. Therefore, the gain G must be small enough to minimize errors due to noise, but large enough to minimize acceleration errors. Loop-gain settings for the helicopter-borne Loran-C receiver in the Variable Geometry BPAS configuration would have to be selected based on flight tests under actual helicopter maneuvers. The error analyses discussed herein are based on a nominal noise standard deviation of σ_u=0.02 μsec.

APPENDIX B

BANDPASS FILTER MODEL

The bandpass filter model employed in the Pulse Retransmission simulations discussed in Appendix F is described by the second-order transfer function

$$\frac{I_o(s)}{I(s)} = G\,\frac{1 + as + bs^2}{1 + ds + bs^2} \qquad \text{(B-1)}$$

where

$I(s)$ = Laplace transform of input current $i(t)$

$I_o(s)$ = Laplace transform of output current $i_o(t)$

s = Laplace transform parameter

G = gain chosen such that maximum of $i_o(t)$ equals maximum of $i(t)$

The bandpass filter frequency spectrum ($s = 2\pi fj$) is characterized by the center frequency (f_p), the -3 dB bandwidth (Δf), and the rejection level (D). These parameters are related to the parameters in Eq. B-1 by

$$\begin{aligned} f_p &= 1/(2\pi\sqrt{b}) \\ \Delta f &= d/(2\pi b) \qquad \text{(B-2)} \\ D &= 20 \log (a/d) \end{aligned}$$

It should be noted that the spectrum approaches a constant value (equal to the value at f_p minus the rejection D) at low and high frequencies. Although bandpass filters typically

APPENDIX C
VARIABLE GEOMETRY CONFIGURATION ERROR MODEL

C.1 INTRODUCTION

In the Variable Geometry BPAS configuration, buoy position is estimated from helicopter-to-buoy microwave range data and synchronous helicopter Loran-C and altimeter position data. Measurements from at least two different helicopter positions are required to compute the position of a buoy. Additional information is needed to resolve the position ambiguity inherent in intersecting two circular lines-of-position (LOPs). The ambiguity is typically resolved by making a third measurement at a helicopter position which is not colinear with the first two positions. Fig. C.1-1 illustrates computation of the buoy position, assuming that there are no

R-49825

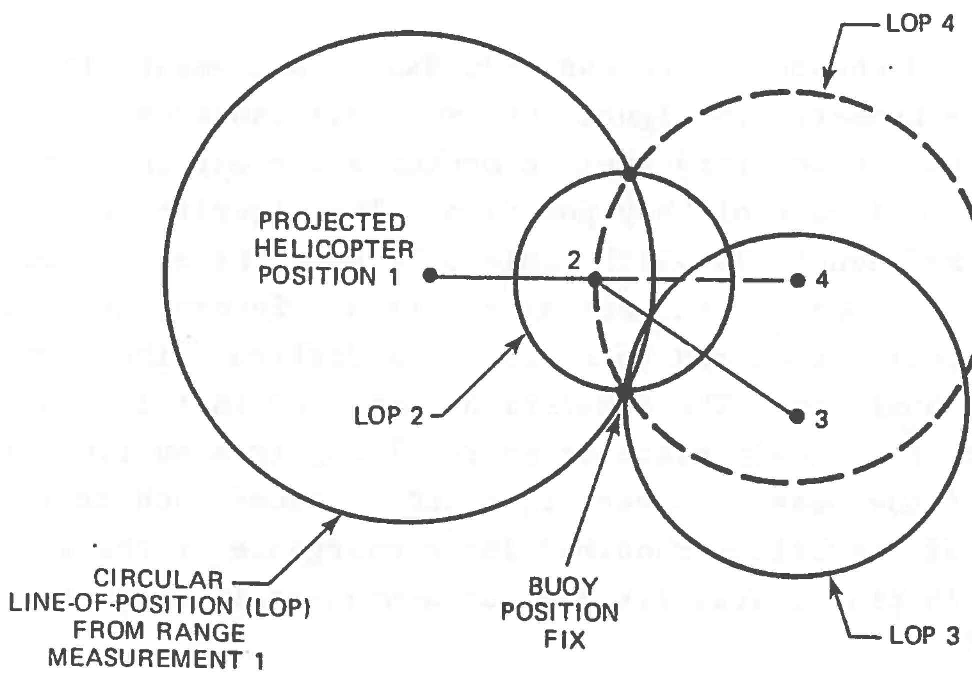

Figure C.1-1 Computation of Coarse Buoy Position Fix

The least-squares algorithm provides an optimal estimate of buoy position in the presence of bias and noise errors, which comprise the error model for this study. A more detailed error model may include errors with dynamic properties intermediate between biases and noises and would be well-suited to a Kalman filter approach (Ref. 17).* A dynamic model is not required for this study, however, because no error sources with time constants comparable to the time interval of the audit are expected. Error sources in the Variable Geometry configuration either change very slowly during the audit (and are modeled as biases), or change fast enough to be independent from measurement to measurement (and are modeled as noises).

C.2 MECHANIZATION AND ERROR MODEL

At each measurement point on the helicopter trajectory (flight pattern), the following quantities are available:

T = measured round-trip travel time of the microwave signal

T_d = specified transponder timing delay (time between reception and transmission of pulse)

z_a = measured helicopter altitude

x_a, y_a = helicopter horizontal position coordinates (east, north) indicated by Loran-C

x_b, y_b = prior estimate of buoy position coordinates (provided by coarse fix or by output of previous iteration of least-squares algorithm).

---

*The least-squares algorithm is a special case of a Kalman filter (i.e., with no dynamics).

k^{th} observation can be related to the error parameters by the equation:

$$\underline{\Delta r}_k = H_k \, \underline{\delta x} + \underline{\delta v}_k \qquad \text{(C.2-5)}$$

where

$\underline{\Delta r}_k$ = vector which includes observation k for each buoy

$\underline{\delta x}$ = state vector of bias errors (including north and east buoy position errors)

$\underline{\delta v}_k$ = vector of noise errors associated with observation k

H_k = matrix of coefficients which defines the geometry for observation k. Loran-C and microwave ranging contributions to H_k are from Eqs. A.4-9 and C.2-4, respectively.

The least-squares algorithm provides a recursive estimate of all bias errors, $\underline{\hat{\delta x}}_k$, (including buoy position error) based on the previous estimate, $\underline{\hat{\delta x}}_{k-1}$, given by the following computational procedure (Ref. 17). The "gain" matrix is first computed by:

$$K_k = P_{k-1} H_k^T \, [H_k P_{k-1} H_k^T + R_k]^{-1} \qquad \text{(C.2-6)}$$

where R_k is the noise error covariance matrix and P_{k-1} is the error covariance matrix for the bias estimate given by the previous step of the recursion algorithm. The initial covariance P_o is a diagonal matrix composed of the initial variances of the bias error sources, as specified in Section C.3. The bias error estimate is given by:

$$\underline{\hat{\delta x}}_k = \underline{\hat{\delta x}}_{k-1} + K_k \, [\underline{\Delta r}_k - H_k \, \underline{\hat{\delta x}}_{k-1}] \qquad \text{(C.2-7)}$$

The initial error estimate $\underline{\hat{\delta x}}_o$ is chosen to be zero. The error covariance matrix is updated by the equation:

TABLE C.3-1

NOMINAL ERROR SOURCES FOR VARIABLE GEOMETRY CONFIGURATION

ERROR SOURCE	SYMBOL	TYPE	STANDARD DEVIATION
Microwave Propagation Velocity Error	δc	Bias	0.015 m/μsec
Microwave Measurement Noise	δT	Noise	0.01 μsec
Common Microwave Timing Error	δT_d	Bias	0.02 μsec
Independent Microwave Timing Error			0.02 μsec
Altitude Error	δz_a	Bias	10 m
Helicopter Loran-C Position Error	$\delta x_a, \delta y_a$	See Appendix A	
A Priori Buoy Position Error	$\delta x_b, \delta y_b$	Bias	Infinite

- A bias which is independent from buoy to buoy and could arise from a random difference in buoy signal delay caused by hardware variability.

The nominal standard deviation of each type of timing bias error is conservatively assumed to be 0.02 μsec in this study.

The helicopter is assumed to be equipped with a radar altimeter characterized by a bias error with a standard deviation of one percent of altitude. For the assumed altitude of 300 m, nominal altitude error (δz_a) standard deviation is conservatively chosen to be 10 m.

APPENDIX D
CORRESPONDENCE WITH MICROWAVE RANGING SYSTEM MANUFACTURERS

This appendix contains copies of correspondence between TASC and two manufacturers of microwave ranging systems, Del Norte Technology, Inc. and Motorola.

TASC
THE ANALYTIC SCIENCES CORPORATION

Six Jacob Way, Reading, MA 01867, (617) 944-6850

21 August 1979

Mr. William O'Donnell - T2020
Motorola - Government Electronics Division
7402 South Price Road
Tempe, Arizona 85282

Dear Mr. O'Donnell:

Please find enclosed tentative requirements for the microwave ranging system which we discussed during our telephone conversation of 1 August 1979. TASC is assisting the Transportation Systems Center and U.S. Coast Guard in evaluating a positioning system which would utilize the specified microwave ranging system in conjunction with airborne Loran-C to audit the positions of U.S. Coast Guard navigational buoys. The microwave ranging/airborne Loran-C system configuration is being compared with an alternative configuration consisting of a Loran-C receiver on each buoy from which time difference data are transmitted over a VHF telemetry link to a shore station or helicopter. Therefore, to provide a meaningful comparison of the candidate systems, TASC needs an estimate of the per unit production costs of buoy equipment and helicopter equipment required for the microwave ranging system, and the cost of developing equipment for experimental system verification.

The microwave ranging system specifications may be modified prior to hardware procurement if a decision is made by the U.S. Coast Guard to pursue the concept. Your inputs to this evaluation are greatly appreciated.

Very truly yours,

Leon M. DePalma

Leon M. DePalma

LMD/p
Enclosures

cc: Mr. Joseph Wolfson
Transportation Systems Center
U.S. Department of Transportation
Kendall Square
Cambridge, MA 02142

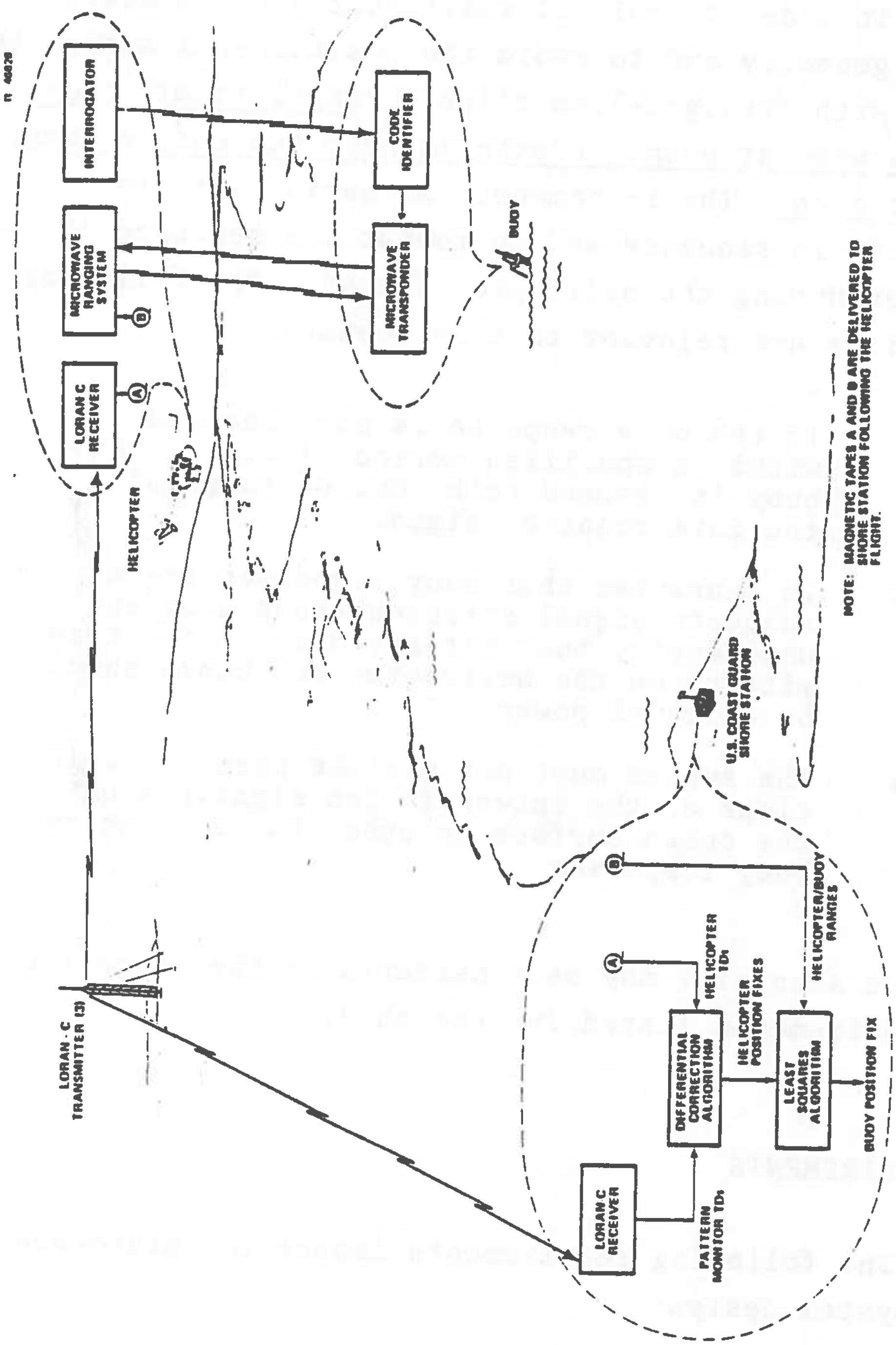

Figure 1-1 Candidate Buoy Position Audit System

- Maximum helicopter-to-buoy range of interest is 30 nm which may be reduced, if necessary, to meet specifications on buoy battery drain; reduction below 10 nm would severely constrain helicopter operations

- Buoy power source is a 12 volt, 1000-6000 amp-hr battery presently on all lighted buoys; battery drain of 7 amp-hr is available for each audit

- Audits are performed once per week on the average; buoy equipment should not require servicing more often than once per year

- Buoy equipment is housed in two cylindrical battery compartments, each measuring at least 22 in. inside diameter by 65 in. deep; one compartment is partially occupied by a 36 in. battery rack; the remainder of this compartment and the entire spare compartment are available for buoy audit equipment

- Battery compartments are vented to the atmosphere, thereby acquiring the temperature (within ±10°F) and humidity of the air above the ocean surface

- Weight of buoy equipment must not exceed 100 lb

- In any particular audit mission, fewer than 300 buoys would be interrogated; therefore, a nine-bit identification code is required

- Range measurement accuracy should be on the order of 10 ft rms at maximum range

- The separation of the buoy antenna and buoy electronics package could vary from 2 ft to 15 ft, depending on the location of the antenna on the buoy structure (see Fig. 3-1 for illustration of a typical buoy); the buoy antenna must have a hemispherical beam pattern

- Maximum helicopter velocity is 80-120 kt, depending on helicopter model; maximum round-trip helicopter flight time is 3 hrs

- The helicopter-borne unit must be capable of displaying the status of the range measurement process -- e.g., a warning could be displayed if no responses are received from a particular buoy; this would prompt the pilot to do a visual survey of the area in which the buoy is expected to be located

- The helicopter-borne unit must be equipped with standard RS-232C digital interfaces to accept interrogation scheduling data from the control unit and to output range data to a tape cassette recorder

- The helicopter-borne unit (excluding antenna) must be portable and capable of being hand-carried by one person; the antenna should be permanently mounted and have a hemispherical beam pattern.

4. COSTING CONSIDERATIONS

The following cost information is required to determine the economic feasibility of the microwave ranging/airborne Loran-C Buoy Position Audit System configuration:

- Production cost per buoy unit (including electronics, antenna, and calibration) for 1000 to 4000 units

- Production cost per helicopter unit (including electronics, display, antenna, and calibration) for fewer than 100 units

- Development and equipment costs for eight buoy units and one helicopter unit for experimental system verification.

A brief description of the recommended design should be provided together with a discussion of potential cost savings afforded by relaxing system specifications or by revising the recommended buoy interrogation scenario.

APPENDIX E
BUOY-TRACKING TECHNOLOGY

In addition to their role as aids to navigation, buoys are applied extensively in hydrographic research. Technology for locating and tracking buoys has received particular attention in the area of ocean current mapping, because the buoys used for this purpose are in a free-drifting mode. Documented methods which have been employed or considered for locating and tracking buoys are summarized in Table E-1. The methods are categorized according to the type of buoy (free-drifting or moored) with which they are associated in the referenced literature. The systems listed in Table E-1 represent a wide range of methods, employing both passive techniques (radar, photography, visual) and active techniques (beacons, transponders, retransmission) and differing significantly in position accuracy, cost, coverage and flexibility.

APPENDIX F

EFFECT OF PULSE RETRANSMISSION ON LORAN-C THIRD-CYCLE IDENTIFICATION

F.1 SIMULATION MODEL

The model utilized in the Pulse Retransmission simulations is illustrated in Fig. F.1-1. The ideal Loran-C current pulse assumed to be received at the buoy is described by the equation

$$i(t) = A\ (t/\Delta)^2\ e^{2\ (1\ -\ t/\Delta)}\ \sin(2\pi ft) \qquad \text{(F.1-1)}$$

where

A = peak envelope current = 1 unit

Δ = peak envelope time = 65 μsec

f = 0.1 cycle/μsec = 100 kHz

t = time (μsec) referenced to start of envelope

Effects of skywave interference, atmospheric noise, and non-zero Envelope-to-Cycle Difference (ECD) are not included in the simulations. The received pulse is passed through a band-pass filter whose transfer function and frequency spectrum are detailed in Appendix B. The bandpass filter parameters -- bandwidth and center frequency -- may vary slightly from buoy to buoy as a result of manufacturing tolerances.

The filtered Loran-C pulse is then distorted by a static (i.e., memoryless) nonlinearity, which is a simple representation of the retransmission process -- including modulation (at the buoy), telemetry, and demodulation (at the shore station or helicopter). A more realistic representation

The Loran-C receiver must be capable of identifying the third cycle of the 100 kHz carrier and of tracking the positive-going zero crossing associated with the third cycle (nominally, the 30 μsec point). A common technique for identifying the third cycle is to form a <u>derived pulse</u> by delaying the original pulse by a half cycle (5 μsec), scaling the delayed pulse by a gain (k) equal to 1.23466, and adding the scaled pulse to the original pulse (Ref. 20). If the ideal Loran-C pulse is processed by such a technique (termed "delay and add"), the <u>envelope</u> of the derived pulse equals zero at the 30 μsec point of the pulse, as shown in Fig. F.1-1. This envelope null is referred to as the <u>envelope tracking point</u>. The objective of the simulations herein is to determine the effect of the filters and nonlinearity on the envelope tracking point.

F.2 EFFECT OF BANDPASS FILTERS

The result of passing the ideal Loran-C pulse through a bandpass filter is to shift the envelope tracking point determined by the "delay and add" envelope deriver. The derived pulses for bandpass filters with bandwidths of 10 and 30 kHz, centered at 100 kHz, are illustrated in Fig. F.2-1 (compare with ideal derived pulse in Fig. 1.1-1). The envelope tracking point* is shifted to the right (>30 μsec) and the length of the shift increases with decreasing bandwidth. Although a bandpass filter causes large shifts in the envelope tracking point, the Loran-C receiver can be calibrated by adjusting the gain k used in the "delay and add" operation. Proper adjustment of k places the envelope tracking point at 30 μsec.

---

*Envelope tracking point is uniquely defined as the derived pulse zero crossing which is not associated with a carrier zero crossing.

However, the Loran-C receiver in the shore station or helicopter in the Pulse Retransmission BPAS configuration must function properly for all buoys in the harbor. Consequently, k must be chosen to guarantee satisfactory envelope tracking for the retransmitted Loran-C pulses from all buoys. It is noted in Ref. 21 that manufacturing tolerances on the bandpass filters utilized at the buoys must be small enough to permit an acceptable harbor-wide calibration. To examine this issue further, the envelope tracking point has been computed versus filter bandwidth (Fig. F.2-2) and versus filter center frequency (Fig. F.2-3). In these simulations, the bandpass filter in the Loran-C receiver is <u>fixed</u> with a bandwidth of 30 kHz and a center frequency of 100 kHz. Slopes of the curves in Figs. F.2-2 and F.2-3 determine the sensitivity of the envelope tracking point to deviations in bandwidth and center frequency, respectively. For a nominal bandwidth of 30 kHz and a nominal center frequency of 100 kHz, the sensitivities are 0.2 μsec per kHz of bandwidth and 0.3 μsec per kHz of center frequency. Since manufacturing tolerances less than 1.0 kHz are easily achievable, the envelope tracking point will vary less than 0.3 μsec from buoy to buoy. If the average envelope tracking point is calibrated to a value of 30 μsec, no third-cycle identification problems due to bandpass filter variability are expected to be encountered.*

F.3 EFFECT OF NONLINEAR MODULATION/DEMODULATION

The effect of a nonlinear modulation/demodulation process on the envelope tracking point is investigated using the model depicted in Fig. F.1-1. Both bandpass filters are

---

*Third-cycle identification problems may occur if the calibrated envelope tracking point lies outside the 25 to 35 μsec time interval.

assumed to have a 30 kHz bandwidth and 100 kHz center frequency. Two classes of static nonlinearity are considered, hard-limiting and "serpentine". The impact of a nonlinearity on the envelope tracking point is an important issue due to the large amplitude range expected between the weakest and the strongest Loran-C pulses received at each buoy. It is shown in Ref. 21 that the modulation/demodulation process must exhibit a minimum dynamic operating range of 78 dB. If a 78 dB dynamic range cannot be achieved due to cost or technical constraints, the strongest pulses would be distorted by nonlinearities. Since the character of the distortion differs for different pulse amplitudes, it may not be possible to compensate for envelope tracking point differences introduced by the distortion.

The hard-limiting nonlinearity is described by the input-output characteristic shown in Fig. F.3-1. The saturation level α determines the degree to which the leading edge of the filtered Loran-C pulse (with peak value of unity) is distorted by the nonlinearity. The output of the hard-limiting nonlinearity is illustrated in Fig. F.3-2 for a saturation level of 0.1. Although the leading edge of the pulse is apparently distorted beyond recognition by the nonlinearity, information regarding the pulse envelope is not lost. The information is contained in the slopes of the carrier below the saturation level. Indeed, passing the distorted pulse through the second bandpass filter nearly replicates the pulse which enters the nonlinearity. This somewhat surprising result can also be explained by the frequency spectrum of the distorted pulse which is plotted in Fig. F.3-3. The shape of the spectrum in the Loran-C band (90-110 kHz) is not significantly different from the shape of the Loran-C spectrum. Harmonics of 100 kHz are introduced by the nonlinearity but are removed by the 30 kHz bandpass filter. The envelope

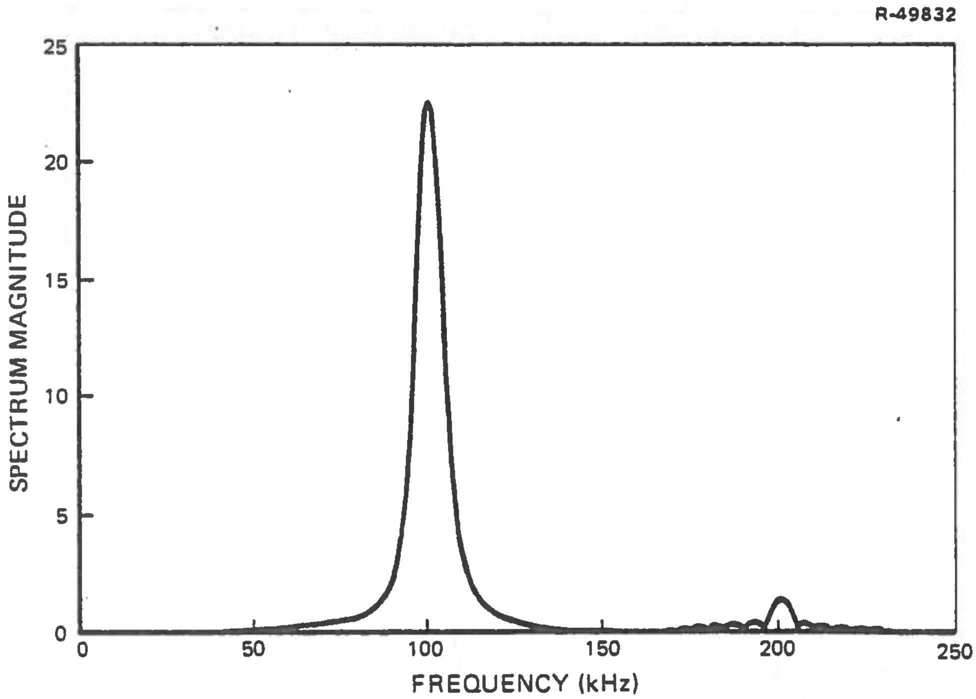

Figure F.3-3 Spectrum of Distorted Loran-C Pulse (α = 0.1)

tracking point is presented in Table F.3-1 for various values of α. Deviation from the nominal value of 37.99 μsec (for no nonlinearity) is less than 0.1 μsec. Therefore, a hard-limiting nonlinearity has no detrimental effect on Loran-C third-cycle identification.

The <u>serpentine nonlinearity</u> has the smooth input-output characteristic illustrated in Fig. F.3-4. The deviation from linearity is expressed by $\beta \sin(2\pi x)$, where β is the maximum deviation and x is the input to the nonlinearity. Pulse distortion depends on the parameter β and the peak amplitude of the input pulse; e.g., maximum pulse distortion occurs for large β and large peak amplitudes. The output of the serpentine nonlinearity is shown in Fig. F.3-5 for β equal to

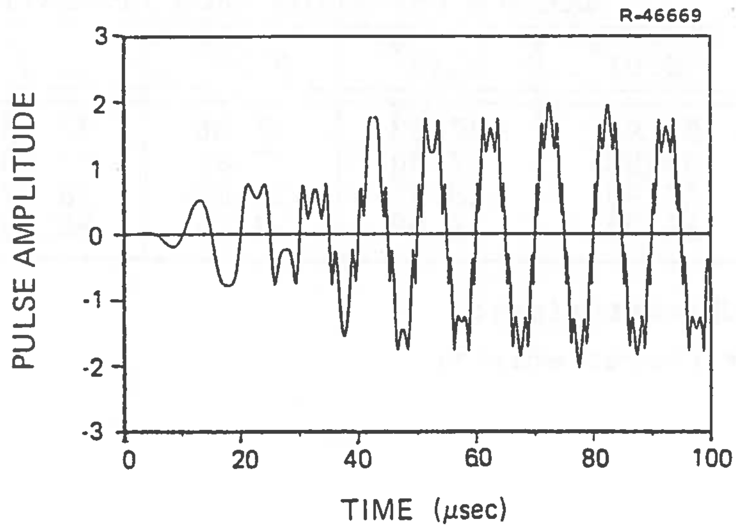

Figure F.3-5 Output of Serpentine Nonlinearity for $\beta=0.5$ and a Peak Amplitude of 2.0

The hard-limiting and serpentine nonlinearities discussed above are both symmetric with respect to the origin -- i.e., $f(-x) = -f(x)$ where f and x denote the nonlinear function and input current value, respectively. An asymmetric nonlinearity was simulated by a serpentine nonlinearity with a cosine rather than a sine characteristic. A somewhat greater effect on the envelope tracking point is found, as shown in the last column of Table F.3-2. However, the maximum deviation from the nominal envelope tracking point is only 2.34 μsec, still within the acceptable ±5 μsec limits.

APPENDIX G

COMMERCIAL EQUIPMENT DATA SHEETS

(1) COMMUNITRONICS LTD.
Telemetry Systems
Models MT-11 and MR-11

(2) COMMUNITRONICS LTD.
VHF Telemetry Transmitter
Model T-111

(3) COMMUNITRONICS LTD.
FM VHF Receiver
Model MR-18-FM

(4) INTERNAV
Loran-C Navigation and Monitor Receiver
Model LCM 404

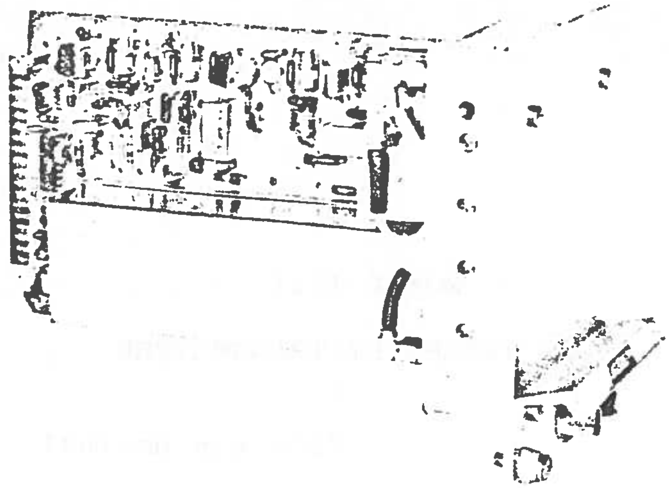

MODEL MR-11

The Model MR-11 Receiver is a crystal controlled dual conversion FM receiver. Utilizing an all solid state construction, the unit can be powered by 115 VAC power or +12 VDC. Since the construction of the MR-11 is modular, a change in the band pass filters allows the unit to process wide or narrow band information. The specifications of the MR-11 are listed below.

SPECIFICATIONS

Frequency Band	- 400 to 500 MHz
Accuracy	- ±.001%
Sensitivity (10 db Sinad)	- Less than 1 uv
Noise Figure	- 3 db
Bandwidth (Post Detection)	- 10 KHz (standard)
Image Rejection	- Greater than 60 db
Spurious Rejection	- Greater than 60 db
Power Requirement	- +12 VDC or 115 VAC
Size	- 5 3/4" x 4" x 10"

PRELIMINARY DATA SHEET

MR-18 FM VHF Receiver

The Communitronics Ltd. MR-18 FM VHF Receiver offers the user a reliable, lo power FM receiver. A unique feature of the receiver is its wide demodulated bandwidth (30 kHz). The MR-18 FM's small size plus low power consumption makes it ideal for compact, battery powered use, such as sonobuoys, command receiver, homing devices and distress beacons. Custom tailoring at the factory allows for different bandwidths as well as channel selection for any frequency from 30-300 MHz.

SPECIFICATIONS

Frequency	30-300 MHz
RF Bandwidth	200 kHz
Modulation Acceptance	FM
Sensitivity	½V for 20 dB quieting
Baseband Frequency Response	+3 dB 5 Hz to 30 kHz
Distortion	<1% @ 30 kHz peak deviation
Supply Voltage	12-15V D.C. (15 typical)
Temperature Range	0^{o} - 50^{o} C.
RF Input Impedance	50 Ohms nominal
Size	2" x 4" x 1" height
Weight	5 oz.

A. Local Mode - In this mode of operation, the LCM 404 is controlled from the front panel and can be used as a normal navigation receiver. The GRI, the secondaries in use, and the cycle sampling points are controlled from the front panel. Simultaneously, the unit can be remotely polled and will reply upon command with time differences and other Loran-C data.

GRI - Determined by Front Panel Switches

TD's displayed - Controlled by front panel switches S1 and S2.

Data to Remote Accessories - Controlled by switches S1 and S2.

Cycle Select Enable/Disable - Controlled by front panel

Up or Down Cycle Commands - From front panel

SNR - Can be displayed on front panel through use of front panel controls.

Communciations - Responds to external requests for time difference or status information.

B. Remote Mode - In this mode, certain receiver functions can be controlled remotely through the communications channel.

GRI - Determined by internal DIP switches (Front Panel GRI switches are ignored)

Secondaries Tracked - Determined by internal DIP switches.

TD's displayed - Selected by front panel switches S1 and S2.

Data to remote accessories - Selected by front panel switches S1 and S2.

Cycle Select Enable/Disable - Remotely controlled

UP of DOWN Cycle Commands - Remotely controlled.

SNR - Can be displayed on front panel using front panel switches

B. Noise

The standard deviation of the time differences will be less than 20 nanoseconds at a signal-to-atmospheric noise ratio of 0 DB.

C. Tracking

Receiver will maintain track over the following range of signal conditions.

a. Signal-to-noise greater than -23 DB atmospheric or better.
b. CW interference S/CWI greater than -40 DB (when notched).
c. Envelope to cycle difference plus or minus 4 μsec.
d. Absolute signal level 10 to 114 DB/luv/meter.

D. Acquisition and Settling

Receiver will acquire and settle to the correct cycle over the following range of signal conditions.

a. Signal-to-noise greater than -15 DB atmospheric.
b. CW interference S/CWI greater than -32 DB (when notched).
c. Envelope to cycle difference plus or minus 3.5 μsec.
d. Absolute signal level 25 to 105 DB/luv/meter.

E. Temperature Range - 0 to 55 degrees C.

F. Size - 5.7" high x 12.6" wide x 13.2" deep.

G. Weight - 20 lbs.

H. Resolution of tracking loop steps 10 nanoseconds.

I. Tracks Master and up to four secondaries.

J. Supply Voltage - 10 to 15 volts DC, 15 watts (with front panel display off).

Byte 3 First Digit - Execute Command on Signal X.

0 = Master

1-8 = MSD of Signal TD

9 = All

Second Digit - Spare

VI. Format of Reply Message

A. TD Reply

Byte 1 - Receiver ID 0 - 255 LSB first

Byte 2 - TDA 1 nanosecond digit LSB first

TDA 10 nanosecond digit

Byte 3 - TDA 100 ns digit

TDA 1 μsec digit

Byte 4 - TDA 10 μsec digit

TDA 100 μsec digit

Byte 5 - TDA 1 MS digit

TDA 10 MS digit

Byte 6-9 TDB 1 nsec digit first

Byte 10-13 TDC (if active)

Byte 14-17 TDD (if active)

Byte 18 - Signal Alert

Bit 0 = 1 if M = $\overline{LS}\cdot\overline{BLK}\cdot STLD$

Bit 1 = 1 if S1 = $\overline{LS}\cdot\overline{BLK}\cdot STLD$+Not Active

Bit 2 = 1 if S2 = $\overline{LS}\cdot\overline{BLK}\cdot STLD$+Not Active

Bit 3 = 1 if S3 = $\overline{LS}\cdot\overline{BLK}\cdot STLD$+Not Active

Bit 4 = 1 if S4 = $\overline{LS}\cdot\overline{BLK}\cdot STLD$+Not Active

Bit 5 = 1 if command executed

Bit 6 = 1 if command rejected.

VII. DIP Switches

DIP Switches are arranged on PC Card as shown:

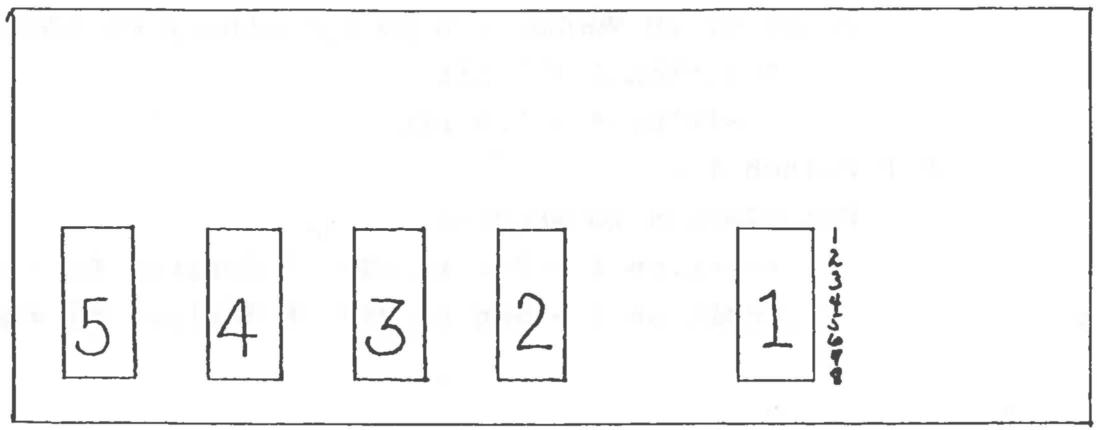

DIP Switch 1 -

Positions 1-4 MSD of GRI (Binary Encoded)

1 = 1 bit, 2 = 2 bit, 3 = 4 bit, 4 = 8 bit

To get 9, set positions 1 and 4.

Positions 5-8 2nd MSD of GRI

5 = 1 bit, 6 = 2 bit, 7 = 4 bit, 8 = 8 bit

DIP Switch 2 -

Positions 1-4 Third Digit of GRI

Positions 5-8 These positions determine whether the receiver is in LOCAL or REMOTE mode. If no switch positions are set, receiver is in LOCAL mode. If

APPENDIX H*

VARIABLE GEOMETRY PN RANGING SYSTEM

For this buoy position measuring system a two way pseudo-noise (PN) ranging signal is contemplated to be utilized. A duplex channel is required. One channel for the forward link (helicopter to buoy) and the other for the return link. To provide frequency isolation, a separation of at least 60 MHz between the channels is desirable. The experimental communication link may operate either microwave (L-Band) or UHF frequencies. The communication requirements are therefore computed for both frequency bands; at these frequencies free space propagation is valid. The free space attenuation between isotropic antenna is given by:

$$\alpha = 37 + 20\log f + 20\log d \qquad (7)$$

where

α = free space attenuation in dB

f = frequency in MHz

d = distance in miles.

In Table 3 are given the availabile carrier-to-noise ratios at the assumed parameters with the baseline values of P_T = 1 watt and d = 25 N.M. where

P_T = transmitter power

d = distance to buoy

P_r = received signal power

*Appendix H was extracted from an internal memorandum. For reasons of expediency equations, tables, and figures were not renumbered.

T_o = reference noise temperature

T_t = equivalent system noise temperature

k = Boltzman constant (1.38 x 10^{-23} w/oK/Hz)

Note that the received signal power P_r is proportional to

$$P_r \propto \frac{P_T}{d^2} \qquad (8)$$

so that P_r and hence C/N_o can be readily scaled as a function of P_T, and d. Table 3 will be used as a baseline reference for estimating the communication requirements for the PN ranging system.

3.1 PN RANGING CODE REQUIREMENTS

An envelope correlating, delay-lock tracking loop is to be used in the PN ranging system. A diagramatic representation of the receiver structure is shown in Figure 2.[2] The PN code must satisfy several requirements.

a) It must provide unambiguous range.

b) It must satisfy the measurement accuracy requirements.

c) It must provide a tolerable acquisition time.

Unambiguous Range: To provide unambiguous range the code length must be chosen so that

$$n\Delta \geq 12 \text{ d in usec.} \qquad (9)$$

where

d is the distance in N.M.

Δ is the width of each code chip in usec.

n is the number of chips in the ranging code

If the distance $d = 25$ N.M., then the code length must be at least 300 usec. If we pick a code chip of $\Delta = 1$ usec and $n = 512$ chips, an unambiguous range will be provided to approximately 42.6 N.M.

Tracking Accuracy: Another requirement is to adjust the system parameters so as to achieve good tracking accuracies with the envelope correlating, delay-lock loop (shown in Figure 2). The jitter in the delay measurements is given by:[3]

$$\frac{\sigma_t}{\Delta} = \left[\frac{B_L}{2C/N_o}\left(1 + \frac{2B_{1F}}{C/N_o}\right)\right]^{1/2} \qquad (10)$$

where

σ_t = tracking rms error in feet

Δ = chip duration in usec

B_{1F} = receiver post correlation 1F bandwidth

B_L = tracking loop bandwidth

Furthermore, if $C/N_o \gg 2\,B_{IF}$, the second term in the above equation can be neglected. If we let $B_{IF} = 10$ KHz (taking into account oscillator drifts), the value of $2\,B_{IF}$ is 43 dB. From Table 3, it is seen that even at L-Band and only with 0.1 watts of transmitted buoy power, the available

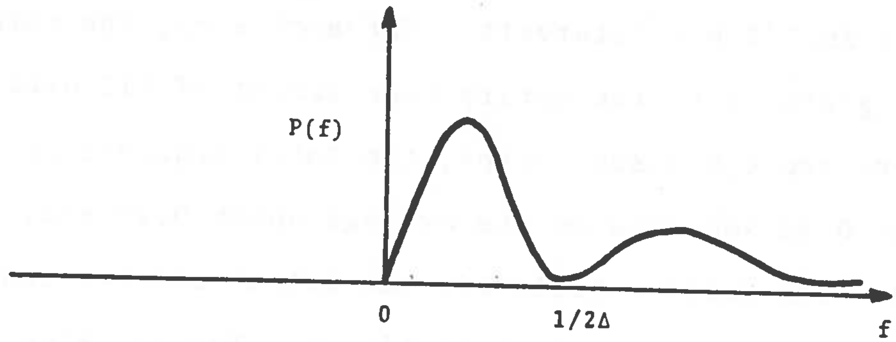

FIGURE 3a. CLOCK X CODE SPECTRUM

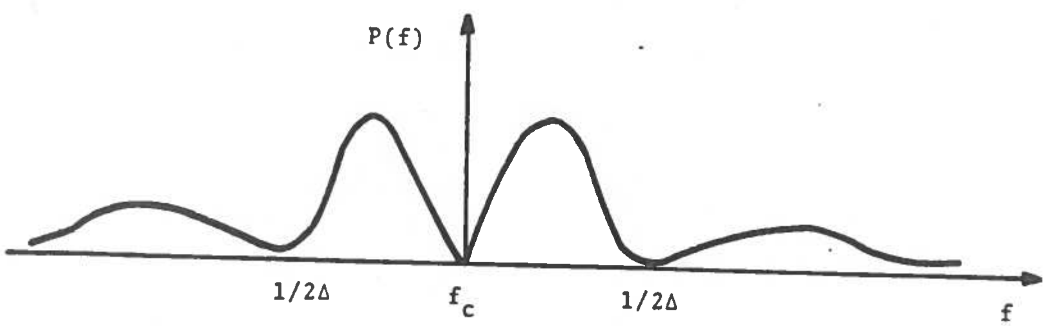

FIGURE 3b. SPECTRUM OF MODULATED CARRIER

TABLE 4. RANGING CODE PARAMETERS

PN code length.....................	=	512 μsec.
n.....................	=	512 (number of chips in the ranging code)
Δ.....................	=	1 μsec. (width of each chip)
Unambiguous range..................	=	42.6 N.M.
Correlator processing gain.........	=	27 dB
Post-correlator IF Bandwidth, B_{IF}..	=	10 KHz
Tracking loop bandwidth B_L.........	=	20 Hz
Tracking delay jitter rms, σ_t......	=	less than 3.3 ft for $C/N_o > 60$ dB
Average estimated acquisition time.	≈	0.36 sec.

noise will be small and for all practical purposes can be neglected. The amplified buoy signal will be in all probability band-pass limited. Since the $(SNR)_{RF}$ at the buoy receiver is larger than unity, there will be some enhancement in the output signal to noise ratio. If the input SNR to the band-pass limter were smaller than unity the output signal to noise ratio would be somewhat degraded. Here, we assume that a band-pass limiter will not degrade system performance. Our task now is to determine the (C/N_o) at the input to the helicopter reciever required for proper operation of the PN ranging system. The post correlation IF signal to noise ratio $(SNR)_{IF}$, at the input to the envelope detectors preceeding the delay lock loop, is given approximately by:

$$(SNR)_{IF} \approx \frac{(SNR)_{RF}}{L} \frac{B_{RF}}{B_{IF}} \qquad (12)$$

where

$(SNR)_{RF}$ = SNR at the input to the envelope correlator

$(SNR)_{IF}$ = post correlation IF signal to noise ratio

$(B)_{RF}$ = 4 MHZ (RF bandwidth)

$(B)_{IF}$ = 10 KHz (post correlation IF bandwidth)

L = 3 dB (assumed decorrelation loss)

Suppose that we require that the $(SNR)_{IF}$ at the input to the delay lock loop be at least 10 dB and preferably 20 dB. Such signal to noise ratios should be adequate for proper operation of the tracking loop since they are above the threshold values of typical phase lock loops.

TABLE 5. L-BAND COMMUNICATION PARAMETERS

Forward Link: (Helicopter to buoy)

P_H = 20 watts (Helicopter transmitted power

d = 25 N.M.

f = 1,500 MHz (assumed)

RF Bandwidth = 4 MHz

Modulation = PSK

data = PN ranging code with 512, 1 usec. code chips

Available $(SNR)_{RF}$ = 16.1 dB (at buoy receiver

Return Link: (Buoy to helicopter)

P_B = 0.246 watts (Buoy transmitted power)

f $\doteq$ 1,500 MHz

RF Bandwidth = same as above

Modulation = same as above

data = same as above

Available C/N_o = 63 dB-Hz

Available $(SNR)_{RF}$ = - 3 dB (at input to helicopter reciever)

Available $(SNR)_{IF}$ = 20 dB (at input to delay lock loop)

Command Link: Can utilize a data link or other means to "turn on" the buoy receiver/transmitter electronics.

APPENDIX I

DESIGN AND PERFORMANCE OF A TONE RANGING SYSTEM FOR BUOYAUDIT

Tone ranging is a range measurement technique which phase modulates an RF carrier with a set of sidetones or sine waves. The sidetones are generated from a master oscillator by digital division. The highest frequency tone is determined by the desired ranging precision; range is determined by measuring the phase shift between transmitted and received tones. The lower frequency tones are used for coarse range measurement, i.e., the phase shift of a lower frequency tone is used to resolve the number of whole wavelengths of phase shift which the higher frequency tone has incurred.

The specific technique described here is derived from an implementation originally proposed and analyzed by J.J. Stiffler (Ref. 36). It is basically a tone ranging system wherein a carrier is angle-modulated by a set of CW tones which are commensurate in frequency and coherent in phase. In his analysis Stiffler showed that under certain constraints, a tone frequency ratio of 2:1 would minimize the time required for signal acquisition. It also results in a particularly simple implementation scheme.

The signal generation process requires a signal countdown chain which divides in frequency by factors of two from the system oscillator to generate the ranging tones. The highest tone is called the clock; it determines the precision of the ranging system. The lowest frequency tone is chosen to have a half-wavelength longer than the minimum range required, thus eliminating range ambiguity problems. The set of tones is then combined in a majority-logic adder (equivalent to hard-limiting) thus providing a binary waveform to the modulator. In practise this same digital logic would drive the buoy clock.

RANGE TONE SELECTION AND IMPLEMENTATION

The block diagram of the chosen tone generator is shown in Figure 1. The highest frequency component has been chosen to be 100 khz; the lowest frequency component is 1.5625 khz. This component has a wavelength of 105.33 nautical

The phase-locked loop in Figure 2 locks to the carrier component of the received signal spectrum (Figure 3).

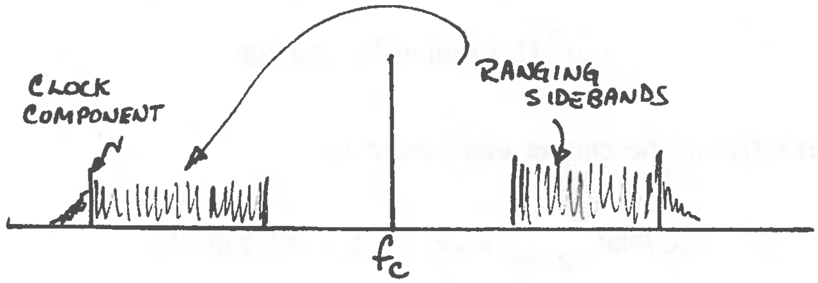

Figure 3. RF Signal Spectrum

The spectrum of the signal has very little energy in the region between the carrier and the lowest frequency tone (1.5625 khz). Consequently, the carrier-tracking loop can have a wide enough bandwidth to insure rapid lock-on, thus minimizing signal acquisition time.

The loop phase detector also functions as a linear phase demodulator. Consequently, the detector output signal contains the ranging signal, which goes from here to the ranging signal processor. The processor filters the noisy receiver output and generates a replica which is coherent in frequency and phase with the received ranging signal.

RANGING SYSTEM PERFORMANCE

The transmission frequency assumed here is about 1600 MHz. At this frequency, transmitter power level on the buoy need be no more than 1 watt. Assuming a range of 25 nautical miles from buoy to helicopter, the signal level received by the helicopter is calculated as follows:

Transmitter Power (1 watt)	+30dBm
Total Net Antenna Gain	0dB
Space Loss (free space)	-130.0dB
Signal Level at Helicopter	-100dBm
Noise Figure	+3dB
System Noise Power Density (assumes antenna temperature of 290°k)	-171dBm/Hz
Received Carrier / Noise Power Density (C/No)	+71dB-Hz

RANGING SIGNAL PROCESSOR - ACQUISITION AND PRECISION

The processor performs a sequential acquisition, first locking to the clock in a phase-locked loop, and then sequentially dividing its output by factors of two, comparing each output with the demodulated signal and making a binary (inphase-out of phase) decision. The decision time is (for each component), an integer multiple of the code length, which is essentially the period of the lowest-frequency code component (1/1562.5 or 0.64 milliseconds.) The clock loop bandwidth will be 20Hz, which will result in an acquisition time of approximately 3/20 = 150 milliseconds.

Each of the other components will require 0.64 milliseconds; therefore, the total system acquisition time, for each buoy transmission, will be:

$$T = 0.63 + 0.15 + (6) \times 0.64 \times 10^{-3} = 0.784 \text{ sec.}$$

which leaves a little over 9 seconds for the actual range measurement.

The precision of the ranging measurement is determined by the clock phase jitter, which in turn is a function fo the clock loop S/N.

$$\sigma^2 = \frac{1}{2\, S/N} (\text{rad})^2 \,;$$

(Ref. 39)

σ^2 = variance of clock phase.
S/N = clock signal/noise ratio.

The clock signal noise ratio is:

$$S/N)_{CL} = \left(C/N_0\right)_{ranging} \cdot 2 B_{L,CL} \cdot \rho \,;$$

$B_{L,CL}$ = clock tracking loop noise bandwidth.

ρ = clock component power relative to total ranging power.

The value of ρ is derived in Ref. 36; for this design, it is -2dB. So

$$S/N)_{CL} = +70.4 - 13 - 2 = +55.4 \text{ dB}$$

REFERENCES

1. Walden, R.G., and Webb, D., "Methods of Locating and Tracking Buoys," Trans. Buoy Technology Symposium, (Washington, D.C.) March 1964, pp. 317-324.

2. Werner, C.D., "Buoy Tracking With Over-the-Horizon (OTH) Radar," Proc. AIAA Drift Buoy Symposium, (Hampton, Virginia) May 1974, pp. 18-33.

3. Cote, C., "The Development of the Satellite Location and Data Collection System Within the National Aeronautics and Space Administration," Proc. AIAA Drift Buoy Symposium, (Hampton, Virginia) May 1974, pp. 351-371.

4. Bumpus, D.F., "The Striffler 'Talking Drift Bottle,' a Free-Drifting Buoy-Location System," Proc. AIAA Drift Buoy Symposium, (Hampton, Virginia) May 1974, pp. 9-17.

5. Webb, D.C., "Measurement of Open Ocean Circulation Using Neutrally Buoyant Floats," Proc. AIAA Drift Buoy Symposium, (Hampton, Virginia) May 1974, pp. 47-55.

6. Turner, S., "The Navy Navigation Satellite System for Buoy Location," Proc. AIAA Drift Buoy Symposium, (Hampton, Virginia) May 1974, pp. 56-70.

7. Johnson, R.E., "A Near Shore Circulation Study of the Chesapeake Bay Entrance Using Radar Tracked Buoys," Proc. AIAA Drift Buoy Symposium, (Hampton, Virginia) May 1974, pp. 34-46.

8. Giovane, F., "A Study of Aerial Semi-Precise Survey Systems for Position Auditing of Coast Guard Aids to Navigation," U.S. Coast Guard Research and Development Center, Report No. CG-D-61-77, October 1977.

9. Lindeblad, J.R., "The Distress Alerting and Locating System (DALS); Summary of Development and Documentation," U.S. Coast Guard Research and Development Center, Report No. CG-D-29-77, April 1977.

10. Swanson, E.R., "Geometric Dilution of Precision," Navigation: Journal of the Institute of Navigation, Vol. 25, No. 4, Winter 1978-1979, pp. 425-429.

22. Goddard, R.B., "Differential Loran-C Time Stability Study," U.S. Coast Guard, Report No. DOT-CG-31146-A, November 1973.

23. Lincoln, W.B., and Rush, R.G., "The Dynamic Behavior of a Particular Chain Mooring Under Tidal Current Excitation," U.S. Coast Guard, unpublished report, March 1978.

24. Campbell, L.W., Doherty, R.H., Johber, J.R.,"Loran-C System Dynamic Model-Temporal Propagation Variation Study", U.S. Dept. of Transportation, Report # DOT-CG-D57-79, July 1979.

25. Beukers, J.M., "Applications of Loran-C Retransmission," Presented at the Wild Goose Association Annual Convention, October 1973.

26. Cassis, R.H. Jr., "A Loran-C Airborne Navigator," Proc. Offshore Technology Conference, (Houston, Texas) May 1976, pp. 251-257.

27. Cassis, R.H. Jr., "An Operational Test and Evaluation of an Airborne Loran-C Navigator System," Proc. Offshore Technology Conference, (Houston, Texas) May 1977, pp. 69-76.

28. Adams, R.J., and McKinley, J.B., "Airborne Evaluation of the Production AN/ARN-133 Loran-C Navigator," Systems Control, Inc. (Vt), Report No. CG-D-32-79, July 1979.

29. Munson, R.C., "Positioning Systems," presented at International Congress of Surveyors, (Stockholm, Sweden) June 1977.

30. Hart, E.D., and Downing, G.C., "Positioning Techniques and Equipment for U.S. Army Corps of Engineers Hydrographic Surveys," U.S. Army, Report No. H-77-10, May 1977.

31. Couchman, R.L., "An Overview of Alternative Techniques for Determining Positions at Sea, with Emphasis on Applicability of Potential Use for Positioning Buoys," U.S. Coast Guard Research and Development Center, Report No. CG-D-20-78, March 1978.

32. "Coast Guard Action Needed to Promote Safer Marine Transportation," Comptroller General of the United States, Report No. CED-79-37, May 1979.